CALIFORNIA INSTITUTE OF TECHNOLOGY

DYNAMICS LABORATORY

THE DYNAMICS OF A SPINNING ELASTIC DISK WITH MASSIVE LOAD

by
Thomas Lee Moeller

Report No. DYNL-73-01

A report on research conducted under a grant from the Burroughs Corporation

October 1973

THE DYNAMICS OF A SPINNING ELASTIC DISK WITH MASSIVE LOAD

Thesis by

Thomas Lee Moeller

In Partial Fulfillment of the Requirements

for the Degree of

Doctor of Philosophy

California Institute of Technology

Pasadena, California

1973

(Submitted August 13, 1973)

The author would like to convey his gratitude to Professor W. D. Iwan for his patience and valuable assistance throughout this investigation. Also, special credit is due Professor Joel Franklin and Professor Thomas Caughey for their consultation.

The author is greatly appreciative of the financial support from the Burroughs Corporation, the California Institute of Technology, the National Science Foundation, and a National Defense Education Act Fellowship.

Sincere thanks are due to the secretarial staff, especially Mrs. Marilyn Hawn and Mrs. Julie Powell for their skillful typing of this manuscript.

The author also wishes to express his deep gratitude to his parents, and to his wife, Jeanie, whose understanding and patience never ceased.

ABSTRACT

This thesis analyzes the dynamics of a spinning elastic disk. The disk rotates at a constant angular velocity and is acted upon by a load consisting of a mass distributed over a finite area of the disk, a spring, and a dashpot. Using a finite mode approximation, the equation of motion of the transverse deflection of the disk is written as a system of ordinary differential equations with constant coefficients.

Analysis of the eigenvalues of the finite mode approximation yields four distinct types of instability. An instability occurs due to the stiffness of the load, terminal instabilities occur due to both the mass of the load and the damping of the load, and an instability occurs as a result of modal coupling.

The multiple mode approximation used in the spinning disk analysis is applied to a stationary disk with a moving load. Comparison of the spinning and stationary disk shows the influence of the centrifugal stress of the rotating disk.

The direct stability methods of Liapunov are applied to the equation of motion for both the spinning and stationary disk and are used to prove the stability of the systems at speeds below certain critical speeds. Upper bounds for the difference between eigenvalues of the finite mode approximation and eigenvalues of a full infinite mode system are derived. These bounds are calculated for the eigenvalues of a modal coupling instability arising from the finite mode analysis to show that the solution of the full set of equations is also unstable.

TABLE OF CONTENTS

I. INTRODUCTION

Interest in the dynamics of spinning disks arises from such diverse areas as turbine rotor dynamics, circular saw vibrations, and stability of computer disk memory units. The study of turbine rotor and circular saw vibrations deals mainly with the response of a rotating disk to external transverse forces. It has been shown that such a system becomes unstable at certain speeds of rotation. These critical speeds depend only upon the natural frequencies of vibration of the disk. For the disk memory analysis, the interaction of the recording head of the disk memory with the surface of the disk requires the mass of the recording head to enter the analysis. If the mass of the load is included in the analysis, instabilities can occur at speeds other than the critical speeds of free vibration.

The physical system investigated here is that of the rotating disk memory. The system consists of a thin metal disk spinning at high speed, upon which information is recorded by means of a recording head. An air bearing separates the recording head from the disk, and the head is attached to the supporting frame by a mounting of some type. The stiffness of the air bearing is much greater than that of the restraint, so that the displacement of the head is essentially equal to the transverse deflection of the disk.

The early work on the vibration of spinning elastic disks concentrated on determining the natural frequencies of vibration of such disks [1 - 4], and of the effect of large amplitude vibrations which introduce non-linearities [5 - 10]. The work of Lamb and

Southwell [1] is of particular value in this thesis as both an upper and lower bound for the natural frequencies of the spinning disk are obtained. Lamb and Southwell show that the natural frequencies of vibration of the spinning disk are given as combinations of terms arising from the centrifugal stress of the rotation and the bending stress of the disk. If bending stresses are ignored the natural frequencies are those of a spinning membrane [11 - 14].

When centrifugal stresses are ignored the natural frequencies of a rotating disk becomes those of a stationary disk. The rotating disk appears as a stationary disk with a moving load in a reference frame fixed in the disk. The vibration of stationary circular disks was studied by Southwell [2] in which the natural frequencies of vibration of the disk are obtained. The topic of moving loads in general is studied by Hegemeir [15] and, with respect to circular plates, by Iwan and Stahl [16], Stahl and Iwan [17], Stahl [18] and Mote [19]. In Iwan and Stahl [16], the load consists of a mass-spring-dashpot system which moves in concentric circles about an elastic disk. An eigenfunction expansion is used to show that instabilities due to the mass, spring, and dashpot of the load occur at certain speeds.

The use of direct stability methods for continuous systems is advantageous since it yields exact results. The direct stability methods of Liapunov have been applied to continuous systems in general theorems put forth by Movchan [20] [21], summarized in Knopps [22], and analyzed for the case of load damping by Caughey and

Dickerson [23], Lee Hsu [24], and D'Souza [25]. Examples of the use of these direct methods in the case of vibrating elastic systems are given by Movchan [21] and Hegemeier [26]. One objective of the present analysis is to use direct stability techniques to demonstrate the stability of the spinning disk system at low speeds of rotation.

Since the direct stability methods fail to yield results for speeds of rotation above certain critical speeds, Galerkin's method is used to study the stability of the spinning disk system at high rates of rotation. Galerkin's method is put forth in many sources such as Mikhlin [27];[28] [29]. The method is applied to physical systems in numerous cases, however of particular interest here is its use in stability analysis.

In Chapter II of this thesis, the partial differential equation of motion of the spinning disk is derived and Galerkin's method is used to obtain an approximate system of equations. The finite mode approximation used with Galerkin's method employs radial eigenfunctions approximating the modes of the freely spinning disk. These approximate eigenfunctions are used in Rayleigh's method to obtain approximate natural frequencies.

Chapters III and IV analyze a truncated system of equations for the spinning disk. First, the single mode system is analyzed to determine if there exist values of angular rotation for which an unstable solution exists. The stiffness of the load causes an unstable solution for an interval of speeds above the critical speed. The mass

and damping of the load are shown to cause terminal instabilities. The multiple mode system exhibits yet another type of instability caused by interaction of the modes. In these two chapters the primary means of presenting the information for the spinning disk is by using the Frequency-Speed diagram. Tobias [6], Iwan and Stahl [16], Stahl [18] and Mote [19], have also used such diagrams in their analysis. The diagrams give the magnitude of the imaginary and real part of the approximate eigenvalues as a function of a normalized angular rotation.

In Chapter V, the approximate radial eigenfunctions of the spinning disk are used to develop a system of equations for a stationary disk with a load system moving in a circular path on the disk. The work of Iwan and Stahl [16] is used as a comparison to establish the effect of using approximate eigenfunctions. In Iwan and Stahl [16], a complete set of eigenfunctions which satisfied all the boundary conditions of the problem were used. Also, comparison with the work of Chapters III and IV is made to determine the effect of the centrifugal stresses in the disk.

In Chapter VI, the direct stability method of Liapunov is used to show that both the spinning and stationary disk are stable below certain critical speeds. An error bound theory is developed for the approximate eigenvalues of infinite matrices. The theory is applied to the spinning disk problem to verify that there exist eigenvalues of the full infinite system with positive real parts, thus making the solution to the full infinite system of equations unstable.

II. FORMULATION

2.1 Introduction

In this chapter, the equation of motion is derived for the transverse vibrations of a spinning elastic disk with massive loading. Galerkin's method is then used to convert the partial differential equation of motion to a system of ordinary differential equations.

The equation of motion has variable coefficients and involves operators arising from both the bending stress of the disk and the centrifugal stress due to the rotation of the disk.

In a fixed inertial reference frame, the system of ordinary differential equations that results from applying Galerkin's method has constant coefficients. By assuming that vibrations occur in only a finite number of modes, a finite set of constant coefficient ordinary differential equations results. These are analyzed by elementary techniques.

The expansion functions used in the Galerkin technique of this analysis are functions which closely approximate the mode shapes of the freely spinning disk.

2.2 Equation of Motion

Consider the physical system consisting of a spinning elastic axisymmetric disk moving in contact with a stationary mass, spring, and dashpot system. The mass is assumed to be in intimate contact

with the surface of the disk and the spring and dashpot are attached to a fixed support above the disk. The entire system is shown in Figure 1.

Let the spinning elastic disk be described in a reference frame R which is rotating with the disk. Let the polar coordinates of R be (r, θ). The equation of motion of the spinning axisymmetric elastic disk in the coordinates (r, θ) is:

$$\rho h u_{tt} + \frac{Eh^3}{2(1-\nu^2)} \nabla^4 u - \frac{h}{r}[P r u_r]_r - \frac{h}{r^2} Q u_{\theta\theta} = 0 \qquad (2.1)$$

The function $u = u(r, \theta, t)$ is the transverse displacement of the point (r, θ) on the disk at time t, and the system parameters are given by:

$$\left.\begin{aligned} P &= A(a^2 - r^2)\rho\Omega^2 \\ Q &= \left(Aa^2 - Br^2\right)\rho\Omega^2 \\ A &= \frac{1}{8}(3+\nu) \\ B &= \frac{1}{8}(1+3\nu) \\ a &= \text{outer radius of disk} \\ \Omega &= \text{angular velocity of disk} \\ \rho &= \text{density of disk} \\ h &= \text{thickness of disk} \end{aligned}\right\} \qquad (2.2)$$

The geometric boundary conditions at $r = 0$ are:

$$u = 0 \;\; ; \;\; u_r = 0 \qquad (2.3)$$

The natural boundary conditions at $r = a$ are

$$B_1 u = 0 \;\; ; \;\; B_2 u = 0 \qquad (2.4)$$

with,

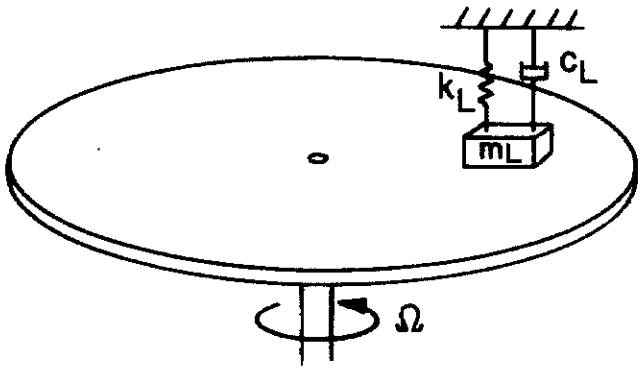

Fig. 1. System Configuration.

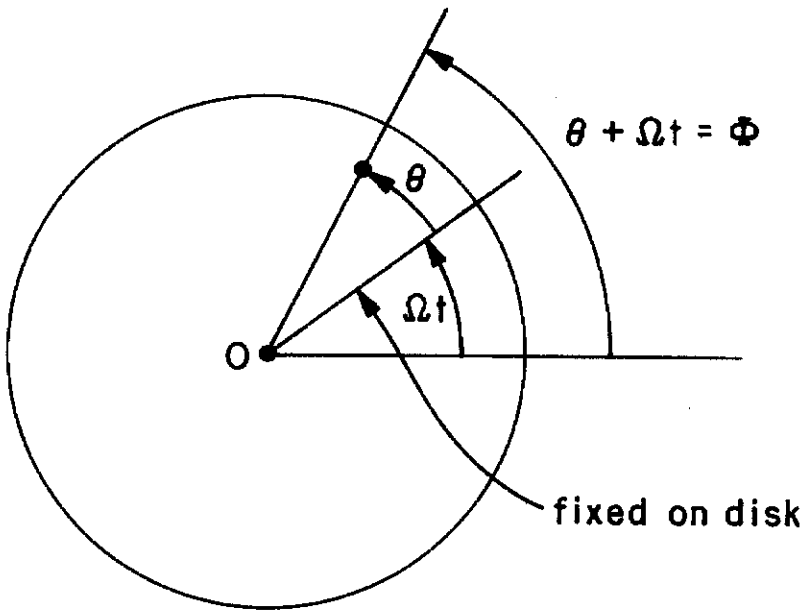

Fig. 2. Angular velocity relationship.

$$B_1 u = \frac{Eh^2}{3(1-\nu^2)}\left[\frac{\partial}{\partial r}(\nabla^2 u) + \frac{1-\nu}{r^2}\frac{\partial^2}{\partial \theta^2}\left(\frac{\partial u}{\partial r} - \frac{1}{r}u\right)\right]$$

$$B_2 u = \frac{Eh^2}{3(1-\nu^2)}\left[\frac{\partial^2 u}{\partial r^2} + \nu\left(\frac{1}{r}\frac{\partial u}{\partial r} + \frac{1}{r^2}\frac{\partial^2 u}{\partial \theta^2}\right)\right] \qquad (2.5)$$

Let the initial conditions be:

$$\left.\begin{aligned} u(r, \theta, 0) &= W_1(r, \theta) \\ u_t(r, \theta, 0) &= W_2(r, \theta) \end{aligned}\right\} \quad \forall r \in [0, a] \text{ and } \forall \theta \in [0, 2\pi] \qquad (2.6)$$

The equation of motion of the spinning disk (2.1) is defined $\forall t > 0$ and $(r, \theta) \in D$, where D is the region of the disk given by:

$$D = \{(r, \theta) \mid 0 \leq r \leq a \ , \ 0 \leq \theta \leq 2\pi\} \qquad (2.7)$$

The equation of motion is now written in a fixed reference frame. Let the reference frame F have the same origin as the frame R and the unit vectors $\{\underset{\sim}{e}_1, \underset{\sim}{e}_2, \underset{\sim}{e}_3\}$ such that the frame R rotates with respect to F with angular velocity $\Omega \underset{\sim}{e}_3$.

In the reference frame F, the region of the disk becomes:

$$D_t = \{(r, \Phi) \mid 0 \leq r \leq a \ , \ \Omega t \leq \Phi \leq \Omega t + 2\pi\} \qquad (2.8)$$

The relationship between the angular coordinates of the frame R and F is shown in Figure 2. Using the angular velocity relationship of the two reference frames, the angular polar coordinate Φ of a material point on the disk can be written in terms of θ as:

$$\Phi = \theta - \Omega t \quad \forall t \in [0, \infty) \text{ and } \forall \theta \in [0, 2\pi] \qquad (2.9)$$

To rewrite Equation (2.1) in terms of the polar coordinates of frame F the following relationships are needed:

$$\left.\begin{aligned}
&\hat{u} = \hat{u}(r, \Phi, t) = u(r, \theta - \Omega t, t) \\
&\frac{\partial u}{\partial r} = \frac{\partial \hat{u}}{\partial r} \quad ; \quad \frac{\partial^2 u}{\partial r^2} = \frac{\partial^2 \hat{u}}{\partial r^2} \quad ; \\
&\frac{\partial u}{\partial \theta} = \frac{\partial \hat{u}}{\partial \Phi}\frac{\partial \Phi}{\partial \theta} = \frac{\partial \hat{u}}{\partial \Phi} \quad ; \quad \frac{\partial^2 u}{\partial \Phi^2} = \frac{\partial^2 \hat{u}}{\partial \Phi^2} \\
&\frac{\partial^2 u}{\partial t^2} = \frac{\partial^2 \hat{u}}{\partial t^2} - 2\Omega \frac{\partial^2 \hat{u}}{\partial t \partial \Phi} + \Omega^2 \frac{\partial^2 \hat{u}}{\partial \Phi^2}
\end{aligned}\right\} \qquad (2.10)$$

Using (2.10), the equation of motion (2.1) is now written in frame F as:

$$\left.\begin{aligned}
&\rho h\left[\hat{u}_{tt} - 2\Omega \hat{u}_{t\Phi} + \Omega^2 \hat{u}_{\Phi\Phi}\right] + h\left[L_1(\hat{u}) + L_2(\hat{u})\right] = 0 \\
&\text{with} \\
&r \in [0, a] \quad , \quad \Phi \in [\Omega t, \Omega t + 2\pi] \quad , \quad t \in [0, \infty) \quad ,
\end{aligned}\right\} \qquad (2.11)$$

and

$$\left.\begin{aligned}
&L_1(\hat{u}) = -\frac{1}{r}\left[Pr\, \hat{u}_r\right]_r - \frac{\Omega}{r^2}\hat{u}_{\Phi\Phi} \\
&L_2(\hat{u}) = \frac{Eh^2}{3(1-\nu^2)}\nabla^4 \hat{u}
\end{aligned}\right\} \qquad (2.12)$$

The geometric boundary conditions (2.4) become:

$$\hat{u}(0, \Phi, t) = \hat{u}_r(0, \Phi, t) = 0 \qquad \forall \Phi \in [\Omega t, \Omega t + 2\pi] \quad , \quad \forall t \in [0, \infty) \qquad (2.13)$$

$$\hat{u}(r, \Phi, t) = \hat{u}(r, \Phi + 2\pi, t) \qquad \forall r \in [0, a] \quad , \quad \forall \Phi \in [\Omega t, \Omega t + 2\pi] \qquad (2.14)$$

The periodic condition given by (2.14) implies that a solution to (2.1) with $0 \le \Phi \le 2\pi$ will also be a solution under the condition (2.14). Thus it is sufficient to consider the problem (2.11) with Φ such that $0 \le \Phi < 2\pi$, i.e.

$$\left.\begin{aligned}
&\rho h\left[\hat{u}_{tt} - 2\Omega \hat{u}_{t\Phi} + \Omega^2 \hat{u}_{\Phi\Phi}\right] + h\left[L_1(\hat{u}) + L_2(\hat{u})\right] = 0
\end{aligned}\right\} \qquad (2.15)$$

with

$$r \in [0, a] \;\; ; \;\; \Phi \in [0, 2\pi] \;\; ; \;\; t \in [0, \infty) \qquad \Big\} \qquad (2.15)\ \text{cont.}$$

To simplify notation in the subsequent analysis, $\hat{u}(r, \Phi, t)$ with $r \in [0, a]$, $\Phi \in [0, 2\pi]$, and $t \in [0, \infty)$ shall be given by $u(r, \Phi, t)$.

The effect of the loading system is now introduced. The force exerted by the load on the disk is given by

$$f(t) = m_L \ddot{z}(t) + c_L \dot{z}(t) + k_L z(t) \qquad (2.16)$$

where $z(t)$ is the vertical displacement of the load as shown in Fig. 1, and m_L, c_L, k_L are the mass, damping coefficient, and spring constant for the load. The region of the disk on which the load acts is given by

$$D_L = \{(r, \Phi) \mid r_1 \le r \le r_2 \;,\; \Phi_1 \le \Phi \le \Phi_2\} \qquad (2.17)$$

and the area of the load is then given by

$$A_L = \frac{1}{2}\left(r_2^2 - r_1^2\right)\left(\Phi_2 - \Phi_1\right) \qquad (2.18)$$

The load area A_L is assumed to be small compared to the area of the disk.

Since the transverse displacement of the disk $u(r, \Phi, t)$ varies over the load region D_L, an approximation must be made for the function $z(t)$. The form of $z(t)$ to be used here shall be the average value of $u(r, \Phi, t)$ over the load region D_L, i.e.

$$z(t) = \frac{1}{A_L} \iint_{D_L} u(r, \Phi, t)\, dA \qquad (2.19)$$

Similar approximations are made for $\dot{z}$, and $\ddot{z}$:

$$\left.\begin{aligned} \dot{z}(t) &= \frac{1}{A_L}\iint_{D_L} u_t(r,\Phi,t)\,dA \\ \ddot{z}(t) &= \frac{1}{A_L}\iint_{D_L} u_{tt}(r,\Phi,t)\,dA \end{aligned}\right\} \tag{2.20}$$

Then the force applied to the disk is given by

$$f(t) = \frac{m_L}{A_L}\iint_{D_L} u_{tt}\,dA + \frac{c_L}{A_L}\iint_{D_L} u_t\,dA + \frac{k_L}{A_L}\iint_{D_L} u\,dA \tag{2.21}$$

The equation of motion for a spinning disk with an applied load is given by

$$\rho h\left[u_{tt} - 2\Omega u_{t\Phi} + \Omega^2 u_{\Phi\Phi}\right] + \left[L_1 + L_2\right](u) = q(r,\Phi,t) \tag{2.22}$$

where $q(r,\Phi,t)$ is the force per unit area applied to the disk. The total force $f(t)$ is related to $q(r,\Phi,t)$ by

$$f(t) = \iint_D q(r,\Phi,t)\,dA \tag{2.23}$$

A representation for $q(r,\Phi,t)$ which yields the assumed total force given by (2.21) may be given by

$$q(r,\Phi,t) = \frac{H(r,\Phi)}{A_L}\left[m_L u_{tt}(r,\Phi,t) + c_L u_t(r,\Phi,t) + k_L u(r,\Phi,t)\right] \tag{2.24}$$

with

$$H(r,\Phi) = \begin{cases} 1 & \text{if } (r,\Phi) \in D_L \\ 0 & \text{if } (r,\Phi) \notin D_L \end{cases} \tag{2.25}$$

Thus, the full equation of motion may be written as

$$\rho h\left[u_{tt} - 2\Omega u_{t\Phi} + \Omega^2 u_{\Phi\Phi}\right] + \left[L_1 + L_2\right](u) = -\frac{H(r,\Phi)}{A_L}\left[m_L u_{tt} + c_L u_t + k_L u\right] \tag{2.26}$$

In the limit as the area of the load goes to zero the force per unit area becomes:

$$q(r,\Phi,t) = \delta^*(r-r_0, \Phi-\Phi_0)[m_L u_{tt} + c_L u_t + k_L u] \tag{2.27}$$

with the point load acting at $r = r_0, \Phi = \Phi_0$ and

$$\delta^*(r-r_0, \Phi-\Phi_0) = \frac{\delta_1(r-r_0)}{r_0} \cdot \delta_2(\Phi-\Phi_0) \tag{2.28}$$

where

$$\left.\begin{aligned} &\int_0^a \frac{\delta_1(r-r_0)}{r_0}\, r\, dr = 1 \qquad \forall\, r_0 \in [0, a] \\ &\int_0^{2\pi} \delta_2(\Phi-\Phi_0)\, d\theta = 1 \qquad \forall\, \Phi_0 \in [0, 2\pi] \end{aligned}\right\} \tag{2.29}$$

$$\left.\begin{aligned} &\delta_1(r-r_0) = 0 \qquad \forall\, r \neq r_0 \\ &\delta_2(\Phi-\Phi_0) = 0 \qquad \forall\, \Phi \neq \Phi_0 \end{aligned}\right\} \tag{2.30}$$

2.3 Reduction to a System of Ordinary Differential Equations

The exact stability analysis of solutions to non-self-adjoint boundary value problems such as (2.26) is very difficult. However, an effective approximate method is to express the solution in the form of a series of coordinate functions which satisfy the boundary conditions of the problem. The partial differential equation can then be reduced

to a system of ordinary differential equations. The technique to be used here is Galerkin's method.

2.3.1 Galerkin's Method

Consider the partial differential equation given by

$$\mathcal{L}u(\underset{\sim}{x},t) + u_{tt}(\underset{\sim}{x},t) = f(\underset{\sim}{x},t) \qquad \forall \underset{\sim}{x} \in R \text{ and } \forall t \in [0,\infty) \tag{2.31}$$

where R is a two dimensional region, and $\mathcal{L}$ is a differential operator (not necessarily linear).

The linear homogeneous boundary conditions are given by

$$Bu(\underset{\sim}{x},t) = 0 \quad \text{on} \quad \partial R \times T \tag{2.32}$$

and the initial conditions are

$$\left.\begin{aligned} u(\underset{\sim}{x},0) &= U(\underset{\sim}{x}) \quad \text{on} \quad R \\ u_t(\underset{\sim}{x},0) &= V(\underset{\sim}{x}) \quad \text{on} \quad R \end{aligned}\right\} \tag{2.33}$$

The function u is defined in an inner product space H with inner product given by

$$\langle v,w \rangle = \iint_D v(\underset{\sim}{x},t)\, w(\underset{\sim}{x},t)\, dA \qquad \forall v,w \in C^2(R \times T) \tag{2.34}$$

An approximate solution to (2.31) is sought in the form

$$u_n(\underset{\sim}{x},t) = \sum_{k,\ell=1}^{n} a_{k\ell}(t)\, \varphi_{k\ell}(\underset{\sim}{x}) \quad \text{on} \quad R \times T \tag{2.35}$$

Here the $\varphi_{k\ell}$ are coordinate functions which satisfy the homogeneous boundary conditions and the $a_{k\ell}$ are to be determined. While the function $u_n(\underset{\sim}{x},t)$ certainly satisfies the boundary conditions (2.32) it does not in general satisfy the equation (2.31). Thus,

$$u_{n,tt}(\underset{\sim}{x},t) + \mathcal{L}u_n(\underset{\sim}{x},t) - f(\underset{\sim}{x},t) = R_n(\underset{\sim}{x},t) \tag{2.36}$$

where R_n is the error function corresponding to the approximate solution u_n.

Galerkin's method for reducing (2.31) to a system of ordinary differential equations is to require that the $a_{k\ell}$ functions be chosen such that R_n is orthogonal to each of the $\varphi_{k\ell}$; $k, \ell = 1, \ldots n$ in the sense that

$$\langle R_n, \varphi_{k\ell} \rangle = 0 \quad \forall\ k, \ell = 1, \ldots, n \tag{2.37}$$

The Galerkin requirement (2.37) assumes that the solution to the original equation can be represented by a series of the form

$$u(\underset{\sim}{x},t) = \sum_{k,\ell=1}^{\infty} a_{k\ell}(t)\varphi_{k\ell}(\underset{\sim}{x},t) \tag{2.38}$$

If (2.37) holds true as $n \to \infty$, then it follows that

$$\lim_{n\to\infty} R_n = 0 \tag{2.39}$$

Suppose further that the operator $\mathcal{L}$ is such that

$$\mathcal{L}(u_n) \to \mathcal{L}(u) \quad \text{as} \quad n \to \infty \tag{2.40}$$

Then (2.39), (2.40) imply that the function $u(\underset{\sim}{x},t)$ defined by (2.38) solves (2.31).

To obtain the system of ordinary differential equations corresponding to (2.37) substitution for R_n is made to obtain

$$\langle (u_{n,tt} + \mathcal{L}u_n - f), \varphi_{ij} \rangle = 0 \quad \forall\ i,j = 1, \ldots, n \tag{2.41}$$

Substitution for u_n from (2.35) yields the system of equations:

$$\left.\begin{aligned} \ddot{a}_{ij}+\nu_{ij} &= \langle f, \varphi_{ij}\rangle \qquad \forall\ i,j = 1,\ldots,n \\ \text{with} \qquad & \\ \nu_{ij} &= \langle \mathcal{L}u_n, \varphi_{ij}\rangle \end{aligned}\right\} \tag{2.42}$$

Note that the form of (2.42) does not depend on $\mathcal{L}$ being linear. If $\mathcal{L}$ is a linear operator however, then

$$\nu_{ij} = \sum_{k,\ell=1}^{n} a_{k\ell}(t)\langle \mathcal{L}\varphi_{k\ell}, \varphi_{ij}\rangle \tag{2.43}$$

and the system (2.42) can be written

$$\ddot{a}_{ij} + \sum_{k,\ell=1}^{n} b_{ijk\ell}\, a_{k\ell} = f_{ij} \qquad \forall i, j = 1,\ldots,n \tag{2.44}$$

with

$$\left.\begin{aligned} b_{ijk\ell} &= \langle \mathcal{L}\varphi_{k\ell}, \varphi_{ij}\rangle \\ f_{ij} &= \langle f, \varphi_{ij}\rangle \end{aligned}\right\} \tag{2.45}$$

To write the equation of motion given by (2.27) as a system of ordinary differential equations, let

$$\left.\begin{aligned} \mathcal{L}(u) &= \left[u_{tt} - 2\Omega u_{t\Phi} + \Omega^2 u_{\Phi\Phi}\right] + L_1 u + L_2 u \\ \eta(u) &= -\frac{H(r,\Phi)}{\rho h A_L}\left[m_L u_{tt} + c_L u_t + k_L u\right] \end{aligned}\right\} \tag{2.46}$$

with L_1 and L_2 given by (2.12) and H and A_L given by (2.25) and (2.18) respectively. The equation of motion (2.31) then becomes

$$\mathcal{L}(u) = \eta(u) \quad ; \quad u = u(r,\Phi,t) \tag{2.47}$$

Let the solution be written as an eigenfunction expansion of the form

$$u(r,\Phi,t) = \sum_{\ell,\, n=1}^{N} [T_{\ell n}(t) \cdot \Psi_{\ell n}(r,\Phi)] \tag{2.48}$$

with $\{\Psi_{\ell n}\}_{\ell,\, n=1}^{\infty}$ a set of orthogonal eigenfunctions of the operator $(L_1 + L_2)$.

Let the inner product on the region of the disk be defined by

$$\langle u,v\rangle = \frac{1}{\pi} \iint_D u(r,\Phi)\, v(r,\Phi)\, dA \quad \forall\, u,v \text{ continuous on region of disk}$$

$$= \frac{1}{\pi} \int_0^{2\pi} \int_0^a u(r,\Phi)\, v(r,\Phi)\, r\, dr\, d\Phi \ , \tag{2.49}$$

The condition (2.36) implies

$$\langle \mathcal{L}(u) - \mathcal{N}(u), \Psi_{\ell n}\rangle = 0 \qquad \forall\, \ell, n = 1,2,\ldots \tag{2.50}$$

Assume that the eigenfunctions $\Psi_{\ell n}$ are separable in r and Φ and let $\{\Psi_{\ell n}\}_{\ell,n=1}^{\infty}$ be the union of

$$\{\cos(n\Phi)\, R_{\ell n}(r)\}_{\ell,n=0}^{\infty} \quad \text{and} \quad \{\sin(n\Phi)\, R_{\ell n}(r)\}_{\ell,n=0}^{\infty} \tag{2.51}$$

with the functions $\{R_{\ell n}\}_{\ell,n=0}^{\infty}$ yet to be determined. Then

$$u(r,\Phi,t) = \sum_{i,j=1}^{N} [A_{ij}(t) R_{ij}(r) \cos j\Phi + B_{ij}(t) R_{ij}(r) \sin j\Phi] \tag{2.52}$$

Using (2.52) in relation (2.50) then yields

$$\left.\begin{aligned}\langle \mathcal{L}(u)-\mathcal{N}(u)\,,\, R_{\ell n}(r)\cos n\Phi\rangle &= 0 \\ \langle \mathcal{L}(u)-\mathcal{N}(u)\,,\, R_{\ell n}(r)\sin n\Phi\rangle &= 0\end{aligned}\right\} \qquad \forall\,\ell,n=0,1,\ldots N \tag{2.53}$$

(2.54)

Expanding (2.53) using (2.46) then implies

$$\langle (u_{tt}-2\Omega u_{t\Phi}+\Omega^2 u_{\Phi\Phi})\,,\, R_{\ell n}(r)\cos n\Phi\rangle + \langle (L_1 u+L_2 u)\,,\, R_{\ell n}(r)\cos n\Phi\rangle$$

$$+\langle \mathcal{N}(u)\,,\, R_{\ell n}(r)\cos n\Phi\rangle = 0 \qquad \forall\,\ell,n=0,1,\ldots N \tag{2.55}$$

Substituting the assumed solution (2.48) in (2.53) gives

$$\ddot{A}_{\ell n}-2\Omega n\dot{B}_{\ell n}+\Omega^2 n^2 A_{\ell n}+\sum_{i,j=1}^{N}\lambda_{ij\ell n}A_{ij}$$

$$+\sum_{i,j=1}^{N}G^{(cc)}_{ij\ell n}\left[m_L\ddot{A}_{ij}+c_L\dot{A}_{ij}+k_L A_{ij}\right]$$

$$+\sum_{i,j=1}^{N}G^{(sc)}_{ij\ell n}\left[m_L\ddot{B}_{ij}+c_L\dot{B}_{ij}+k_L B_{ij}\right]=0 \qquad \forall\,\ell,n=1,\ldots,N \tag{2.56}$$

with

$$\left.\begin{aligned}\lambda_{ij\ell n} &= \langle (L_1+L_2)(R_{ij}(r)\cos j\Phi)\,,\, R_{\ell n}(r)\cos n\Phi\rangle \\ G^{cc}_{ij\ell n} &= \langle \frac{H(r,\Phi)}{\rho h A_L}R_{ij}(r)\cos j\Phi\,,\, R_{\ell n}(r)\cos n\Phi\rangle \\ G^{sc}_{ij\ell n} &= \langle \frac{H(r,\Phi)}{\rho h A_L}R_{ij}(r)\sin j\Phi\,,\, R_{\ell n}(r)\cos n\Phi\rangle\end{aligned}\right\} \tag{2.57}$$

and the initial conditions

$$\left.\begin{aligned}A_{\ell n}(0) &= w^{(1)}_{\ell n} \\ B_{\ell n}(0) &= w^{(2)}_{\ell n}\end{aligned}\right\} \tag{2.58}$$

where $w_{\ell n}^{(1)}$ and $w_{\ell n}^{(2)}$ are such that

$$\left.\begin{aligned} U(r,\Phi) &= \sum_{\ell,n=1}^{N} w_{\ell n}^{(1)} R_{\ell n} \cos n\Phi \\ V(r,\Phi) &= \sum_{\ell,n=1}^{N} w_{\ell n}^{(2)} R_{\ell n} \sin n\Phi \end{aligned}\right\} \qquad (2.59)$$

Similarly, the requirement (2.54) yields the system

$$\begin{aligned} &\ddot{B}_{\ell n} + 2\Omega n \dot{A}_{\ell n} + \Omega^2 n^2 B_{\ell n} \\ &+ \sum_{i,j=1}^{N} \lambda_{ij\ell n} B_{ij} + \sum_{i,j=1}^{N} G_{ij\ell n}^{(cs)} [m_L \ddot{A}_{ij} + c_L \dot{A}_{ij} + k_L A_{ij}] \\ &+ \sum_{i,j=1}^{N} G_{ij\ell n}^{(ss)} [m_L \ddot{B}_{ij} + c_L \dot{B}_{ij} + k_L B_{ij}] = 0 \qquad \forall \ell,n=0,1,\ldots N \end{aligned} \qquad (2.60)$$

with

$$\left.\begin{aligned} \lambda_{ijk\ell} &= \langle (L_1+L_2)(R_{ij}(r)\cos j\Phi), R_{\ell n}(r)\cos n\Phi \rangle \\ G_{ij\ell n}^{(cs)} &= \langle \frac{H(r,\Phi)}{\rho h A_L} R_{ij}(r)\cos j\Phi , R_{\ell n}(r)\sin n\Phi \rangle \\ G_{ij\ell n}^{(ss)} &= \langle \frac{H(r,\Phi)}{\rho h A_L} R_{ij}(r)\sin j\Phi , R_{\ell n}(r)\sin n\Phi \rangle \end{aligned}\right\} \qquad (2.61)$$

The set of equations defined by (2.56) and (2.60) will be referred to as the "N-mode system" corresponding to the equation (2.46) and the eigenfunctions $\{\psi_{ij}\}_{i,j=1}^{N}$.

2.3.2 The Approximate Radial Eigenfunctions

The eigenvalue problem which generates the raidal eigenfunctions $\left\{R_{\ell n}\right\}_{\ell,n=0}^{\infty}$ is derived by substituting

$$u(r,\Phi,t) = e^{i\mu_{\ell n}t} R_{\ell n}(r) \cos n\Phi \tag{2.62}$$

into the partial differential equation

$$u_{tt} + (L_1 + L_2)(u) = 0 \tag{2.63}$$

with L_1 and L_2 given by (2.12), and the boundary conditions

$$\left.\begin{aligned} \hat{B}_1(R_{\ell n}) = B_1(R_{\ell n}(r)\cos n\Phi) = 0 \quad \text{at} \quad r = a \\ \hat{B}_2(R_{\ell n}) = B_2(R_{\ell n}(r)\cos n\Phi) = 0 \quad \text{at} \quad r = a \end{aligned}\right\} \tag{2.64}$$

where B_1 and B_2 are given by (2.5) and

$$\left.\begin{aligned} R_{\ell n} = 0 \quad \text{at} \quad r = 0 \\ \frac{d}{dr} R_{\ell n} = 0 \quad \text{at} \quad r = 0 \end{aligned}\right\} \tag{2.65}$$

Using (2.62) in (2.63) gives the eigenvalue problem

$$L_r^{(n)}(R_{\ell n}) = \mu_{\ell n}^2 R_{\ell n} \tag{2.66}$$

with

$$L_r^{(n)} = \left\{\left[\frac{d^2}{dr^2} + \frac{1}{r}\frac{d}{dr} - \frac{n^2}{r^2}\right]^2 - P\frac{d^2}{dr^2} + \frac{\Omega}{r^2}n^2\right\} \tag{2.67}$$

As shown by Lamb and Southwell [1], the modes of a spinning elastic disk are characterized by both modal circles and modal diameters. In the present analysis, the load system has no radial motion.

For this reason, it is felt here that the most significant behavior of the system will be obtained from an assumed solution that has zero modal circles. Thus, only $\{R_{0n}\}_{n=0}^{\infty}$ will be used in the assumed expansion of the solution.

The eigenfunctions $\{R_{0n}\}_{n=0}^{\infty}$ are solutions of Equation (2.66) together with the boundary conditions (2.65). A closed form algebraic expression for the solution of (2.66) is very difficult to obtain. Thus recourse is made to an approximation of the eigenfunctions.

Since the operator $L_r^{(n)}$ of Equation (2.67) is an ordinary differential operator with respect to r, Rayleigh's method can be used to determine approximate eigenvalues μ_{0n}, n=1,2,..., i.e.

$$(\mu_{0n})^2 = \min_{R \in G} V_n(R) \tag{2.68}$$

where

$$G = \left\{R(r) \,|\, R(0) = R'(0) = 0,\ R \in C^2[0,a] \text{ and } \iint_D \cos^2 n\Phi\, R^2(r)\, dA = 1\right\} \tag{2.69}$$

$$V_n(R) = V_1(\cos n\Phi\, R(r)) + V_2(\cos n\Phi\, R(r)) \tag{2.70}$$

with

$$V_1(u) = \iint_D \left\{P\left(\frac{\partial u}{\partial r}\right)^2 + \frac{Q}{r^2}\left(\frac{\partial u}{\partial \Phi}\right)^2\right\} dA \tag{2.71}$$

and

$$V_2(u) = \frac{Eh^3}{3(1-\nu)} \iint_D \left\{(\nabla^2 u)^2 + 2(1-\nu)(u_{xy} - u_{xx}u_{yy})\right\} dA \tag{2.72}$$

where

$$u_{xy}-u_{xx}u_{yy}=\left(\frac{1}{r}\frac{\partial^2 u}{\partial r\partial\Phi}-\frac{1}{r^2}\frac{\partial u}{\partial\Phi}\right)^2-\frac{\partial^2 u}{\partial r^2}\left(\frac{1}{r^2}\frac{\partial^2 u}{\partial r^2}+\frac{1}{r}\frac{\partial u}{\partial r}\right) \tag{2.73}$$

Let

$$\mathcal{G}_1=\left\{p_n\in\mathcal{G}\,|\,p_n=\left(1+\beta_n r^2\right)r^n \text{ with } \beta_n \text{ real}\right\} \tag{2.74}$$

Furthermore, let the approximate eigenfunction be called $\tilde{R}_n$ and let

$$\tilde{R}_n=\left(1+\beta_n^* r^2\right)r^n \qquad n=1,2,\ldots \tag{2.75}$$

with β_n^* chosen such that

$$V_n(\tilde{R})=\min_{p\in\mathcal{G}_1} V_n(P) \qquad n=1,2,\ldots \tag{2.76}$$

Then $\tilde{R}_n$ gives the best approximation to the radial eigenfunction over all functions in the class $\mathcal{G}_1$. The approximate eigenvalues obtained from $\tilde{R}_n$ are

$$(\tilde{\mu}_{0n})^2=V_n(\tilde{R}_n) \qquad n=1,2,\ldots \tag{2.77}$$

The accuracy of these approximate eigenfunctions is evaluated on the basis of how close the approximate eigenvalues are to exact eigenvalues. This topic is discussed next. For each $n=1,2,3$ approximate radial eigenfunctions have been obtained. They are shown in Figure 3.

In order to indicate the accuracy of the approximate radial eigenfunctions $\tilde{R}_n$, they will be used in Rayleigh's method to determine an upper bound for the square of the natural frequency μ_n of the operator (L_1+L_2). Then a lower bound for μ_n^2 is determined as

$$\left(\mu_n^{ub}\right)^2=V_n(\tilde{R}_n) \tag{2.78}$$

where $V_n(\tilde{R}_n)$ is given by (2.70).

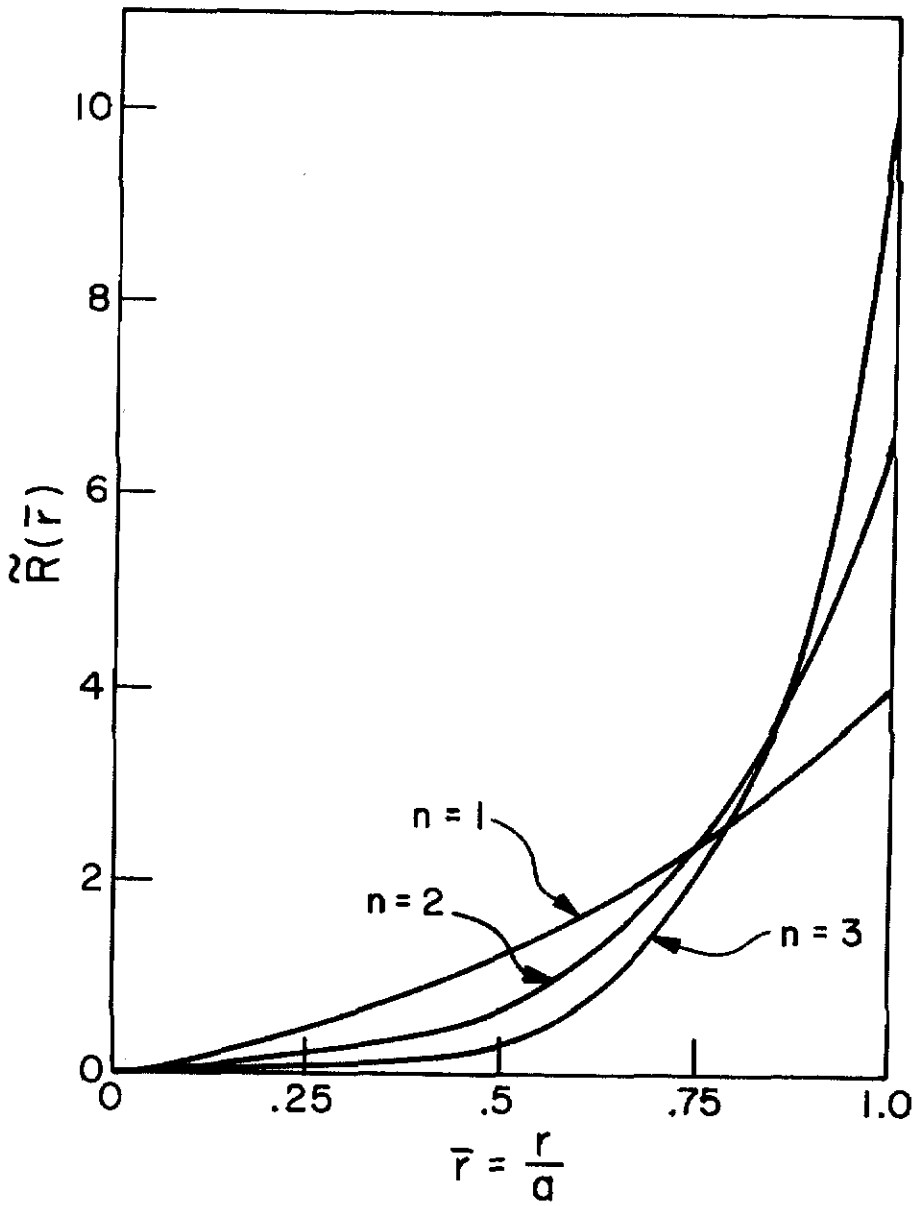

Fig. 3. Approximate radial eigenfunctions.

The lower bound for μ_n^2 is obtained using the fact that the sum of the squares of the natural frequencies of the operators L_1 and L_2 are a lower bound for the square of the natural frequency of $(L_1 + L_2)$. To show this let w_1, w_2 and w^* be such that

$$\min_{w \in G} \left\{ V_1^{(n)}(w \cos n\Phi) \right\} = V_1^{(n)}(w_1 \cos n\Phi) = \left(P_1^n\right)^2 \tag{2.79}$$

$$\min_{w \in G} \left\{ V_2^{(n)}(w \cos n\Phi) \right\} = V_2^{(n)}(w_2 \cos n\Phi) = \left(P_2^n\right)^2 \tag{2.80}$$

$$\min_{w \in G} \left\{ V_n(w) \right\} = V_n(w^*) = \mu_n^2 \tag{2.81}$$

with V_1 and V_2 given by (2.71) and (2.72) and

$$G = \left\{ w \in C^2[0,1] \mid w = w_r = 0 \text{ at } r = 0 \; ; \; \int_0^1 w^2 r \, dr = 1 \right\} \tag{2.82}$$

Since $w^* \neq w_1$, Rayleigh's principle implies

$$V_1^n(w^*) > V_1^n(w_1) = \left(P_1^n\right)^2 \tag{2.83}$$

Similarly,

$$V_2^n(w^*) > V_2^n(w_2) = \left(P_2^n\right)^2 \tag{2.84}$$

Now (2.83) and (2.84) together with (2.81) imply

$$\mu_n^2 > \left(P_1^n\right)^2 + \left(P_2^n\right)^2 \tag{2.85}$$

The lower bound to μ_n^2 defined by (2.85) can be combined with the upper bound given by Relation (2.81) to obtain

$$\left(\mu_n^{ub}\right)^2 \geq \left(\mu_n\right)^2 \geq \left(P_1^n\right)^2 + \left(P_2^n\right)^2 \tag{2.86}$$

The values of $\left(P_1^n\right)^2$ and $\left(P_2^n\right)^2$ are known to be

$$\left(P_1^n\right)^2 = \lambda_n \Omega^2 \tag{2.87}$$

and

$$\left(P_2^n\right)^2 = \xi_n^4 \frac{Eh^2}{3\rho(1-\nu^2)} \tag{2.88}$$

where λ_n and ξ_n are given in Table 2.1. The upper and lower bounds for μ_n^2 defined by (2.86) are shown in Figure 4 as a function of Ω for the case $n = 2$. In the subsequent analysis, the lower bound to μ_n^2 defined by (2.86) shall be referred to as $(\tilde{\mu}_n)^2$ and given by

$$\tilde{\mu}_n^2 = \left(P_1^n\right)^2 + \left(P_2^n\right)^2 \tag{2.89}$$

	n=1	n=2	n=3	n=4
λ_n	1.00	2.35	4.05	6.16
ξ_n	1.01	2.29	3.50	4.64

Table 2.1. Values of λ_n and ξ_n.

2.3.3 The System of Ordinary Differential Equations

Using the approximate radial eigenfunctions, an approximate solution can be defined as

$$\tilde{u}(r,\phi,t) = \sum_{n=1}^{N} [A_n(t) \cos n\phi + B_n(t) \sin n\phi] \tilde{R}_n(r) \tag{2.90}$$

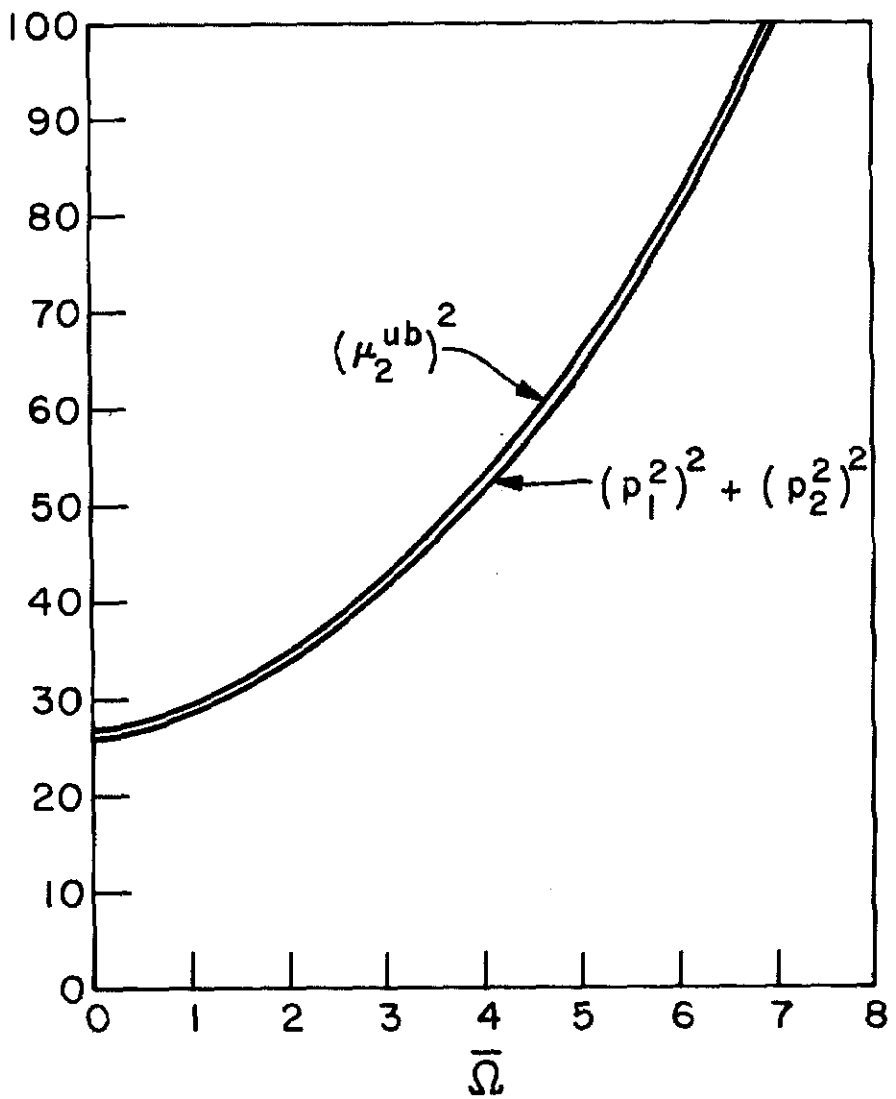

Fig. 4. Upper and lower bounds for the natural frequency of a spinning disk.

Limiting the approximate solution to a finite number of modes and using the approximate radial eigenfunctions $\tilde{R}(r)$ which satisfy only the geometric boundary conditions results in an approximate solution for the equation of motion. However, the use of a finite number of modes and the approximate radial eigenfunctions does not change the qualitative nature of the stability analysis. This will be shown in Chapter 5 by comparison with results using exact eigenfunctions. Using the assumed solution (2.90) in the equation of motion (2.27) and applying the Galerkin requirement (2.36) yields

$$\ddot{A}_n - 2\Omega n \dot{B}_n + \Omega^2 n^2 A_n + \sum_{\ell=1}^{N} \lambda_{\ell n} A_\ell + \sum_{\ell=1}^{N} \tilde{G}^{cc}_{\ell n} [m_L \ddot{A}_\ell + c_L \dot{A}_\ell + k_L A_\ell] + \sum_{\ell=1}^{N} \tilde{G}^{sc}_{\ell n} [m_L \ddot{B}_\ell + c_L \dot{B}_\ell + k_L B_\ell] = 0 \qquad \forall\, n = 1,\ldots,N \qquad (2.91)$$

and

$$\ddot{B}_n + 2\Omega n \dot{A}_n + \Omega^2 n^2 B_n + \sum_{\ell=1}^{N} \lambda_{\ell n} B_n + \sum_{\ell=1}^{N} \tilde{G}^{cs}_{\ell n} [m_L \ddot{A}_\ell + c_L \dot{A}_\ell + k_L A_L] + \sum_{\ell=1}^{N} \tilde{G}^{ss}_{\ell n} [m_L \ddot{B}_\ell + c_L \dot{B}_\ell + k_L B_L] = 0 \qquad \forall\, n = 1,\ldots,N \qquad (2.92)$$

with

$$\left.\begin{aligned}
\lambda_{\ell n} &= \langle (L_1 + L_2)(\widetilde{R}_\ell(r)\cos\ell\Phi)\ ,\ \widetilde{R}_n(r)\cos n\Phi\rangle \\
\widetilde{G}^{cc}_{\ell n} &= \langle \frac{H(r,\Phi)}{\rho h A_L}\widetilde{R}_\ell(r)\cos\ell\Phi\ ,\ \widetilde{R}_n(r)\cos n\Phi\rangle \\
\widetilde{G}^{sc}_{\ell n} &= \widetilde{G}^{cs}_{\ell n} = \langle \frac{H(r,\Phi)}{\rho h A_L}\widetilde{R}_\ell(r)\cos\ell\Phi\ ,\ \widetilde{R}_n(r)\cos n\Phi\rangle \\
\widetilde{G}^{ss}_{\ell n} &= \langle \frac{H(r,\Phi)}{\rho h A_L}\widetilde{R}_\ell(r)\sin\ell\Phi\ ,\ \widetilde{R}_n(r)\sin n\Phi\rangle
\end{aligned}\right\} \qquad (2.93)$$

By specifying the load region parameters Φ_1 and Φ_2 to be symmetric about the x-axis, the $\widetilde{G}^{sc}_{\ell n}$ and $\widetilde{G}^{cs}_{\ell n}$ terms are eliminated. To see this let

$$\left.\begin{aligned}
\Phi_1 &= -\theta_0 \\
\Phi_2 &= +\theta_0
\end{aligned}\right\} \qquad (2.94)$$

With such load region angular parameters the function $H(r,\Phi)$ becomes

$$H(r,\Phi) = \begin{cases} 1 & \text{if } \Phi\in[-\theta_0,\theta_0] \text{ and } r\in[r_1,r_2] \\ 0 & \text{otherwise} \end{cases} \qquad (2.95)$$

and $\widetilde{G}_{\ell n}$ becomes

$$\left.\begin{aligned}
\widetilde{G}^{sc}_{\ell n} &= \langle \frac{H(r,\Phi)}{\rho h A_L}\widetilde{R}_\ell(r)\sin\ell\Phi\ ,\ \widetilde{R}_n(r)\cos n\Phi\rangle \\
&= \frac{1}{\rho h A_L}\left[\int_{r_1}^{r_2}\widetilde{R}_\ell(r)\widetilde{R}_n(r)r\,dr\right]\left[\int_{-\theta_0}^{+\theta_0}\sin\ell\Phi\cos n\Phi\,d\Phi\right] \\
&= 0 \quad \forall\ \ell, n=1,\ldots,N
\end{aligned}\right\} \qquad (2.96)$$

The systems (2.91) and (2.92) can be normalized by letting

$$\left.\begin{aligned} \tau = P_2^1 t,\ \bar{\mu}_n = \frac{\mu_n}{P_2^1},\ \bar{\Omega} = \frac{\Omega}{P_2^1} \\ \bar{m}_L = m_L,\ \bar{c}_L = \frac{c_L}{P_2^1},\ \bar{k}_L = \frac{k_L}{(P_2^1)^2} \end{aligned}\right\} \tag{2.97}$$

with P_2^1 defined by (2.88). Using these normalization constants, the systems (2.91) and (2.92) may be written as a first order system of vector equations by letting

$$\underset{\sim}{Y}_n = \begin{pmatrix} \dot{A}_n(\tau) \\ \dot{B}_n(\tau) \\ A_n(\tau) \\ B_n(\tau) \end{pmatrix} \quad \forall\, \tau \in [0, \infty) \tag{2.98}$$

with $A_n(\tau)$ and $B_n(\tau)$ given in Equation (2.90). Using (2.98), the systems (2.91) and (2.92) can be written as

$$P_n \dot{\underset{\sim}{Y}}_n + Q_n \underset{\sim}{Y}_n = \sum_{\substack{e=1 \\ e \neq n}}^{N} \left[\mathscr{F}_{en} \underset{\sim}{Y}_e + \mathscr{G}_{en} \dot{\underset{\sim}{Y}}_e \right] \quad \forall n = 1, \ldots, N \tag{2.99}$$

with

$$
P_n = \left[\begin{array}{cc|cc} (1+m_1) & 0 & 0 & 0 \\ 0 & (1+m_2) & 0 & 0 \\ \hline 0 & 0 & 1 & 0 \\ 0 & 0 & 0 & 1 \end{array}\right]; \quad \begin{array}{l} m_1 = \bar{m}_L \, \tilde{G}^{cc}_{nn} \\ m_2 = \bar{m}_L \, \tilde{G}^{ss}_{nn} \end{array}
$$

$$
Q_n = \left[\begin{array}{cc|cc} c_1 & -2\bar{\Omega}n & (\bar{\mu}_n^2 - \bar{\Omega}^2 n^2 + k_1) & 0 \\ +2\bar{\Omega}n & c_2 & 0 & (\bar{\mu}_n^2 - \bar{\Omega}^2 n^2 + k_2) \\ \hline -1 & 0 & 0 & 0 \\ 0 & -1 & 0 & 0 \end{array}\right]; \quad \begin{array}{l} c_1 = \bar{c}_L \, \tilde{G}^{cc}_{nn} \\ c_2 = \bar{c}_L \, \tilde{G}^{ss}_{nn} \\ k_1 = \bar{k}_L \, \tilde{G}^{cc}_{nn} \\ k_2 = \bar{k}_L \, \tilde{G}^{ss}_{nn} \end{array}
$$

$$
\mathscr{F}_{en} = \left[\begin{array}{cc|cc} \bar{c}_L \, \tilde{G}^{cc}_{en} & 0 & \bar{k}_L \, \tilde{G}^{cc}_{en} & 0 \\ 0 & \bar{c}_L \, \tilde{G}^{ss}_{en} & 0 & \bar{k}_L \, \tilde{G}^{ss}_{en} \\ \hline 0 & 0 & 0 & 0 \\ 0 & 0 & 0 & 0 \end{array}\right]
$$

$$
\mathscr{G}_{en} = \left[\begin{array}{cc|cc} \bar{m}_L \, \tilde{G}^{cc}_{en} & 0 & 0 & 0 \\ 0 & \bar{m}_L \, \tilde{G}^{ss}_{en} & 0 & 0 \\ \hline 0 & 0 & 0 & 0 \\ 0 & 0 & 0 & 0 \end{array}\right]
$$

(2.100)

2.4 Discussion

The use of Galerkin's method in this investigation reduces the problem from that of the stability of a partial differential equation to the determination of the eigenvalues of a linear system of equations.

The use of approximate eigenfunctions to generate the N-mode approximation does not change the qualitative nature of the stability results of the N-mode system. The validity of these approximate stability criteria is discussed in Chapter VI.

The equation of motion is written in a reference frame in which the load is not rotating. The equation could have been written in the rotating reference frame in which case the load would have appeared to be rotating. This, however, would have introduced variable coefficients in the N-mode approximation. In the stationary frame, the equations have constant coefficients and thus can be analyzed using elementary techniques.

III. STABILITY ANALYSIS OF A SINGLE MODE APPROXIMATION

3.1 Introduction

In this chapter and in Chapter 4, analysis of the solution to the boundary value problem (2.26) will be accomplished by analyzing the stability of solutions to the system (2.99). Since this involves finding the eigenvalues of matrices defined by the system (2.99), numerical and algebraic techniques will be used.

In this chapter, a single mode approximation to the solution is analyzed. The characteristic equation for the single mode approximation is studied algebraically to determine values of the parameters which yield eigenvalues with positive real parts. The existence of positive real parts in the eigenvalues is the criterion of instability. The Routh Hurwitz criteria is used for the case including load damping. Numerical techniques are employed to obtain the frequency-speed diagrams for the one mode approximation. The effect of using approximate radial eigenfunctions is also analyzed.

The single mode approximation is the only approximation which allows algebraic analysis. Since the qualitative aspects of the stability of the single mode analysis appear in the multiple mode analysis, this simplified system provides insight into the behavior of the more complex approximations.

3.2 Nature of Solutions

The basic equation derived in Chapter II to be analyzed here is Equation (2.99). It may be written as

$$\gamma_n \ddot{\underset{\sim}{x}}_n + a_n \dot{\underset{\sim}{x}}_n + \beta_n \underset{\sim}{x}_n = -\sum_{\substack{e=1 \\ e\neq n}}^{N} \left[k_L F_{en} \underset{\sim}{x}_e + \right.$$

$$\left. + c_L F_{en} \dot{\underset{\sim}{x}}_e + m_L F_{en} \ddot{\underset{\sim}{x}}_e \right] \quad \forall n = 1, 2, \ldots N \qquad (3.1)$$

with

$$\gamma_n = \begin{bmatrix} (1+m_1) & 0 \\ 0 & (1+m_2) \end{bmatrix}$$

$$a_n = \begin{bmatrix} c_1 & -2\bar{\Omega}n \\ +2\bar{\Omega}n & c_2 \end{bmatrix}$$

$$\beta_n = \begin{bmatrix} (\bar{\mu}_n^2 - \bar{\Omega}^2 n^2 + k_1) & 0 \\ 0 & (\bar{\mu}_n^2 - \bar{\Omega}^2 n^2 + k_2) \end{bmatrix}$$

$$F_{en} = \begin{bmatrix} \bar{G}_{en}^{cc} & 0 \\ 0 & \bar{G}_{en}^{ss} \end{bmatrix}$$

and m_i, k_i, c_i, $i = 1, 2$ given by (2.100)

If it is assumed that vibration occurs in one mode only then Equation (3.1) becomes:

$$\gamma_n \ddot{\underset{\sim}{x}}_n + a_n \dot{\underset{\sim}{x}} + \beta_n \underset{\sim}{x}_n = \underset{\sim}{0} \quad \forall n = 1, \ldots, N \qquad (3.2)$$

Assume a solution to (3.2) of the form

$$\underset{\sim}{x} = \underset{\sim}{\eta}\, e^{st} \quad s \text{ complex}$$

with

$$\underset{\sim}{\eta} = \begin{pmatrix} \eta_1 \\ \eta_2 \end{pmatrix}, \qquad (3.3)$$

Using (3.3) in Equation (3.2) implies

$$\{ \gamma_n s^2 + \alpha_n s + \beta_n \} \underset{\sim}{\eta} e^{st} = \underset{\sim}{0} \tag{3.4}$$

For a nontrivial solution of (2.2) it is necessary that

$$\det \{ \gamma_n s^2 + \alpha_n s + \beta_n \} = 0 \tag{3.5}$$

Equation (3.5) can be expanded using Relations (2.102) to obtain

$$\det \begin{bmatrix} (1 + m_1) s^2 + c_1 s + (\bar{\mu}_n^2 - n^2 \bar{\Omega}^2 + k_1) & -2 \bar{\Omega} n s \\ +2 \bar{\Omega} n s & (1+m_2) s^2 + c_2 s + \bar{\mu}_n^2 - \bar{\Omega}^2 n^2 + k_2 \end{bmatrix} = 0 \tag{3.6}$$

This yields the characteristic equation

$$a_0 s^4 + a_1 s^3 + a_2 s^2 + a_3 s + a_4 = 0 \tag{3.7}$$

with

$$\left.\begin{aligned} a_0 &= (1 + m_1)(1 + m_2) \\ a_1 &= c_1 (1 + m_2) + c_2 (1 + m_1) \\ a_2 &= (1 + m_1)(\bar{\mu}_n^2 - \bar{\Omega}^2 n^2 + k_2) + (1 + m_2)(\bar{\mu}_n^2 - \bar{\Omega}^2 n^2 + k_1) \\ &\quad + c_1 c_2 + (2 \bar{\Omega} n)^2 \\ a_3 &= (\bar{\mu}_n^2 - \bar{\Omega}^2 n^2 + k_1)(c_2) + (\bar{\mu}_n^2 - \bar{\Omega}^2 n^2 + k_1)(c_1) \\ a_4 &= (\bar{\mu}_n^2 - \bar{\Omega}^2 n^2 + k_1)(\bar{\mu}_n^2 - \bar{\Omega}^2 n^2 + k_2) \end{aligned}\right\} \tag{3.8}$$

The lower bound approximation to μ_n^2 developed in Chapter II is now used. From Equation (2.89a) the approximation is given by

$$(\bar{\mu}_n)^2 = (p_1^n)^2 + (p_2^n)^2 \tag{3.9}$$

where $(p_1^n)^2 = \lambda_n \bar{\Omega}^2$ (3.10)

and $$(p_2^n)^2 = \xi_n \frac{Eh^2}{\rho a^4} \tag{3.11}$$

Using (3.9) in (3.8) yields

$$\left.\begin{aligned}
a_0 &= (1+m_1)(1+m_2) \\
a_1 &= c_1(1+m_2) + c_2(1+m_1) \\
a_2 &= (1+m_1)\left[(p_2^n)^2 + \lambda_n\overline{\Omega}^2 - n^2\overline{\Omega}^2 + k_2\right] \\
&\quad + (1+m_2)\left[(p_2^n)^2 + \lambda_n\overline{\Omega}^2 - n^2\overline{\Omega}^2 + k_1\right] \\
&\quad + c_1c_2 + (2\overline{\Omega}n)^2 \\
a_3 &= \left[(p_2^n)^2 + \lambda_n\overline{\Omega}^2 - n^2\overline{\Omega}^2 + k_1\right](c_2) \\
&\quad + \left[(p_2^n)^2 + \lambda_n\overline{\Omega}^2 - n^2\overline{\Omega}^2 + k_2\right](c_1) \\
a_4 &= \left[(p_2^n)^2 + \lambda_n\overline{\Omega}^2 - n^2\overline{\Omega}^2 + k_1\right]\left[(p_2^n)^2 + \lambda_n\overline{\Omega}^2 - n^2\overline{\Omega}^2 + k_2\right]
\end{aligned}\right\} \tag{3.12}$$

3.3 Analysis of Characteristic Equation

The value of the real part of the roots of Equation (3.7) determine the stability of the solution of the one-mode approximation. If there is a root s_1 of Equation (3.7) with positive real part, then there will exist a solution to Equation (3.2) of the form

$$\binom{\eta_1}{\eta_2} e^{Re(s_1)t} \cdot \cos(Im(s_1)\cdot t) \tag{3.13}$$

with $Re(s_1) > 0$.

Thus, there exists a solution which is unbounded for $t \in [0, \infty]$. Analysis of the roots of Equation (3.7) is now made for various values of $\overline{m}_L$, $\overline{c}_L$, and $\overline{k}_L$.

3.3.1 Spinning Disk With No Load

With $\bar{m}_L = \bar{k}_L = \bar{c}_L = 0$, Equation (3.7) becomes

$$s^4 + \left[2(p_2^n)^2 + 2\lambda_n\bar{\Omega}^2 + 2n^2\bar{\Omega}^2\right]s^2 + \left[(p_2^n)^2 + \lambda_n\bar{\Omega}^2 - n^2\bar{\Omega}^2\right]^2 = 0 \qquad (3.14)$$

Hence:

$$s^2 = -\left[(p_2^n)^2 + \lambda_n\bar{\Omega}^2 + n^2\bar{\Omega}^2\right] \pm \left\{\left[(p_2^n)^2 + \lambda_n\bar{\Omega}^2 + n^2\bar{\Omega}^2\right]^2 - \left[(p_2^n)^2 + \lambda_n\bar{\Omega}^2 - n^2\bar{\Omega}^2\right]^2\right\}^{\frac{1}{2}} \qquad (3.15)$$

Since $\lambda_n > 0$ and $n^2\bar{\Omega}^2 > 0$,

$$\left[(p_2^n)^2 + \lambda_n\bar{\Omega}^2 + n^2\bar{\Omega}^2\right]^2 \geq \left[(p_2^n)^2 + \lambda_n\bar{\Omega}^2 - n^2\bar{\Omega}^2\right] \qquad (3.16)$$

Inequality (3.16) implies that

$$\left\{\left[(p_2^n)^2 + \lambda_n\bar{\Omega}^2 + n^2\bar{\Omega}^2\right]^2 - \left[(p_2^n)^2 + \lambda_n\bar{\Omega}^2 - n^2\bar{\Omega}^2\right]^2\right\}^{\frac{1}{2}}$$

is real. It follows that the two solutions $(s_1)^2$ and $(s_2)^2$ defined by (3.15) are negative real numbers.

This implies that the roots of (3.14) s_i $i = 1, \ldots, 4$ will all be pure imaginary numbers. These are given by:

$$s_1 = +i\,|s_1| \qquad s_2 = +i\,|s_2|$$
$$s_3 = -i\,|s_1| \qquad s_4 = -i\,|s_1| \qquad (3.17)$$

3.3.2 Spinning Disk With Mass and Spring Load

For the case of undamped load, $\bar{m}_L \neq 0$, $\bar{k}_L \neq 0$, $\bar{c}_L = 0$, the characteristic equation (3.7) becomes

$$a_0 s^4 + a_2 s^2 + a_4 = 0 \qquad (3.18)$$

with

$$\left.\begin{aligned} a_0 &= (1+m_1)(1+m_2) \\ a_2 &= (1+m_1)\left[(p_2^n)^2 + \lambda_n \bar{\Omega}^2 - n^2\bar{\Omega}^2 + k_2\right] \\ &\quad + (1+m_2)\left[(p_2^n)^2 + \lambda_n \bar{\Omega}^2 - n^2\bar{\Omega}^2 + k_1\right] + 4n^2\Omega^2 \\ a_4 &= \left[(p_2^n)^2 + \lambda_n\bar{\Omega}^2 + n^2\bar{\Omega}^2 + k_1\right]\left[(p_2^n)^2 + \lambda_n\bar{\Omega}^2 + n^2\bar{\Omega}^2 + k_2\right] \end{aligned}\right\} \quad (3.19)$$

Since Equation (3.18) is quadratic in s^2 the solution for s^2 can be represented as:

$$(s^2)_{1,2} = \frac{a_2}{2a_0} \pm \frac{1}{2a_0}\cdot\left[(a_2)^2 - 4a_0a_4\right]^{\frac{1}{2}} \quad (3.20)$$

If $4a_0a_4 < 0$ then $\left[(a_2)^2 - 4a_0a_4\right]^{\frac{1}{2}} > |a_2|$

and $2a_0(s_1)^2 = -a_2 + \left[(a_2)^2 - 4a_0a_4\right]^{\frac{1}{2}} > 0.$

Since $(s_1)^2 1 > 0$ this yields a positive real value for s_1 and a root of Equation (3.18) will possess a positive real part. To investigate whether $4a_0a_4$ can be negative consider

$$4a_0a_4 = 4(1+m_1)(1+m_2)\left[(p_2^n)^2 + (\lambda_n - n^2)\bar{\Omega}^2 + k_1\right]\cdot \left[(p_2^n)^2 + (\lambda_n - n^2)\bar{\Omega}^2 + k_2\right] \quad (3.21)$$

Since $m_1 > 0$, and $m_2 > 0$

$$4a_0a_4 < 0 \iff \left[(p_2^n)^2 + (\lambda_n - n^2)\bar{\Omega}^2 + k_1\right]\left[(p_2^n)^2 + (\lambda_n - n^2)\bar{\Omega}^2 + k_2\right] < 0 \quad (3.22)$$

Suppose $k_2 < k_1$. If $\bar{\Omega}$ is such that

$$\left[(p_2^n)^2 + k_2\right] < |2n - n^2|\,\bar{\Omega}^2 < \left[(p_2^n)^2 + k_1\right] \quad (3.23)$$

then $\left[(p_2^n)^2 + (\lambda_n - n^2)\bar{\Omega}^2 + k_1\right]\left[(p_2^n)^2 + (\lambda_n - n^2)\bar{\Omega}^2 + k_2\right] < 0 \quad (3.24)$

and it is clear that one root of the Equation (3.18) possesses a positive real part. Thus, there will be an instability in the solution of Equation (3.2) if $c_L = 0$ and $\bar{\Omega}$ is such that

$$\frac{(p_2^n)^2 + k_2}{n^2 - \lambda_n} < \bar{\Omega}^2 < \frac{(p_2^n)^2 + k_1}{n^2 - \lambda_n} \tag{3.25}$$

To determine if there exist instabilities at speed other than those defined by relation (3.25), the term in brackets in equation (3.20) is analyzed. If there are speeds for which $[\ (a_2)^2 - 4a_0a_4\ ]$ is negative then complex conjugate roots are produced and thus roots with positive real parts are introduced. Using relations (3.19) implies that

$$\begin{aligned}
&[(a_2)^2 - 4a_0\ a_4\ ] = \\
&[\ (1+m_1)\ (\ (p_2^n)^2 + \lambda_n\bar{\Omega}^2 - n^2\bar{\Omega}^2 + k_2) + (1+m_2)\ (\ (p_2^n)^2 + \lambda_n\bar{\Omega}^2 - n^2\ \bar{\Omega}^2 + k_1\ ) + \\
&+ 4n^2\bar{\Omega}^2\ ]^2 - 4\ (1+m_1)(1+m_2)[\ (p_2^n)^2 + \lambda_n\bar{\Omega}^2 - n^2\ \bar{\Omega}^2 + k_1\ ] \\
&[(p_2^n)^2 + \lambda_n\bar{\Omega}^2 - n^2\bar{\Omega}^2 + k_2\ ]
\end{aligned} \tag{3.26}$$

Equation (3.26) is now examined to determine the values of m_1 which render it zero. First Equation (3.26) is rearranged as follows:

$$\begin{aligned}
&[(a_2)^2 - 4\ a_0\ a_4\ ] = [(p_2^n)^2 + \lambda_n\bar{\Omega}^2 - n^2\bar{\Omega}^2]\ (m_1)^2 \\
&+ [2\ (2\ (p_2^n)^2 + 2\lambda_n\bar{\Omega}^2 + 2n^2\ \bar{\Omega}^2 + k_1)(\ (p_2^n)^2 + \lambda_n\bar{\Omega}^2 - n^2\bar{\Omega}^2) \\
&-4\ (\ (p_2^n)^2 + \lambda_n\bar{\Omega}^2 - n^2\ \bar{\Omega}^2 + k_1)\cdot\ (\ (p_2^n)^2 + \lambda_n\bar{\Omega}^2 - n^2\bar{\Omega}^2)\ ]\ (m_1) + \\
&+ [\ (2(p_2^n)^2 + 2\ \lambda_n\bar{\Omega}^2 + 2n^2\bar{\Omega}^2 + k_1)^2\ - 4\cdot[(p_2^n)^2 - \lambda_n\bar{\Omega}^2 - n^2\bar{\Omega}^2 + k_1\ ]\cdot \\
&\quad [\ (p_2^n)^2 + \lambda_n\bar{\Omega}^2 - n^2\bar{\Omega}^2\ ]
\end{aligned} \tag{3.27}$$

The values of m_1 which make (3.27) zero are shown as a function of $\bar{\Omega}$ in the Figure 5. The effect of increasing the stiffness is shown to increase the value of the mass parameter required to obtain instability. The effect of the load radius is shown in Figures 6 and Figure 7.

3.3.3 Spinning Disk With Load Damping

For the case including the mass, spring, and dashpot the full characteristic Equations (3.7) must be used. The Routh Hurwitz criteria will be used to determine if there are values of $\bar{\Omega}$ for which there exist roots of Equation (3.7) that have positive real parts. Let

$$\left.\begin{aligned} \Delta_1 &= a_1 \\ \Delta_2 &= \begin{vmatrix} a_1 & a_0 \\ a_3 & a_2 \end{vmatrix} \\ \Delta_3 &= \begin{vmatrix} a_1 & a_0 & 0 \\ a_3 & a_2 & a_1 \\ 0 & a_4 & a_3 \end{vmatrix} \\ \Delta_4 &= a_4 \, \Delta_3 \end{aligned}\right\} \qquad (3.28)$$

with a_0, a_1, a_2, a_3 and a_4 given by (3.12).

The Routh Hurwitz criteria states that all roots of Equation (3.7) will have negative real parts if and only if all $\Delta_i > 0$ ($i = 1, \ldots, 4$). Using Relations (3.12) for the constant a_1 in Δ_1 yields

$$\Delta_1 = c_1 (1+m_2) + c_2 (1+m_1) \qquad (3.29)$$

Since $c_i > 0$ and $m_i > 0$ $i = 1, 2$ then $\Delta_1 > 0$.

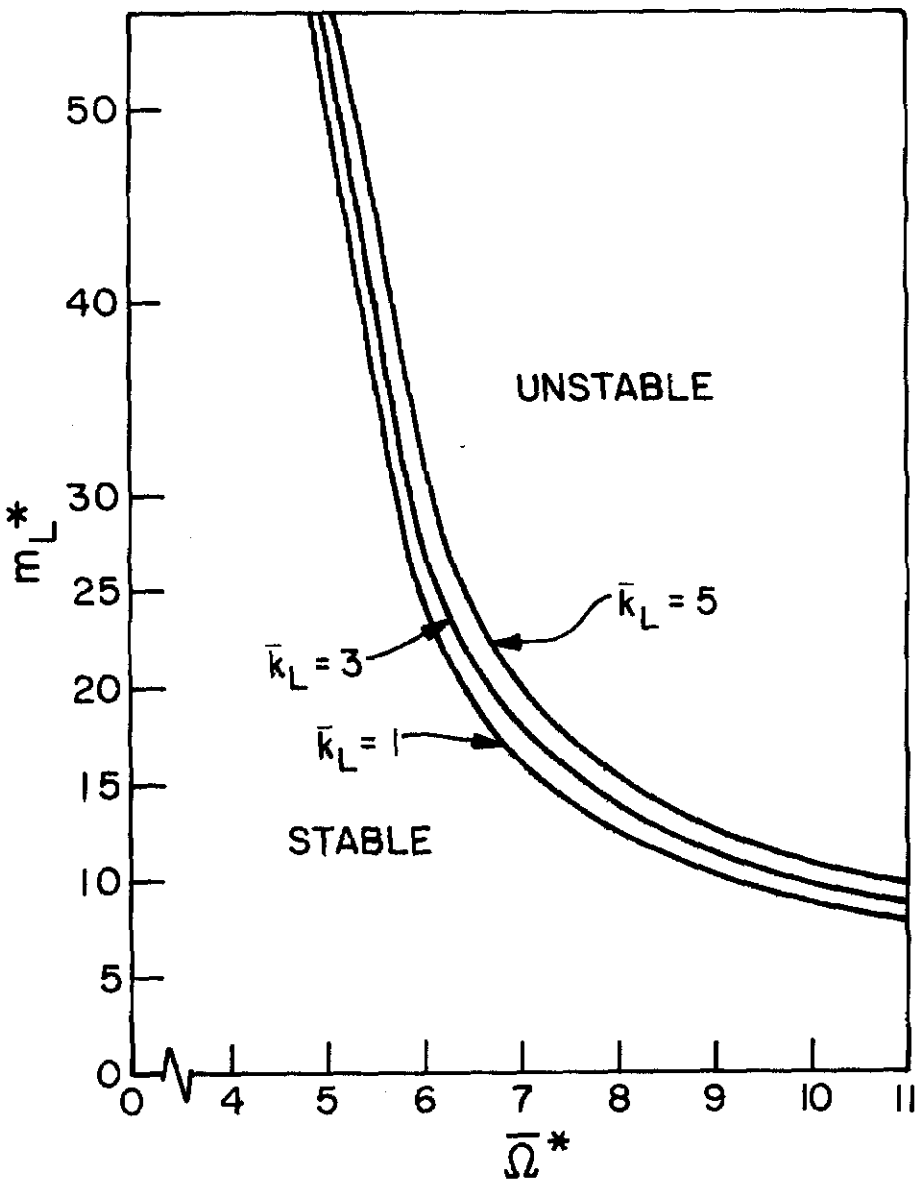

Fig. 5. Terminal speeds of rotation as a function of $\bar{m}_L$ for $\bar{r}_L = .6$.

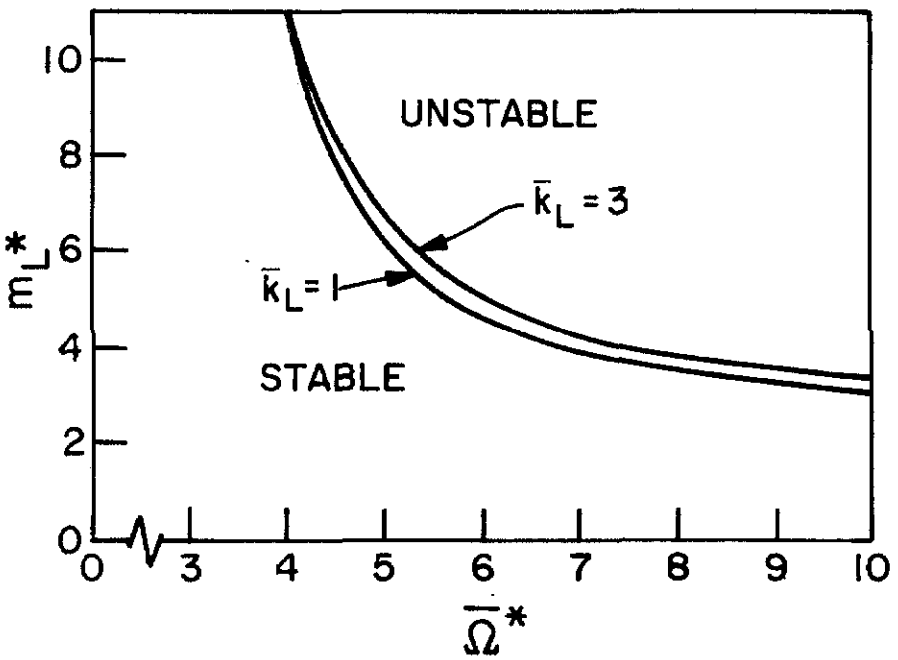

Fig. 6. Terminal speeds of rotation as a function of $\bar{m}_L$ for $\bar{r}_L = .8$.

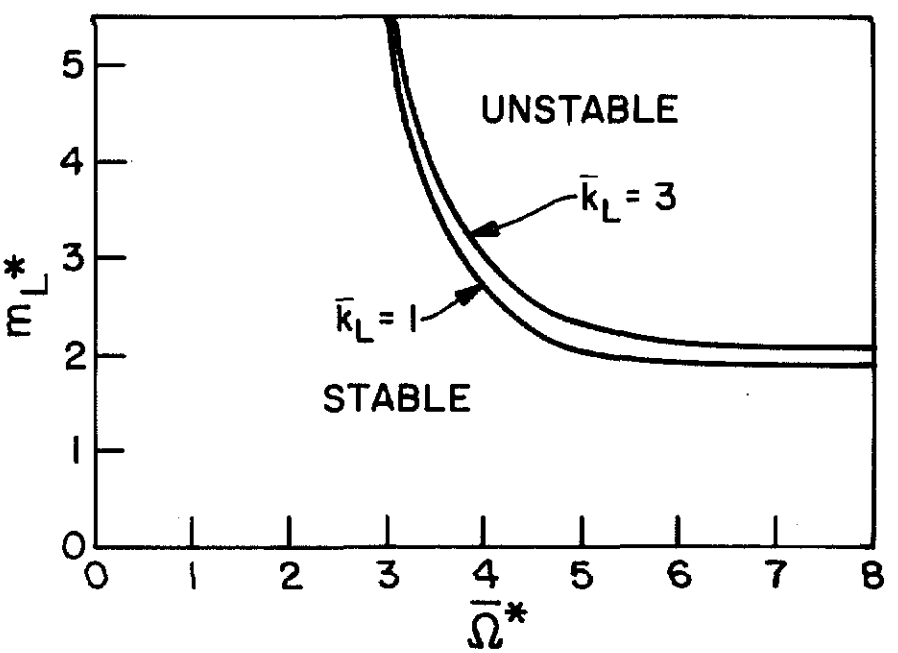

Fig. 7. Terminal speeds of rotation as a function of $\bar{m}_L$ for $\bar{r}_L = .9$.

Similarly, using (3.12) for the constants a_0, a_1, a_2, a_3 in Δ_2 yields

$$\Delta_2 = c_1 (1+m_1)(c_1 c_2 + 4n^2\overline{\Omega}^2) + c_2 (1+m_1)(c_1 c_2 + 4n^2\overline{\Omega}^2) + c_1 (1+m_2)^2 [(p_2^n)^2 + \lambda_n \overline{\Omega} + k_1] + c_2 (1+m_1)^2 [(p_2^n)^2 + \lambda_n \overline{\Omega}^2 - n^2\overline{\Omega}^2 + k_2] \quad (3.30)$$

From Equation (3.30), it follows that a sufficient condition for Δ_2 to be positive is that

$$(1+m_i)\, 4_n \overline{\Omega}^2 > (1+m_i)^2 \left| \lambda_n - n^2 \right| ; \; i = 1, 2 \quad (3.31)$$

For $n = 2$, $\lambda_2 = 2.35$ and Inequality (2.31) implies that m_i must be such that

$$16 > (1+m_i)(1.45); \; i = 1, 2 \quad (3.32)$$

Since m_i is a ratio of the mass of the disk to the mass of the load, relation (3.32) is certainly satisfied for values of m_i of practical interest.

Since $\Delta_4 = a_4 \Delta_3$, assume for the present that Δ_3 is positive and examine a_4. From Relations (3.12)

$$a_4 = [(p_2^n)^2 + \lambda_n \overline{\Omega}^2 - n^2\overline{\Omega}^2 + k_1][(p_2^n)^2 + \lambda_n \overline{\Omega}^2 - n^2\overline{\Omega}^2 + k_2] \quad (3.33)$$

The form of Equation (3.12) implies that the conditions necessary for a_4 to be negative are exactly those derived earlier as the stiffness instability region of Relation (3.25). If Δ_3 is positive for values of $\overline{\Omega}$ defined by (3.25) then the stiffness instability is present.

The Δ_3 expression is now investigated. Since as $\overline{\Omega} \to \infty$, the parameters m_i, c_i, k_i all converge to bounded limits, the

behavior of Δ_3 for $\bar{\Omega} >> 1$ can be studied if the limiting values for m_i, c_i, k_i are substituted for m_i, c_i, k_i in Δ_3. Let the limiting values of m_i, c_i, k_i be called m_i^*, c_i^*, k_i^*. Then Δ_3 can be written as:

$$\Delta_3 = \{[c_2(\lambda_n - n^2) + c_1(\lambda_n - n^2)] \cdot$$
$$[c_1(1+m_2^*)^2 \lambda_n + c_2(1+m_1^*)^2 \lambda_n + c_1(1+m_2^*)(4n^2)$$
$$+ c_2(1+m_1^*)(4n^2) - c_1(1+m_2^*)^2 n^2 - c_2(1+m_1^*)^2 n^2]$$
$$- [c_1(1+m_2^*) + c_2(1+m_1^*)]^2 [\lambda_n - n^2]^2 \} \bar{\Omega}^4 + O(\bar{\Omega}^2) \qquad (3.34)$$

Now Δ_3 will be positive (or negative) for $\bar{\Omega} >> 1$ if the term in braces in Equation (3.34) is positive (or negative). Equation (3.34) can be rewritten as:

$$\Delta_3 = \{ [(c_1 c_2)^{\frac{1}{2}} (\lambda_n - n^2)(1+m_2^*) - (c_1 c_2)^{\frac{1}{2}} (\lambda_n - n^2)(1+m_1^*)]^2$$
$$+ c_1^2 (\lambda_n - n^2)(1+m_2^*)(4n^2) + c_1 c_2 (\lambda_n - n^2)(1+m_1^*)(4n^2)$$
$$+ c_1 c_2 (\lambda_n - n^2)(1+m_2^*)(4n^2) + c_2^2 (\lambda_n - n^2)(1+m_1^*)(4n^2) \} \bar{\Omega}^4$$
$$+ O(\bar{\Omega}^3) \qquad (3.35)$$

For the case of $m_i = 0$, Equation (3.35) becomes

$$\Delta_3 = \{ 4n^2 (\lambda_n - n^2)(c_1 c_2) \} \bar{\Omega}^4 + O(\bar{\Omega}^3) \qquad (3.36)$$

Since $\lambda_n < n^2$, $n = 2,3,\ldots$ Equation (3.36) implies that the coefficient of the highest power of $\bar{\Omega}$ in Δ_3 is negative. Thus, for sufficiently large values of $\bar{\Omega}$, Δ_3 will be negative and there will exist roots of Equation (3.7) with positive real parts. For $m_i \neq 0$ consider the case of a point load. This makes $c_2 = 0$, and Equation (3.36) becomes

$$\Delta_3 = \{ c_i^2 \, (\lambda_n - n^2) \, (4n^2) \, \} \bar{\Omega}^4 + O(\bar{\Omega}^2) \tag{3.37}$$

Again, since $\lambda_n < n^2$, $n = 2, 3\ldots$ the coefficient of the highest power of $\bar{\Omega}$ in Δ_3 is negative and the existence of a root of Equation (3.7) with positive real parts for sufficiently large $\bar{\Omega}$ is assured.

3.4 Validity of the Stability Analysis for a Single Mode Approximation

Since the exact radial eigenfunctions defined by (2.66) satisfy

$$R_{on}(r) > 0 \quad \forall \; r \in [o, a] \text{ and } \forall \, n = 1, 2\ldots \tag{3.38}$$

This implies that m_i, k_i, c_i defined through (2.100) using the exact eigenfunctions are all positive. Since the approximate eigenfunctions $\tilde{R}_n$ satisfy

$$\tilde{R}_n(r) > 0 \quad \forall \; r \in [o, a] \text{ and } \forall \, n = 1, 2, \ldots \tag{3.39}$$

then all terms in the matrices of (3.2) have the same sign for both the exact and approximate eigenvalues.

Now consider the Routh-Hurwitz criteria for the system (3.2) obtained using exact eigenfunctions. Equations (3.29) and (3.32) and the above discussion imply that Δ_1 and Δ_2 for such a system are both positive. From the analysis of Δ_3 a necessary and sufficient condition for the existence of a damping instability

for $\bar{\Omega} >> 1$ is that

$$\lambda_n^* < n^2 \tag{3.40}$$

where λ_n^* is the exact natural frequency of the operator $\frac{1}{\Omega^2} L_1$. Thus if an upper bound λ_n^{ub} for λ_n^* is such that

$$\lambda_n^{ub} < n^2 \tag{3.41}$$

then it is established that the instability of the approximate system implies an instability exists in the exact solution to the single mode system. The same condition applies for the existence of a stiffness instability.

3.5 Numerical Examples

Figure 8 is the frequency-speed diagram for a single mode approximation of a spinning disk with no transverse loading. The frequency-speed diagram gives the real and imaginary parts of the roots of Equation (3.14) as a function of the angular velocity $\bar{\Omega}$. The real part of all roots of (3.14) are zero as given by (3.17) and the solution to the single mode equation (3.2) is therefore periodic in time and is bounded. For $\bar{\Omega} < 4$, the branch of the Imag(s) versus $\bar{\Omega}$ curves which decreases as $\bar{\Omega}$ increases represents the frequency of a forward traveling wave in the disk. The speed at which the frequency of this wave becomes zero will be called the critical speed of the disk and denoted by Ω_2^* . A constant force applied to the disk while the disk is rotating at this speed causes an unstable response. The branch of the Imag(s) versus $\bar{\Omega}$ curves which

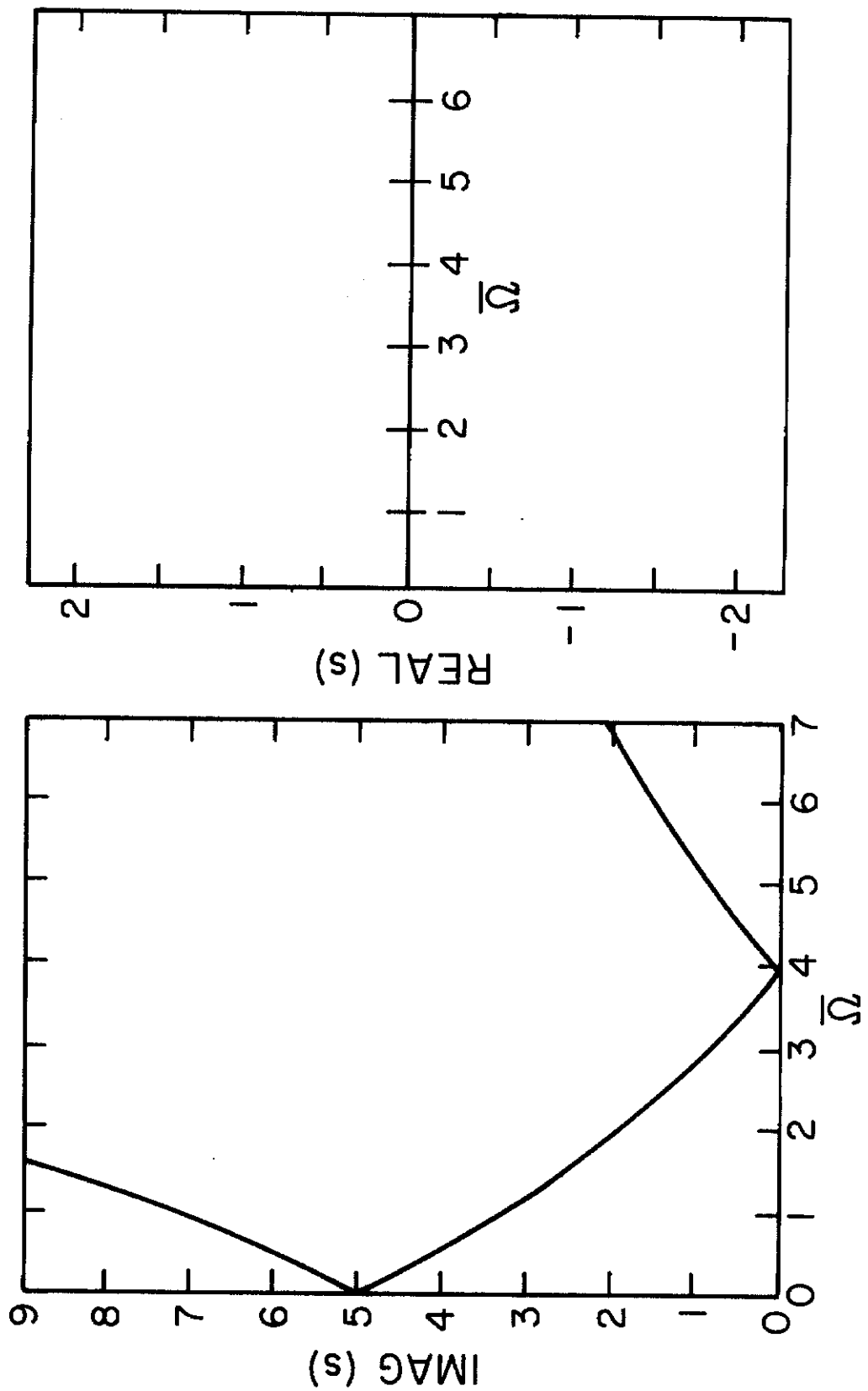

Fig. 8. Frequency-speed diagram for a freely spinning disk ($m_L = c_L = k_L = 0$).

increases with increase in $\bar{\Omega}$ for all values of $\bar{\Omega}$ represents the frequency of a backward traveling wave in the disk. For $\bar{\Omega} > \Omega_2^*$ both branches of the Imag(s) versus $\bar{\Omega}$ curve increase with increase in $\bar{\Omega}$, and the branch corresponding to the forward traveling wave shall be called the reflected branch.

Figure 9 gives the frequency-speed diagram for the single mode approximation including the effects of load mass and spring. The stiffness instability predicted for $\bar{\Omega}$ which satisfy relation (3.25) results from the root of Equation (3.18) with positive real part.

Figure 10 shows the effect of increased load mass over that of Figure 9. A positive real part for one of the roots of Equation (3.18) occurs for $\bar{\Omega} > 5.4$ and this results in an unbounded solution for the single mode system of equations.

Figure 11 gives the frequency-speed diagram for the roots of the full characteristic equation (3.7). The root with positive real part for all values of $\bar{\Omega}$ greater than those of the stiffness instability region appears even though the value of the load mass is well below the instability boundary shown in Figure 5. Thus, the instability here is due to the damping term as the Routh-Hurwitz criteria predicted.

Figure 12 gives the real part of a frequency-speed diagram for the values of $\bar{m}_L$, $\bar{c}_L$, and $\bar{k}_L$ of Figure 9 but the value of $\bar{r}_L$, the load radius is varied. The effect of increasing the load radius is to increase the value of k_i, m_i, and c_i in the Equation (3.7). This has a dramatic effect on the real part of the roots of Equation

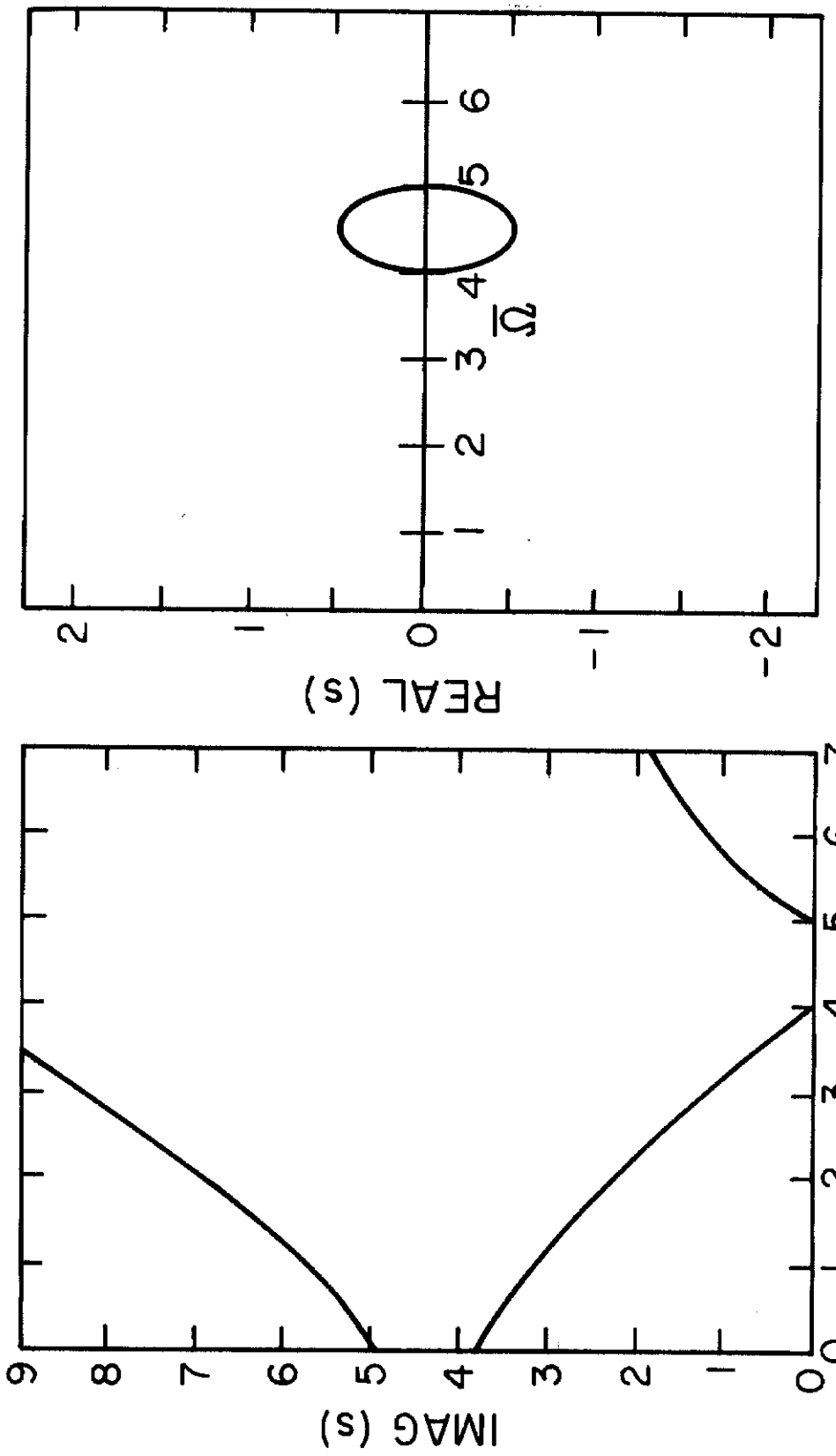

Fig. 9. Frequency-speed diagram for a spinning disk ($\bar{r}_L = .9$, $\bar{m}_L = .1$, $\bar{c}_L = 0$, $\bar{K}_L = 1.0$).

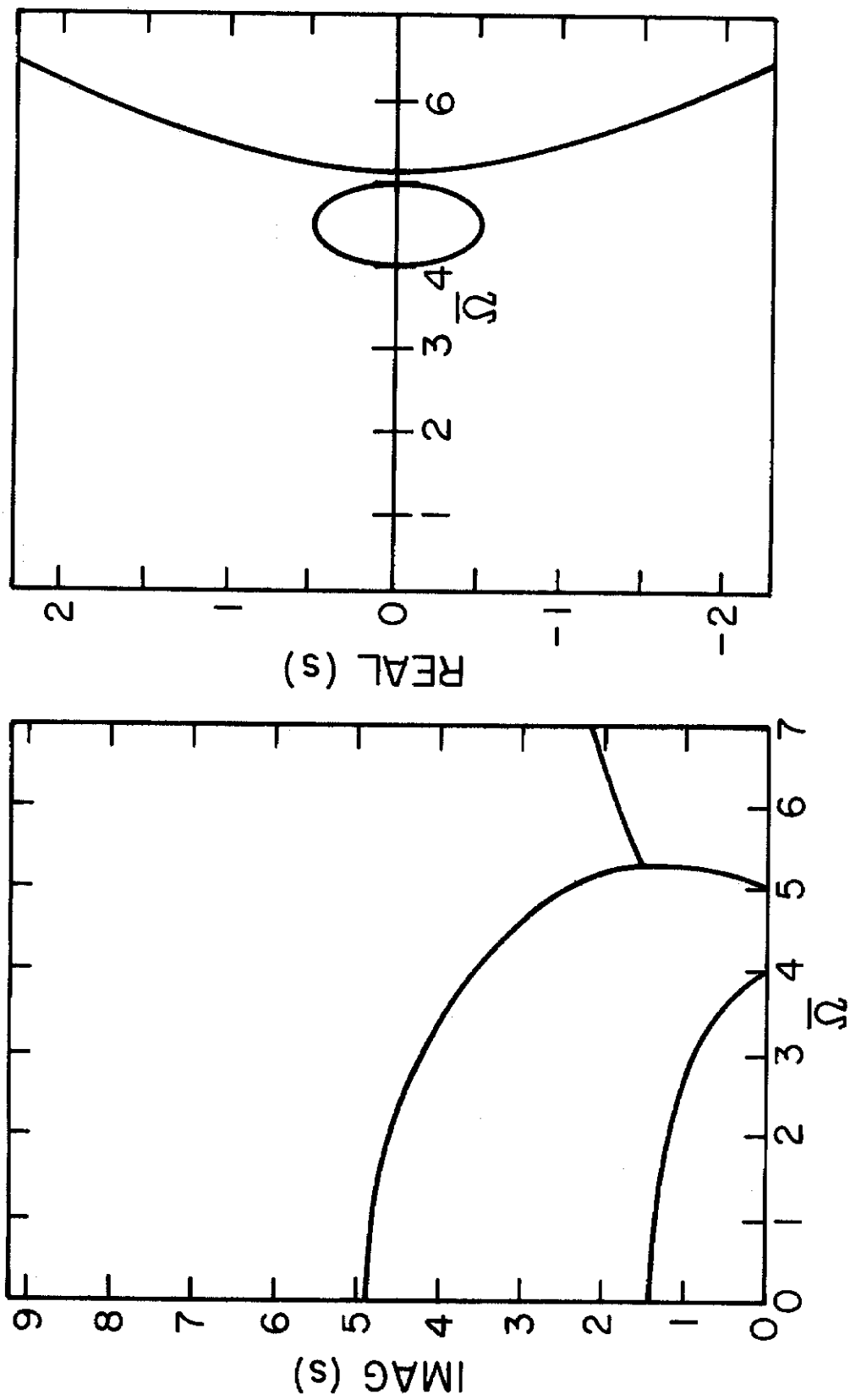

Fig. 10. Frequency-speed diagram for spinning disk ($\bar{r}_L = .9$, $\bar{m}_L = 2.0$, $\bar{c}_L = 0$, $K_L = 1.0$).

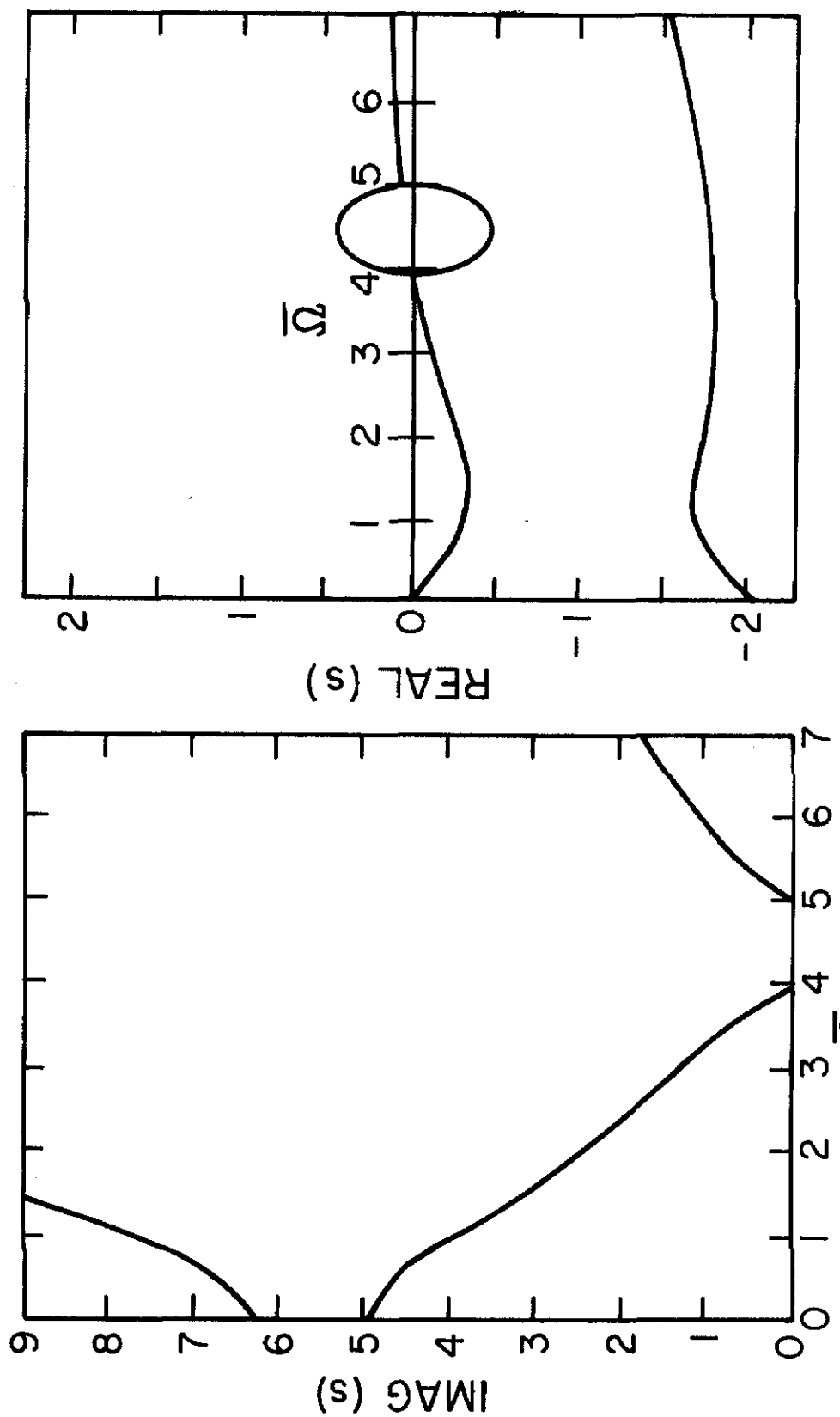

Fig. 11. Frequency-speed diagram for spinning disk with load damping ($\bar{r}_L = .9$, $\bar{m}_L = .1$, $\bar{c}_L = 1.0$, $\bar{K}_L = 1.0$).

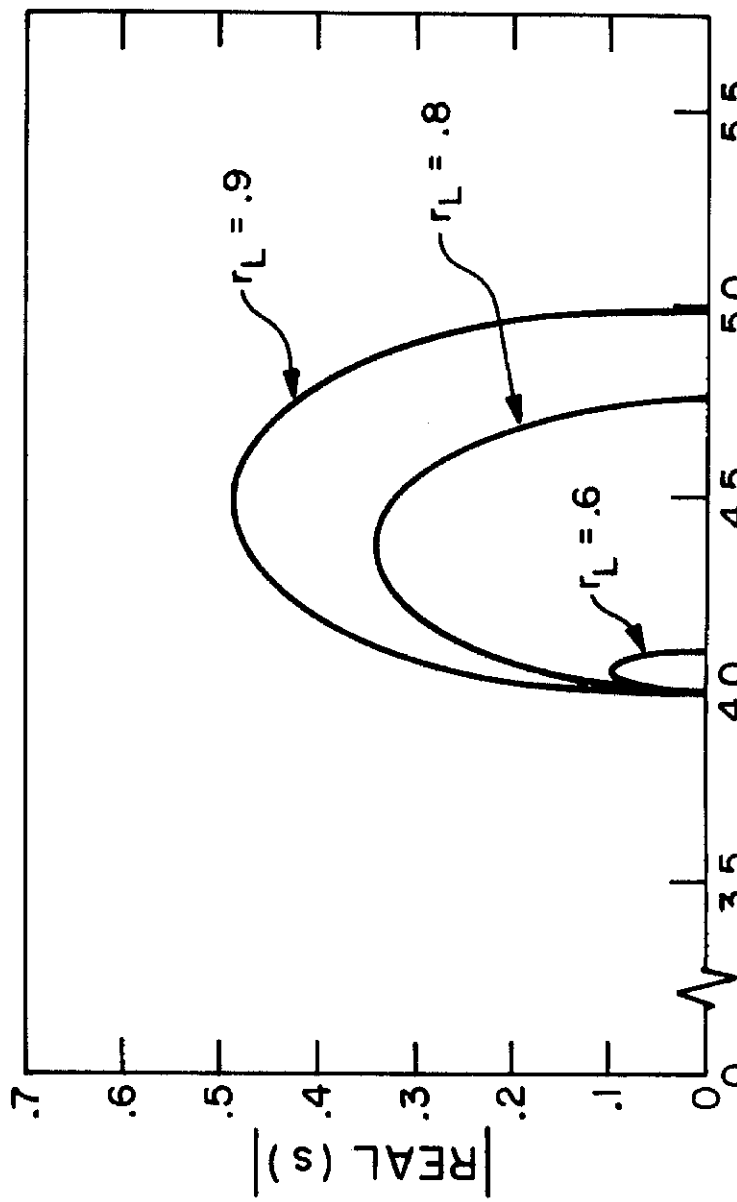

Fig. 12. The effect of load radius on the stiffness instability ($\bar{m}_L = .1$, $\bar{K}_L = 1.0$, $\bar{c}_L = 0$).

(3.7). However, the rotational speed of the disk for the onset of the stiffness instability region is never decreased.

3.6 Discussion

The results of this chapter will be fundamental to the understanding of the dynamics of the N-mode system and to the elastic disk itself. The fact that the system of equation has constant coefficients makes it possible to obtain directly the stability of the single mode system.

When the eigenvalues are graphed against the angular rotation of the disk, the stability of the disk over a range of speeds may be presented in one diagram. Thus, the frequency-speed diagram is used as the primary means of presenting results. The imaginary part of the eigenvalues give the steady state oscillations of the disk whenever the real part of the eigenvalues is zero.

The frequency-speed diagram shows the nature of instabilities that occur. The stiffness instability appears as an interval above the value of speed equal to the critical speeds of the spinning elastic disk with no load.

It is found by algebraic analysis of the characteristic equation of the single mode system that the values of load mass which yield unstable solutions must be larger than that of the disk itself. This makes the instability due to the mass of the load valid only for cases of little practical interest. The terminal instability due to load damping is of interest because its boundary of instability is independent of the amount of damping present. It causes the solution to be

unstable for all speeds greater than those of the stiffness instability.

The ability to compute upper and lower bounds for the natural frequency of the spinning elastic disk is of particular value in the stability analysis. The nature of the stiffness instability is such that a bound on the natural frequency of the spinning disk can be used to establish the speed at which the onset of instability of the disk occurs.

IV. MULTIPLE MODE ANALYSIS OF SPINNING DISK

4.1 Introduction

In the previous chapter, the single mode approximation was studied and approximate stability criteria based on the eigenvalues corresponding to the single mode approximation were developed. In this chapter, the effect of additional modes in the assumed solution on the stability analysis will be developed.

The eigenvalue problem for a multiple mode system is derived and its eigenvalues are calculated numerically. It is shown by the frequency-speed diagram for the multiple mode approximation that the instabilities which exist in the single mode analysis also appear in the multiple mode analysis.

4.2 Formulation of Multiple Mode Approximation

The equation from Chapter II to be used here in the study of the stability of the solution to the multiple mode approximation is Equation (2.99). The system (2.99) is written here as a single equation:

$$\mathbb{m}\ddot{\underset{\sim}{z}}_N + \mathcal{A}\underset{\sim}{z}_N = \underset{\sim}{0} \qquad (4.1)$$

with,

$$\left.\begin{aligned} \mathcal{M} &= \begin{bmatrix} P_1 & \mathcal{G}_{12} \cdots & \mathcal{G}_{1N} \\ \mathcal{G}_{21} & P_2 & \vdots \\ \vdots & & \ddots \\ \mathcal{G}_{N1} & \cdots & P_N \end{bmatrix} \\ \mathcal{A} &= \begin{bmatrix} Q_1 & \mathcal{F}_{12} \cdots & \mathcal{F}_{1N} \\ \mathcal{F}_{21} & Q_2 & \vdots \\ \vdots & & \ddots \\ \mathcal{F}_{N1} & \cdots & Q_N \end{bmatrix} \\ \underset{\sim}{z}_N &= \begin{pmatrix} \chi_1 \\ \vdots \\ \chi_N \end{pmatrix} \end{aligned}\right\} \qquad (4.2)$$

where P_i, Q_i, $\mathcal{G}_{ij}$, $\mathcal{F}_{ij}$, are given by (2.100) and the χ_i, $i = 1, \ldots, N$ are given by (2.98).

Let a solution to (4.1) be of the form

$$\underset{\sim}{x}(t) = \underset{\sim}{\eta}\, e^{st} \qquad (4.3)$$

Then (4.1) reduces to an eigenvalue problem given by

$$s\,\mathcal{M}\,\underset{\sim}{\eta} + \mathcal{A}\,\underset{\sim}{\eta} = \underset{\sim}{0} \qquad (4.4)$$

If the substitution

$$\mathcal{A}^* = \mathcal{M}^{-1}\mathcal{A} \tag{4.5}$$

is made in (4.4) then the eigenvalue problem becomes

$$s\,\underset{\sim}{\eta} + \mathcal{A}^*\underset{\sim}{\eta} = \underset{\sim}{0} \tag{4.6}$$

For the case of a two mode approximation (4.6) becomes

$$s\,\underset{\sim}{\eta} + \begin{bmatrix} P_1 & \mathcal{G}_{12} \\ \mathcal{G}_{21} & P_2 \end{bmatrix}^{-1} \begin{bmatrix} \Omega_1 & \mathcal{F}_{12} \\ \mathcal{F}_{21} & \Omega_2 \end{bmatrix} \underset{\sim}{\eta} = \underset{\sim}{0} \tag{4.7}$$

4.3 Stability of the Multiple Mode Approximation

The solution of the eigenvalue problem (4.7) requires that

$$\det\{\mathcal{A}^* + sI\} = 0 \tag{4.8}$$

Since the order of the matrices in (4.8) is 4*N even a two mode approximation yields an eighth order polynomial for the characteristic values. Because of the size of the matrices involved, recourse is made to numerical techniques to obtain the eigenvalues of (4.7). Here as in Chapter III, a lower bound approximation will be made for the natural frequency μ_k in the matrices Ω_k.

Figure 13 shows the frequency-speed diagram of a spinning elastic disk with no loading. As in the case of the single mode approximation, an unstable solution results from the application of a constant load when the disk is rotating at one of its critical speeds.

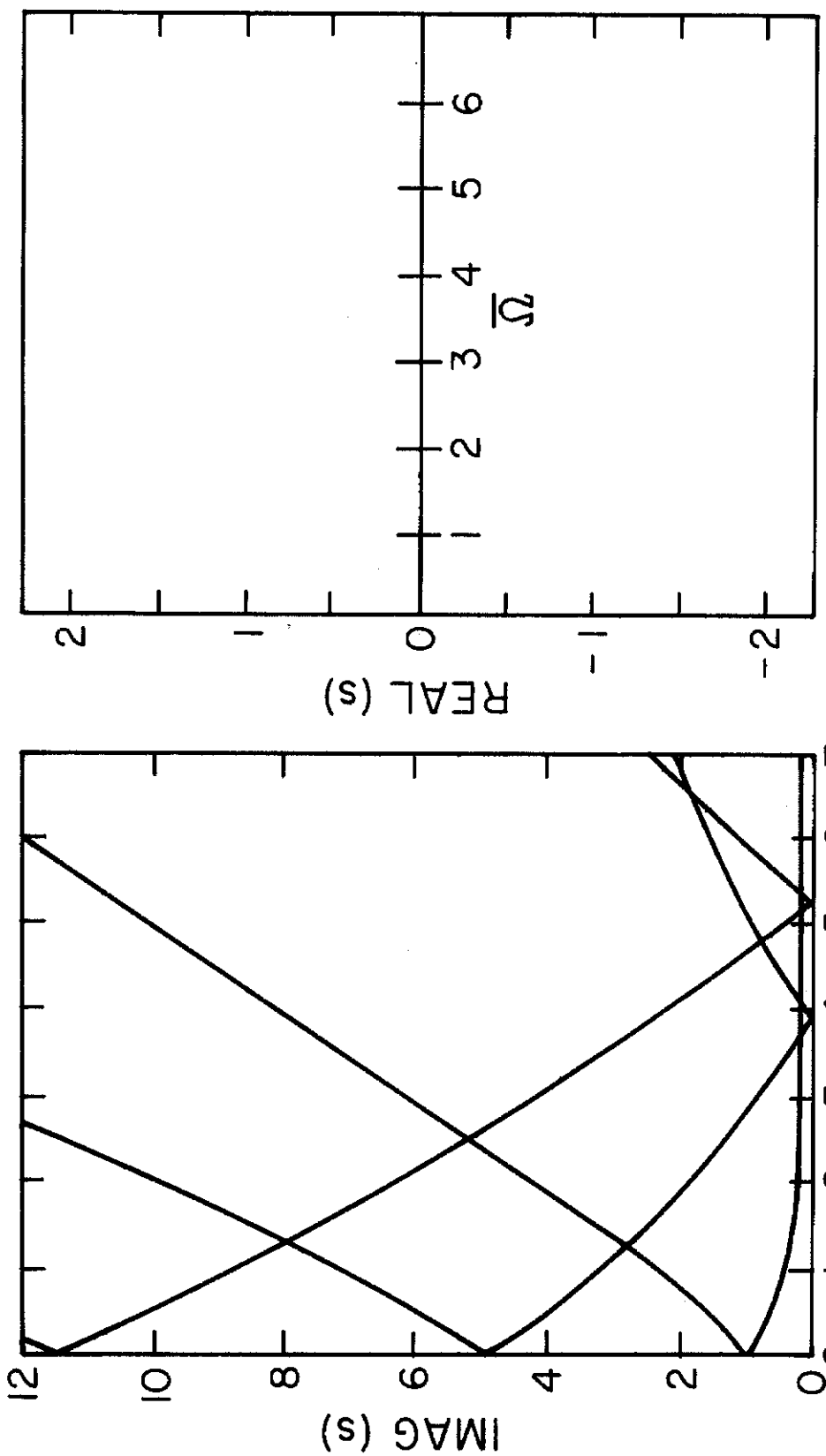

Fig. 13. Three-mode approximation of freely spinning disk ($m_L = c_L = k_L = 0$).

The critical speeds are given for the spinning elastic disk with no load, as the speeds for which a branch of the Imag(s) versus $\bar{\Omega}$ curve becomes zero.

The normalized critical speeds $\bar{\Omega}_n^*$ for the spinning disk are given in Table 4.1

	n = 1	n = 2	n = 3	n = 4
$\bar{\Omega}_n^*$	∞	4.06	5.35	7.06

Table 4.1 Critical Speeds

The approximate solution of the equation of motion is given by

$$u_N = \sum_{k=1}^{N} [A_k(t) \cos k\Phi + B_k(t) \sin k\Phi] \tilde{R}_k(r) \qquad (4.9)$$

Thus if one of the eigenvalues of (4.7) has positive real part, then the approximate solution (4.9) will be unstable.

4.4 Numerical Examples

The nature of the eigenvalues of a two-mode approximation with loading are given in the frequency-speed diagrams for the spinning disk in Figures 14 and 15.

In Figure 14 the normalized load parameters are given by $\bar{r}_L = .6$, $\bar{k}_L = 1.0$, $\bar{m}_L = .1$, $\bar{c}_L = 0$. In this two mode approximation, it is assumed that the solution is composed of modes having one and two modal diameters. These modes are used because they have the lowest critical speeds, and will yield instabilities at the lowest speeds.

The feature of interest regarding stability is that the real part of s becomes positive at two ranges of speed. The lower of these corresponds to the stiffness instability which was present in the single mode approximation. There, the instability resulted from the load parameter $\bar{k}_L$ being non-zero. In this two mode approximation this is also the case. The other interval in which the real part becomes positive occurs at the same speed at which the imaginary parts of s corresponding to the first and second mode intersect. Figure 14 shows that it is the reflected branch of the second mode which intersects an unreflected branch of the first mode curve. This instability does not appear in the single mode approximation and shall be called the modal coupling instability.

In Figure 15 the normalized load parameters are given by $\bar{r}_L = .6$, $\bar{k}_L = 1.0$, $\bar{c}_L = 2.0$, $\bar{m}_L = .1$. This two mode frequency-speed diagram shows the effect of load damping on the eigenvalues. The result of adding load damping is to reduce the size of the stiffness instability region, and to cause one of the eigenvalues to become positive and to continue to grow in magnitude as the speed increases. This behavior of the eigenvalues is analogous to that of the single mode approximation with load damping.

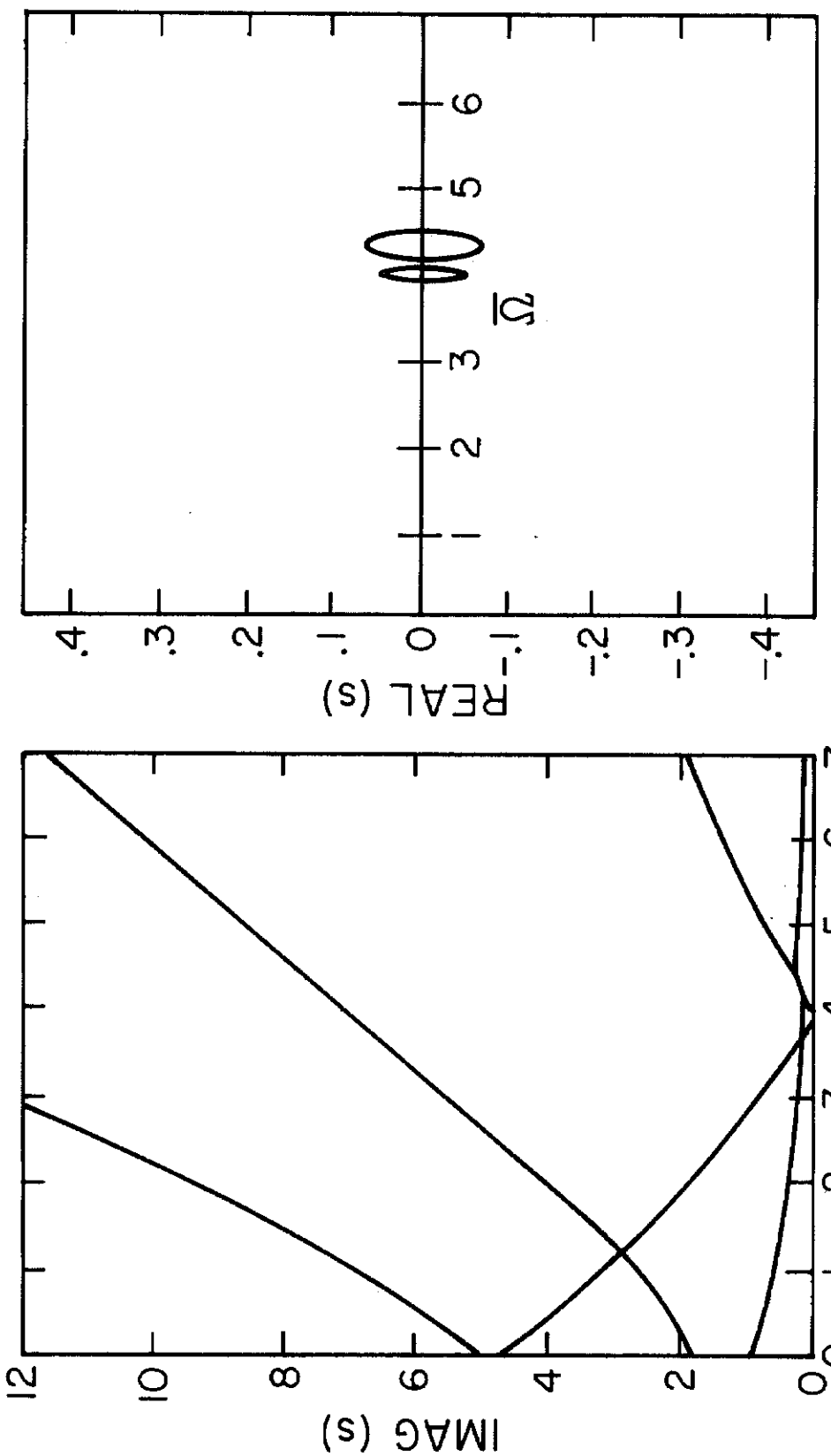

Fig. 14. Two-mode approximation of spinning disk ($\bar{r}_L = .6$, $\bar{m}_L = .1$, $\bar{c}_L = 0$, $\bar{K}_L - 1.0$).

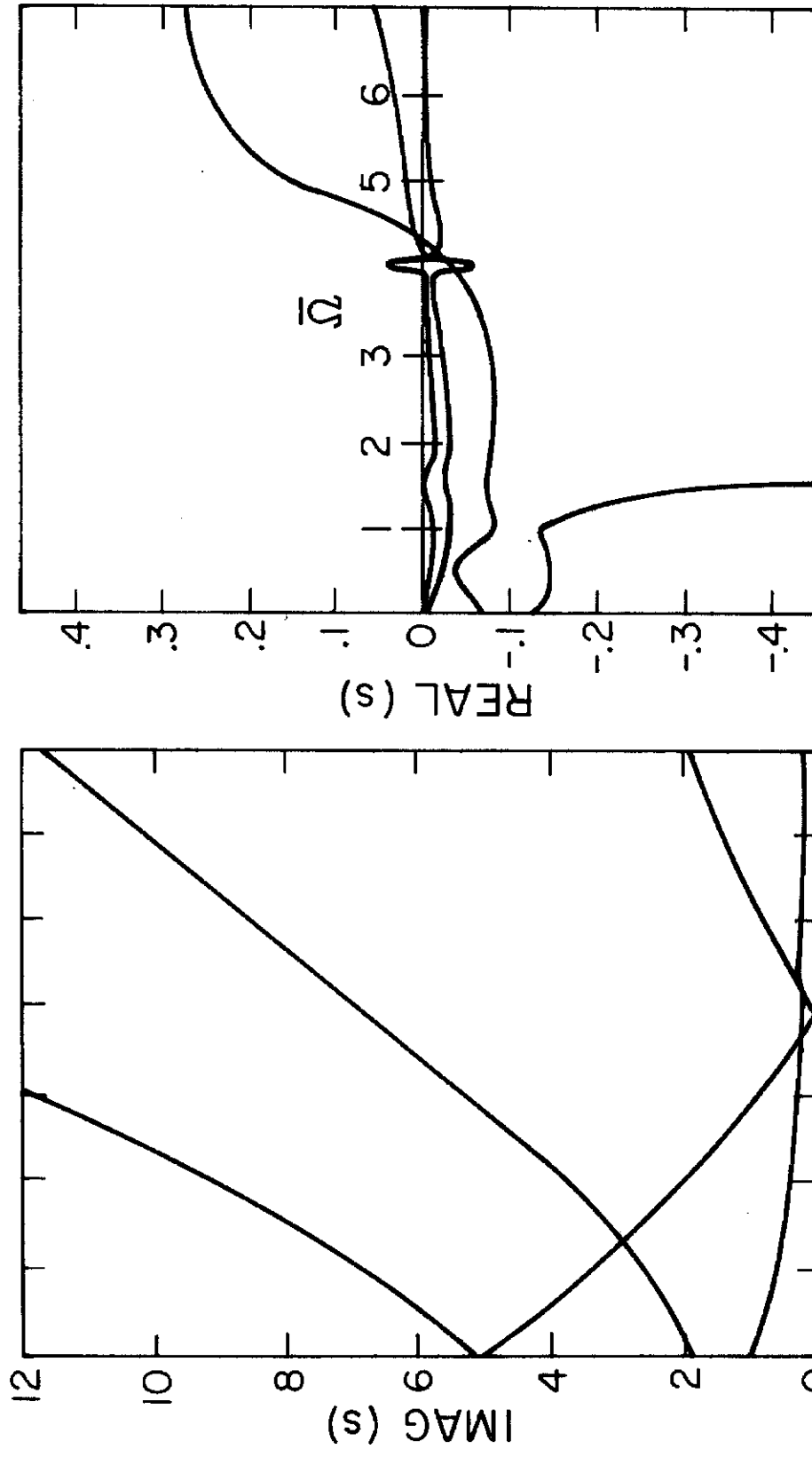

Fig. 15. Two-mode approximation of spinning disk with load damping ($\bar{r}_L = .6$, $\bar{m}_L = .1$, $\bar{c}_L = 2.0$, $\bar{k}_L = 1.0$).

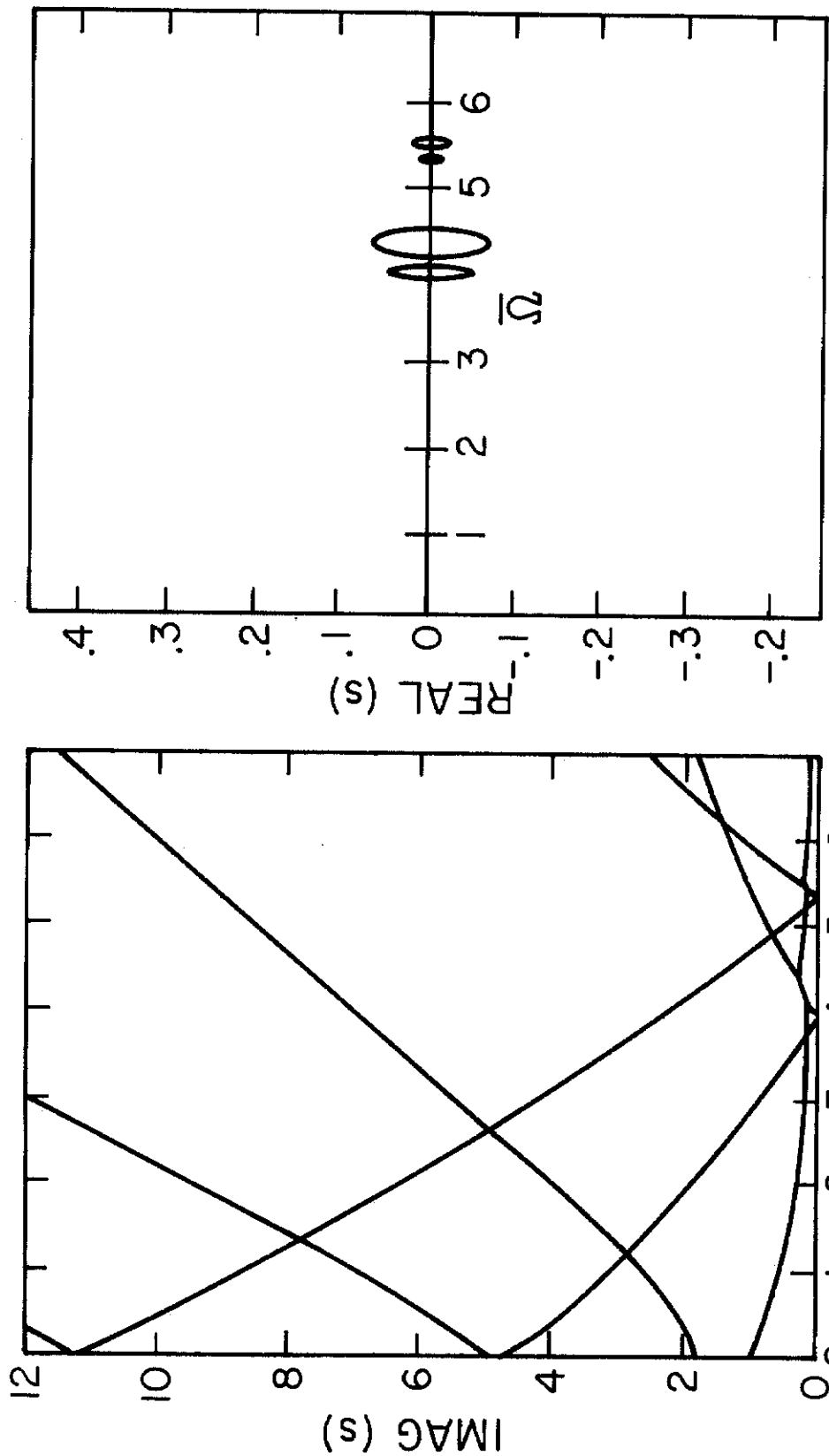

Fig. 16. Three-mode approximation of spinning disk ($\bar{r}_L = .6$, $\bar{m}_L = .1$, $\bar{c}_L = 0$, $K_L = 1.0$).

In the three mode approximation given in Figure 16, the load parameters are given by $\bar{r}_L = .6$, $\bar{k}_L = 1.0$, $\bar{c}_L = 0$, $\bar{m}_L = .1$. This frequency-speed diagram shows again the appearance of modal coupling instabilities. They appear at speeds for which reflected branches of the Imag(s) curves for the second and third modes intersect an unreflected branch of the first mode. Also appearing in this frequency-speed diagram are the stiffness instability regions which occur at speeds above each of the critical speeds.

4.5 Discussion

It is apparent from the frequency-speed diagrams for the two and three mode approximations that stiffness and damping instabilities analogous to the single mode analysis are present. However, also appearing in the multiple mode analysis are model coupling instabilities. These instabilities represent the contribution to the stability theory from the multiple mode approximation. It is thus clear from the analysis of the multiple mode approximation that the stability of the elastic disk cannot be taken as the superposition of single mode stability criteria.

V. COMPARISON OF STATIONARY AND SPINNING DISKS

5.1 Introduction

While the investigation up to this point has been motivated by the goal of including the effect of disk rotation, it is interesting to examine the system response when the centrifugal stress due to the rotation of the disk is neglected.

In the analysis of this chapter, the circular disk remains stationary, while the load system travels in a circular path around the disk. Systems of this type were studied by Iwan and Stahl [16] using an eigenfunction expansion. The effect of the load mass, spring, and damping caused instabilities at certain speeds. The present analysis differs from that of Iwan and Stahl in that approximate radial eigenfunctions are used in the expansion of the solution and the load is taken to be distributed over a finite area of the surface of the disk.

The goal of the analysis of this chapter has two parts. First, it is to show that the use of approximate radial eigenfunctions does not effect the qualitative nature of the stability analysis for the stationary disk. Second, is to show that the effect of rotation of the disk has a significant effect on the stability of the system.

Comparison with Iwan-Stahl [16] will be made to verify that the approximate eigenfunctions yield the same stability criteria for the stationary disk as do those of the exact eigenfunctions. The effect of disk rotation will be shown by comparison of the frequency-speed diagrams of this chapter with the frequency speed diagrams

of Chapter III and IV.

The set of radial eigenfunctions used in the previous analysis of Iwan and Stahl [16] were a complete set of functions which satisfied all the boundary conditions of the problem. They were eigenfunction of the biharmonic operator ∇^4 and were used in the expansion of the assumed solution. The approximate radial eigenfunctions used in the present analysis yield an upper bound for the natural frequencies appearing in the system equations. This has the effect of making the critical speeds greater than if exact natural frequencies were used. However, for the cases considered in this analysis, the error is on the order of .5%.

5.2 Formulation of the Stationary Disk System

The equation of motion for a stationary disk with a moving massive load system is given by

$$\left.\begin{aligned} &\rho u_{tt} + \frac{Eh^3}{3(1-\nu^2)}\nabla^4 u = \frac{1}{2\pi h} q(r, \theta, t) \\ &u = u_t = 0 \quad \text{at} \quad r = 0 \\ &\left.\begin{aligned} B_1 u &= 0 \\ B_2 u &= 0 \end{aligned}\right\} \text{ at } r = a \end{aligned}\right\} \tag{5.1}$$

with B_1 and B_2 given by (2.5).

The function $q(r, \theta, t)$ is the force per unit area applied to the disk by the moving mass-spring-damper system. The distributed load is given by

$$q(r,\theta,t) = \frac{H(r,\ \theta-\Omega t)}{A_L}\left[m_L\left(u_{tt} + 2\Omega u_{t\theta} + \Omega^2 u_{\theta\theta}\right) + c_L\left(u_t + \Omega u_\theta\right) + k_L u\right] \qquad (5.2)$$

with $H(\cdot\,,\cdot)$ given by (2.25) and A_L the area of the load.

Transforming the equation of motion given by (5.1) to a reference frame which rotates with the load yields the equation

$$\rho\left[u_{tt} - 2\Omega u_{t\Phi} + \Omega^2 u_{\Phi\Phi}\right] + L_2(u) = -\frac{1}{2h}\frac{H(r,\Phi)}{A_L}\left[m_L u_{tt} + c_L u_t + k_L u\right] \qquad (5.3)$$

$$u = u_t = 0 \quad \text{at} \quad r = 0$$

$$B_1 u = B_2 u = 0 \ \text{at} \ r = a$$

Using the same approximate radial eigenfunctions as for the spinning disk results in the approximate solution to (5.3)

$$\tilde{u}(r,\Phi,t) = \sum_{n=1}^{N}\left[A_n(t)\cos n\Phi + B_n(t)\sin n\Phi\right]\tilde{R}_n(r) \qquad (5.5)$$

with the $\tilde{R}_n(r)$ given by (2.75).

Applying Galerkin's method to the Equation (5.3) with the assumed solution (5.5) results in the system of equations:

$$\left.\begin{aligned}
&\ddot{B}_n(t) + 2\Omega n\,\dot{A}_n(t) + [\,\tilde{u}_n^{\,2} - \Omega^2 n^2\,]\,B_n(t) = \\
&\qquad \sum_{\substack{j=1\\ j\neq n}}^{N} W_{jn}^{(1)}\,[m_L\,\ddot{B}_j(t) + c_L\,\dot{B}_j(t) + k_L B_j(t)\,] \\
&\ddot{A}_n(t) - 2\Omega n\,\dot{B}(t) + [\,\tilde{u}_n^{\,2} - \Omega^2 n^2\,)\,A_n(t) = \\
&\qquad \sum_{\substack{j=1\\ j\neq n}}^{N} W_{jn}^{(2)}\,[m_L\,\ddot{A}_j(t) + c_L\,\dot{A}_j(t) + k_L A_j(t)\,]
\end{aligned}\right\} \qquad (5.6)$$

with $\tilde{u}_n^{\,2} = \langle L_2\,(R_2 \cos n\,\Phi),\ R_2 \cos n\,\Phi \rangle$ (5.7)

Let

$$\underset{\sim}{y}_n(t) = \begin{pmatrix} \dot{A}_n(t) \\ \dot{B}_n(t) \\ A_n(t) \\ B_n(t) \end{pmatrix} \qquad (5.8)$$

Then the system (5.6) may be written as

$$P_n\,\dot{\underset{\sim}{y}}_n + Q_n\,\underset{\sim}{y}_n = \sum_{\substack{e=1\\ e\neq n}}^{N} [\,\mathcal{F}_{en}\,\underset{\sim}{y}_e + \mathcal{G}_{en}\,\dot{\underset{\sim}{y}}_e\,] \qquad (5.9)$$

with P_n, Q_n, $\mathcal{F}_{en}$, $\mathcal{G}_{en}$ as given in (2.99)

and

$$\hat{Q}_n = \left[\begin{array}{cc|cc} c_1 & -2\bar{\Omega}n & (\tilde{\omega}_n^2 - \bar{\Omega}^2 n^2 + k_1) & 0 \\ +2\bar{\Omega}n & c_2 & 0 & (\tilde{\omega}_n^2 - \bar{\Omega}^2 n^2 + k_2) \\ \hline -1 & 0 & 0 & 0 \\ 0 & -1 & 0 & 0 \end{array}\right] \tag{5.10}$$

The question of the validity of using the radial eigenfunctions for the spinning disk in this approximation for the stationary disk is now investigated. As seen from Figure 4 when $\bar{\Omega} = 0$ the value of $\tilde{\omega}_n^2$ is equal to $(p_2^n)^2$ and the error from the exact natural frequency is less than $\frac{1}{2}\%$ for modes 1, 2, and 3. Thus even though the value of $(\tilde{p}_2^n)^2$ used in the analysis will be an upper bound of the exact value, the two are so close as not to change the results of the stability analysis.

It is shown by comparison of Fig. 17, 18, 20, 22 with those of Iwan-Stahl [16] that the use of approximate radial eigenfunctions does not alter the stability behavior.

5.3 Algebraic Analysis of the Single Mode Approximation

If it is assumed that the solution is of the form

$$\tilde{u} = [A_2(t) \cos 2\phi + B_2(t) \sin 2\phi\ ]\tilde{R}_2(r) \tag{5.11}$$

then the single mode approximation results in the characteristic equation

$$a_0 s^4 + a_1 s^3 + a_2 s^2 + a_3 s + a_4 = 0 \tag{5.12}$$

with a_i, $i = 1, 2, 3, 4$ given by (3.8).

Case 1 $(\bar{m}_L \neq 0,\ \bar{k}_L \neq 0,\ \bar{c}_L = 0)$

For this case the characteristic equation becomes

$$\begin{aligned}(1+m_1)(1+m_2)\, s^4 + \{&(1+m_1)[p_2^2 - n^2\bar{\Omega}^2 + k_2] \\ &+ (1+m_2)[p_2^2 - n^2\bar{\Omega}^2 + k_1] + 4n^2\bar{\Omega}^2\ \}\, s^2 \\ &+ [p_2^2 - n^2\bar{\Omega}^2 + k_1][p_2^2 - n^2\bar{\Omega}^2 + k_2\ ] = 0\end{aligned} \tag{5.13}$$

The zeroes of Equation (5.13) are the eigenvalues of the system (5.9). Thus the solution to (5.9) will be unstable if any of the roots of (5.13) have positive real parts. Analysis reveals that a sufficient condition for a root of (5.13) to have positive real part is that $\bar{\Omega}$ be such that

$$\frac{\sqrt{p_2^2 + k_2}}{n} < \bar{\Omega} < \frac{\sqrt{p_2^2 + k_1}}{n} \quad \text{for } n = 1, 2, \ldots \tag{5.14}$$

Further analysis reveals that if $\bar{m}_L$ is such that $m_1 > m_1^*$ with m_1^* a root of

$$(p_2^3 - n^2\bar{\Omega}^2)\, m_1^2 + [-3k_1\,(p_2^3 - n^3\,\bar{\Omega}^3)\,]m_1 + [\,(2p_2^3 + 2n^3\bar{\Omega}^3 + k_1)^3 - 4\,(p_2^3 - n^3\bar{\Omega}^3 + k_1)^3\,] = 0 \qquad (5.15)$$

then there exists a critical speed Ω_1^* such that for $\bar{\Omega} > \Omega_1^*$, the solution to (5.13) always has a root with positive real part.

Case 2 $(\bar{m}_L = 0,\ \bar{c}_L \neq 0,\ \bar{k}_L \neq 0)$

For the case of no load mass the characteristic equation becomes

$$s^4 + [c_1 + c_2]\, s^3 + [\,2p_2^3 - \{[\,p_2^3 - \bar{\Omega}^3 n^3 + k_1\,]c_2 + (p_2^3 - \bar{\Omega}^3 n^3 + k_1)c_1\,\}\, s + [\,p_2^3 - \bar{\Omega}^3 n^3 + k_1\,][\,p_2^3 - \bar{\Omega}^3 n^3 + k_2\,] = 0 \qquad (5.16)$$

A solution of the fourth order polynomial (5.16) which has positive real part implies that the solution to Equation (5.9) is unstable. As in Chapter III, the Routh Horwitz criteria may be used to establish that there exists on Ω_2^* such that for $\bar{\Omega} > \Omega_2^*$ there exist roots of (5.16) that have positive real parts.

The only two non-trivial criteria for the existence of positive real roots are that of $\Delta_2 > 0$ and $\Delta_3 > 0$. $\Delta_2 > 0$ yields

the stiffness instability region. $\Delta_3 > 0$ yields the terminal instability due to damping. Using Equation (3.34) with $\lambda_n = 0$, the term Δ_3 can be written as:

$$\Delta_3 = \{ [(c_1 c_2)^{\frac{1}{2}} (-n^2) - (c_1 c_2)^{\frac{1}{2}} (-n^2)]^2 + c_1^2 (-n^2) 4n^2 + c_1 c_2 (-n^2) 4n^2 + c_1 c_2 (-n^2) 4n^2 + c_2 (-n^2) 4n^2 \} \bar{\Omega}^4 + O(\bar{\Omega}^3) \quad (5.18)$$

$$\Delta^3 = \{ -4n^4 (c_1 + c_2) \} \bar{\Omega}^4 + O(\bar{\Omega}^3) \quad (5.19)$$

Since the coefficient of the highest power of $\bar{\Omega}$ is negative, the existence of a root of Equation (5.16) with positive real part is assured.

The algebraic analysis of the single mode equation has shown that the spring constant of the load causes an instability for an interval of speed above each of the critical speed of the stationary disk. It has also shown that the mass and damping of the load cause an unstable solution for speeds above certain terminal speeds. Finding these terminal speeds is the subject of the next section.

5.4 Numerical Examples

Figure 17 gives the frequency-speed diagram for a three mode approximation of the stationary disk with no loading. The solution is assumed to have the form

$$\tilde{u}_3 = \sum_{k=1}^{3} [A_n(t) \cos n\phi + B_n(t) \sin n\phi] \tilde{R}_n(r). \qquad (5.20)$$

This assumed solution results in the eigenvalue problem

$$[\lambda I + \alpha] \underset{\sim}{\eta} = \underset{\sim}{0} \qquad (5.21)$$

The solution of the matrix eigenvalue problem (5.21) is carried out numerically. The matrices involved are 12 x 12 and there are thus 12 eigenvalues generated for each value of $\bar{\Omega}$. For the case of no load, all eigenvalues of (5.21) are pure imaginary and occur in conjugate pairs. As was the case in the spinning disk analysis, each mode in the assumed solution has associated with it two eigenvalues. These correspond to a forward and backward traveling wave in the solution $\tilde{u}(r, \phi, t)$.

As can be seen in Figure 17, the eigenvalue for each mode corresponding to the backward traveling wave becomes zero at a rotation speed equal to the natural frequency p_2^n. As noted by Iwan-Stahl [16] Mote [19] and Lamb and Southwell [1], a constant transverse force applied to the disk while it is rotating at this speed $\bar{\Omega} = p_2^n$ causes a solution which has exponentially growing amplitude.

Figures 18 and 19 give a comparison of a single mode approximation for both the spinning and stationary disk. The first mode approximation of the stationary disk in Figure 18 shows both

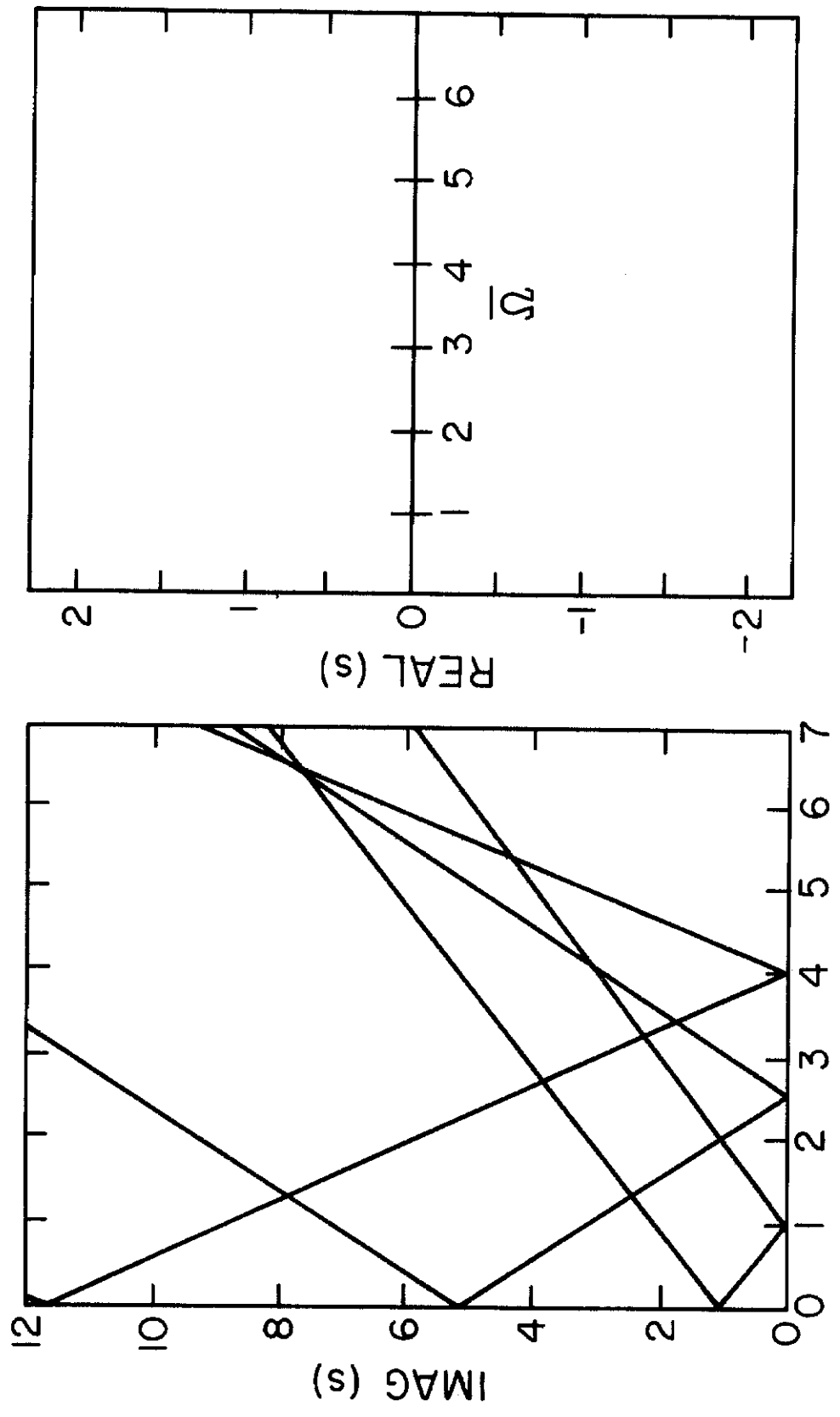

Fig. 17. Three-mode approximation for a stationary disk ($\bar{m}_L = \bar{K}_L = \bar{c}_L = 0$).

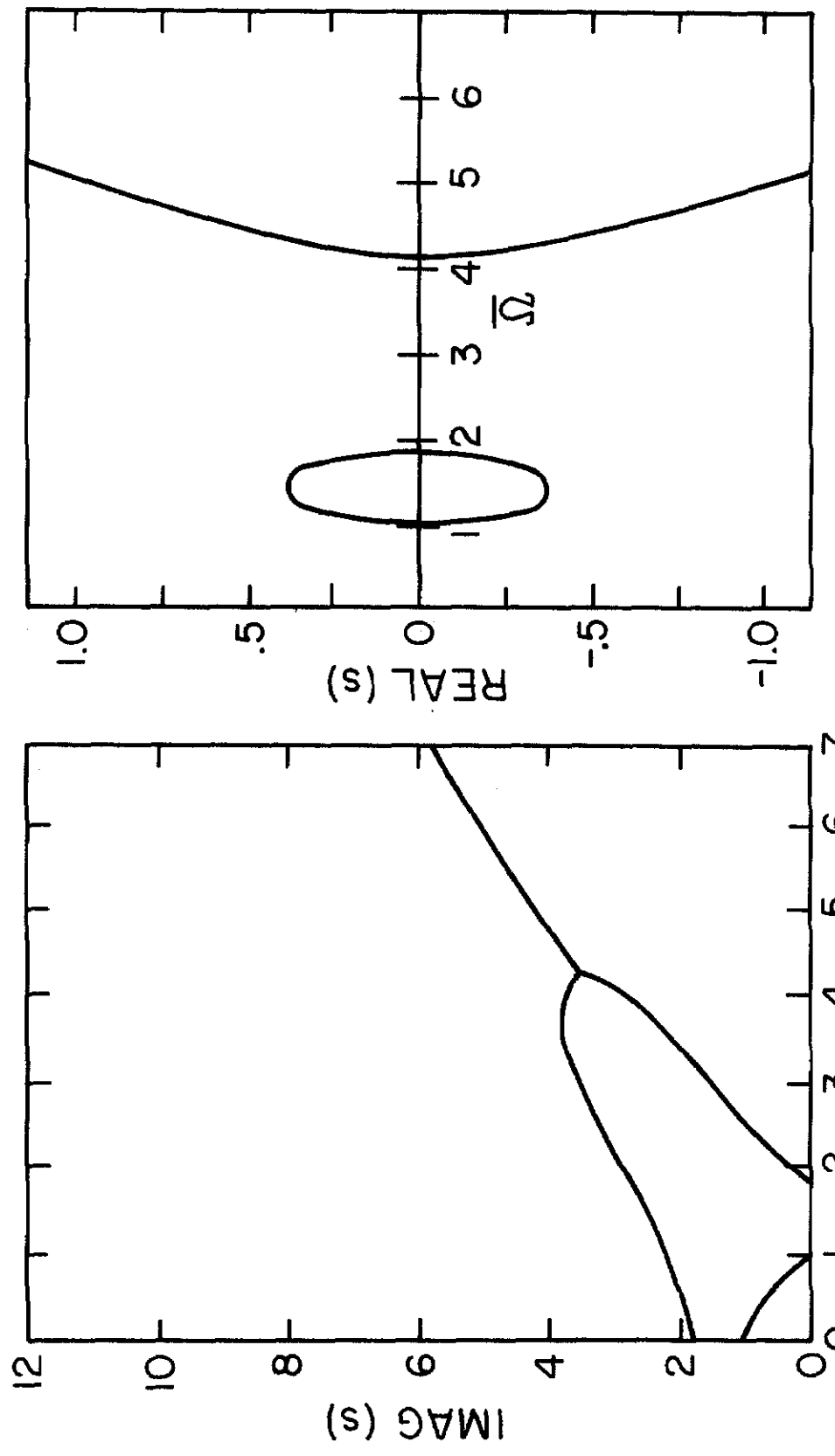

Fig. 18. Single-mode approximation for a stationary disk ($n = 1$, $\bar{m}_L = .1$, $\bar{c}_L = 0$, $\bar{K}_L = 1.0$, $\bar{r}_L = .6$).

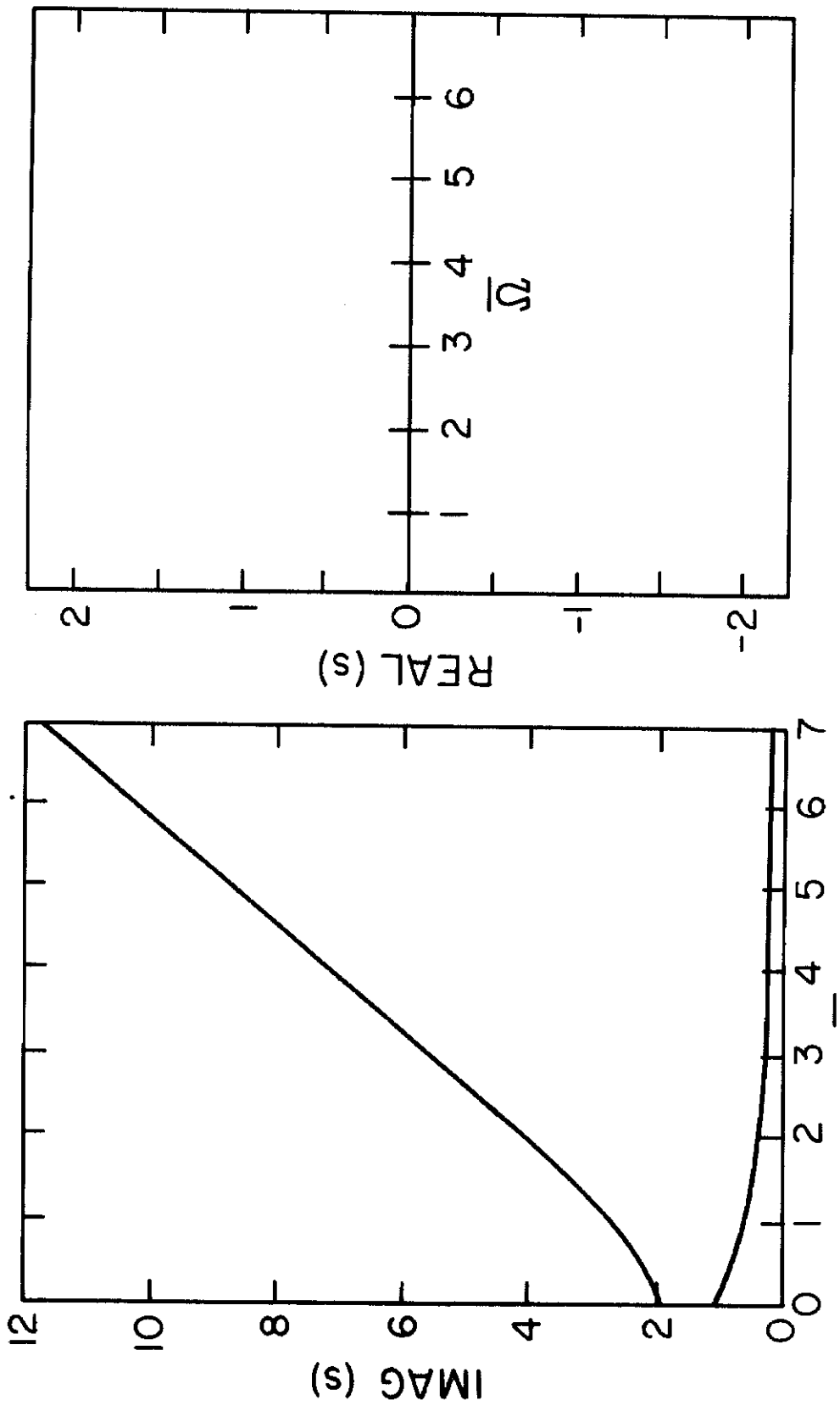

Fig. 19. Single-mode approximation for a spinning disk ($n = 1$, $\overline{m}_L = .1$, $\overline{c}_L = 1.0$, $\overline{K}_L = 1.0$, $\overline{r}_L = .6$).

the stiffness instability above the speed $\bar{\Omega} = p_2^2$ and the onset of the terminal instability at $\bar{\Omega} = 4.5$ caused by the load mass. These instabilities were predicted algebraically in section 5.3.

Figure 19 gives a single mode Frequency-Speed diagram for the spinning disk using the same mode n = 1. The eigenvalue corresponding to the backward traveling wave never becomes zero for the case of the spinning disk in the first mode. This is due to the inclusion of the centrifugal stresses in the equation of motion, and the form of this first mode curve is unaltered by the mass, spring, and damping of the load. Experimental results of Tabias [5] and Mote [19] confirm the form of this Frequency-Speed diagram for the first mode.

Figures 20 and 21 show a single mode approximation Frequency-Speed diagram for the stationary and spinning disk using the mode n = 2. The form of solution assumed in both cases is

$$\tilde{u}(r, \Phi, t) = [A_2(t) \cos 2\Phi + B_2(t) \sin 2\Phi]\tilde{R}_2(r) \qquad (5.23)$$

Since the shape of each single mode approximation for $n > 1$ is similar to that of the second mode, the qualitative difference between Figures 20 and 21 will also be true for single mode approximations with $n > 2$.

First consider the stiffness instability region of the two figures. In Figure 20 for the stationary disk, the region of instability is defined by

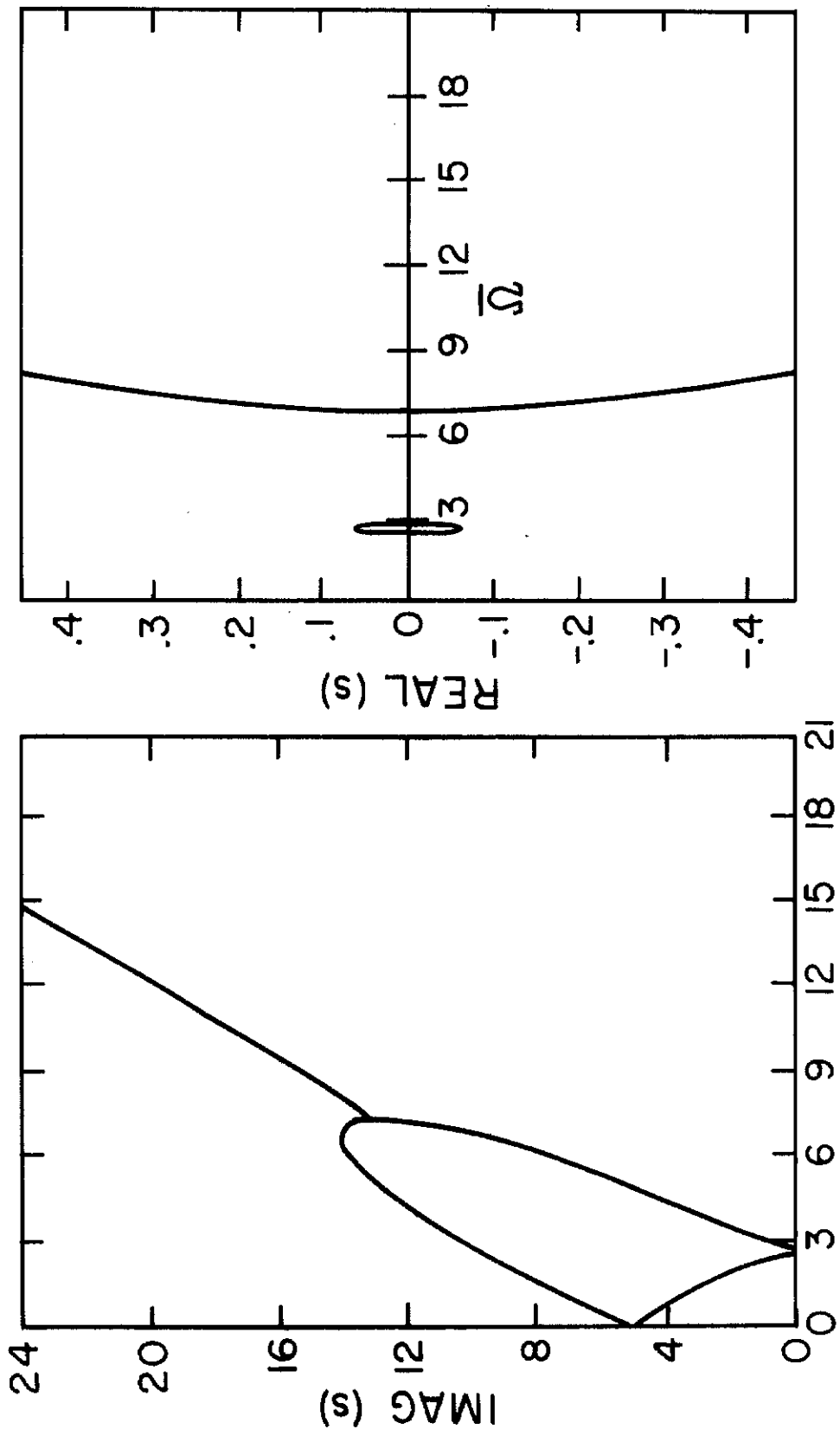

Fig. 20. Single-mode approximation for a stationary disk ($n = 2$, $\overline{m}_L = .1$, $\overline{\epsilon}_L = 0$, $\overline{K}_L = 1.0$, $\overline{F}_L = .6$).

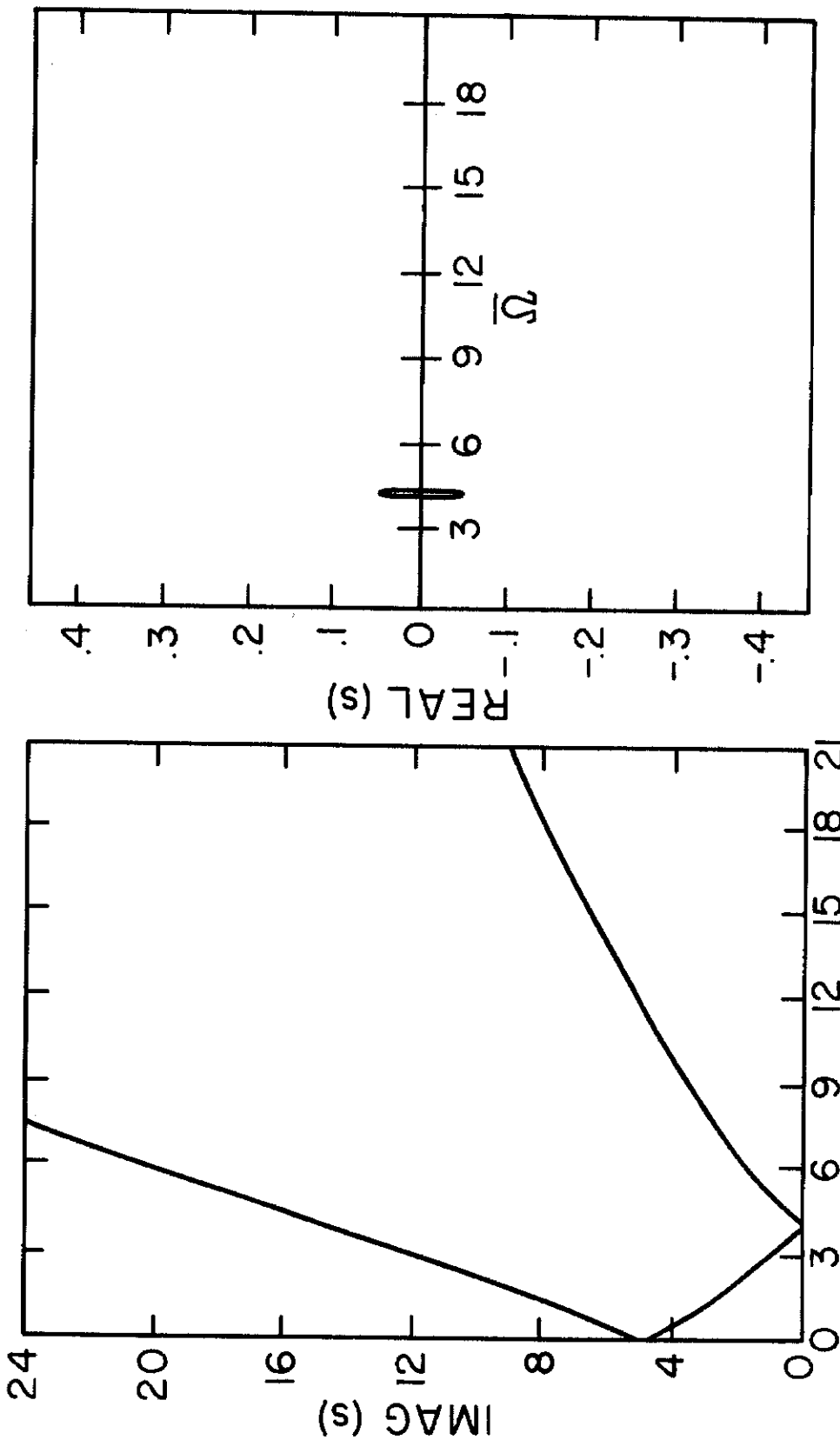

Fig. 21. Single-mode approximation for a spinning disk ($n = 2$, $\overline{m}_L = .1$, $\overline{\epsilon}_L = 0$, $\overline{K}_L = 1.0$, $\overline{F}_L = .6$).

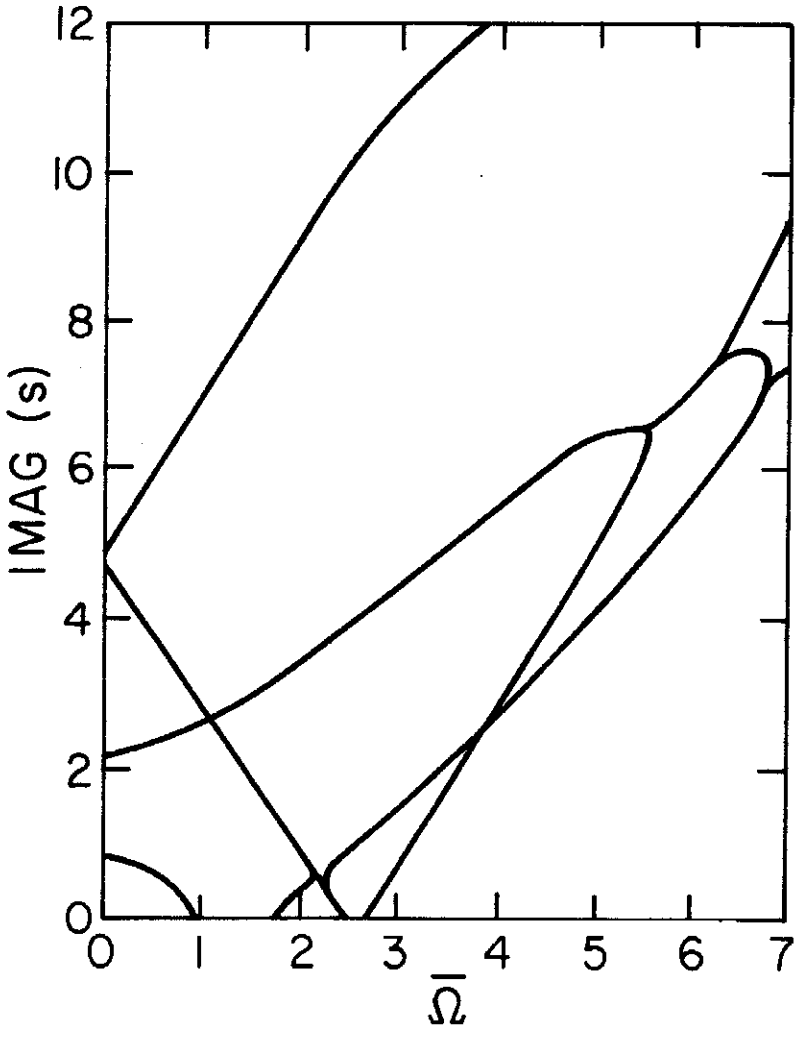

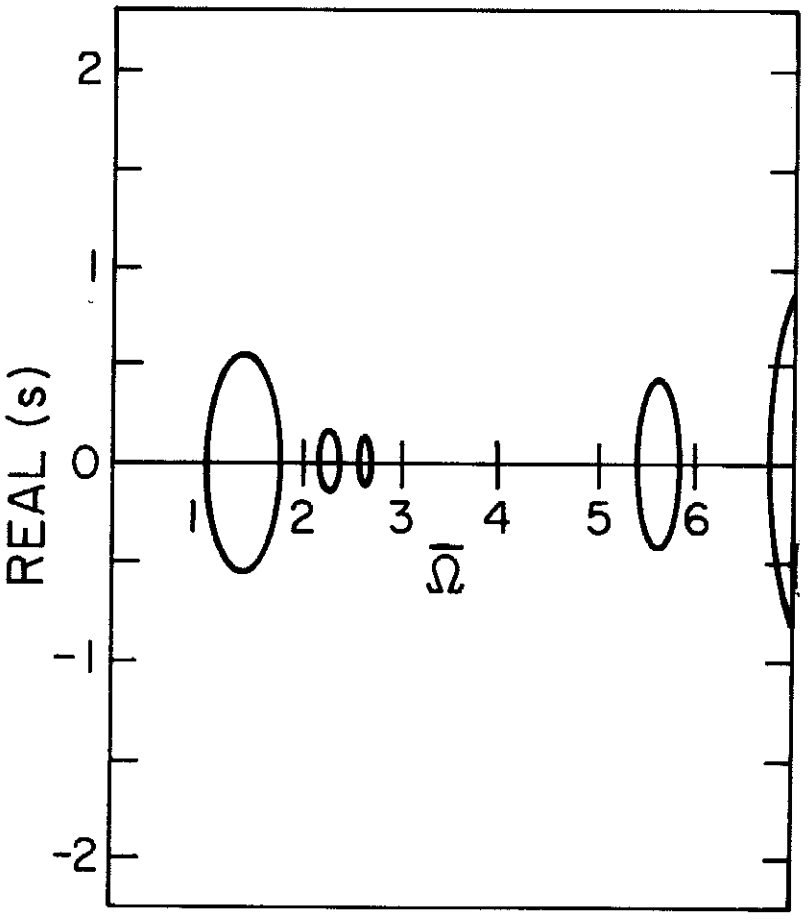

Fig. 22. Two-mode approximation of stationary disk ($r_L = .6$, $\bar{m}_L = .1$, $\bar{c}_L = 0$, $\bar{K}_L = 1.0$).

$$\frac{\sqrt{p_2^2 + k_1}}{2} < \bar{\Omega} < \frac{\sqrt{p_2^2 + k_1}}{2} \qquad (5.24)$$

For the spinning disk case, the instability occurs for $\bar{\Omega}$ such that

$$\sqrt{\frac{p_2^2 + k_1}{4 - \lambda_2}} < \bar{\Omega} < \sqrt{\frac{p_2^2 + k_1}{4 - \lambda_2}} \qquad (5.25)$$

It is seen that the inclusion of the centrifugal stress terms in the equation of motion causes a shift in the placement of the stiffness instability region. Negligible amounts of centrifugal stress reflected in an extremely small value of λ_2 cause the stiffness instability region of the spinning disk to revert to that of (5.24) for the stationary disk.

The major qualitative difference between the Figures 20 and 21 occurs for $\bar{\Omega} > 1$. The terminal instability due to the mass of the load in the stationary disk case does not appear in the spinning disk. The reason for this can be seen in the graphs for $\bar{m}_L$ versus critical speed in Figure 5. The instability due to the mass of the load in the spinning disk case occurs only for large values of $\bar{m}_L$ ($\bar{m}_L > 2.0$). However, the stationary disk analysis reveals that even for the system such as in Figure 21, an instability due to the mass of the load is present. This change in behavior at high speed is due to the inclusion of the centrifugal stress terms in the equation of motion.

Figure 22 shows the Frequency-Speed diagram for a stationary disk with mass and spring load using a two mode approximation. The solution is of the form

$$\tilde{u}(r, \Phi, t) = \sum_{n=1}^{2} [A_n(t) \cos n\Phi + B_n(t) \sin n\Phi] \tilde{R}_n(r) \qquad (5.26)$$

This figure may be compared to that of Figure 14 of Chapter IV for the two mode approximation of the spinning elastic disk with mass and spring load. The effect of modal coupling in the stationary disk is apparent in Figure 22, as displayed by the intersection of the reflected branch of the first mode and the unreflected branch of the second mode at rotational speed $\bar{\Omega} = 2.2$. The stiffness instability for the first mode of the stationary disk does not appear in the spinning disk and the instability due to the mass of the load at $\bar{\Omega} = 5.5$ for the stationary disk is also not present in the spinning disk.

5.5 Discussion

Analysis of the system of equations for the stationary disk using the eigenfunctions of the spinning disk problem has been carried out. A comparison with the results of the investigations of the stationary disk problem using exact eigenfunctions by Iwan and Stahl [16] shows no qualitative difference in the stability analysis due to the approximate eigenfunctions.

The centrifugal stress terms effect the dynamics of the disk in a significant manner. The load mass, spring, and dashpot cause no instabilities for the first mode of the spinning disk but cause instabilities for the stationary disk. For modes with two or more modal diameters, the terminal instability due to the load mass may be eliminated for the spinning disk by choosing the values of load mass sufficiently small. Also, for modes with two or more modal diameters, the stiffness instabilities for the spinning disk are shifted to higher speeds than those of the stationary disk.

The qualitative effect of the load damping and the modal coupling remains the same for both the spinning and stationary disk systems. The damping of the load causes the solution to be unstable for all speeds greater than the first stiffness instability region. A modal coupling instability occurs at speeds for which a reflected branch of one mode intersects an unreflected branch of another mode.

VI. STABILITY AND ERROR BOUND ANALYSIS

6.1 Introduction

The N-mode approximations of Chapters II through Chapter V yield stability criteria for the system of equations defined by Equation (2.98). These stability criteria represent approximate criteria for the solution to the equation of motion. Since it is not possible to obtain a closed form representation for the eigenvalues of the full infinite set of equations, the approach taken here is to first analyze the partial differential equation of motion from the standpoint of the direct stability methods of Liapunov. They will be used to verify the stability of the system at low speeds of rotation. The instabilities given by the N-mode approximation arise from the fact that there is at least one eigenvalue of the system matrix which has positive real parts. Error bound techniques will be employed to show that the eigenvalues of the full infinite matrix also have positive real parts.

The matrix error bound results are based on a number of theorems on nxn matrices. These theorems are generalized to infinite matrices and techniques are developed to relate the eigenvalues of the N-mode approximation to the eigenvalues of the infinite matrices.

The error bound result is used to analyze the approximate eigenvalues obtained from the spinning disk analysis.

6.2 Liapunov Analysis of Stability for Stationary and Spinning Disks

The advantage of the direct stability method of Liapunov is that the stability of the solution to an equation may be analyzed without solving the equation. Direct stability techniques have been used by Movchan [21], Lee et al [24], and others [25], [26], [27], in applications to partial differential equations.

The goal of this section is to establish the stability of the solution to the equation of motion for both the spinning and stationary disk at speeds below a certain critical speed, and at all speeds for the case $u_\theta = 0$.

6.2.1 Basic Definitions and Theorems

DEF 1 (positive definite)

Let R be a metric space with metric $d(\cdot,\cdot)$ and elements a, b, ...

Let $a(\cdot)$ be a function which maps $[t_0, \infty)$ into R,

Let BVP be the set of all $a(\cdot)$ such that $a(\cdot)$ satisfies a given boundary value problem,

Let $f(\cdot)$ be a functional which maps R into real numbers, $\hat{a}(\cdot) \in$ BVP

We say $f(\cdot)$ is positive definite with respect to BVP and $\hat{a}(\cdot)$ if

$$\forall \epsilon > 0 \text{ and } \forall a(\cdot) \in \text{BVP} \ni d(\hat{a}(\cdot), a(t)) > \epsilon \ \forall t \in [t_0, \infty)$$

$$\exists \mu(\epsilon) \ni \cdot f(a(t)) \geq \mu(\epsilon) \ \forall t \in [t_0, \infty) \text{ with } \mu > 0.$$

DEF 2 (infinitessimal upper bound)

Let R, BVP, f, and $\hat{a}(\cdot)$ be as in definition 1.

We say that f admits an infinitesimal upper bound with respect to BVP and $\hat{a}(\cdot)$ if

$$\forall \mu > 0 \; \exists \; \delta(\mu) > 0 \quad \ni \; |f(a(t))| < \mu \; \forall \; t \in [t_o, \infty) \quad \text{and}$$

$$\forall \, a(\cdot) \in BVP \ni d(\hat{a}(\cdot), a(t)) < \delta$$

DEF 3 (non-increasing)

Let R, BVP, f be as in definition 1.

We say that f is non-increasing with respect to BVP if

$$\frac{d}{dt} f \; (a(t)) \leq 0 \quad a(\cdot) \in BVP \quad \text{and} \quad \forall \; t \in [t_o, \infty)$$

DEF 4 (Liapunov function)

Let R, BVP, $\hat{a}(\cdot)$ be as in definition 1.

Let $f(\cdot)$ be a functional on R.

We say $f(\cdot)$ is a Liapunov functional with respect to BVP and $\hat{a}(\cdot)$ if the following properties hold:

(i) $f(\cdot)$ is finite positive with respect to BVP and $\hat{a}(\cdot)$ if

(ii) $f(\cdot)$ admits an infinitesimal upper bound

(iii) $f(\cdot)$ is non-increasing with respect to BVP.

DEF 5 (stability)

Let R, BVP, $\hat{a}(\cdot)$ be as in definition 1.

We say that $\hat{a}(\cdot)$ is stable if

$$\forall \in > 0 \exists \delta > 0 \ni d \, (\hat{a}(\cdot), \; a(t)) < \in \forall \, t \in [t_o, \infty) \quad \text{and}$$

$$\forall \; a(\cdot) \in BVP \ni a(t_o) = a_o \quad \text{and} \quad d(\hat{a}(\cdot), \; a_o) < \delta$$

THEOREM 6.1 (stability)

Let R, BVP, and $\hat{a}(\cdot)$ be as in definition 1.

If $\exists$ a Liapunov functional on R with respect to BVP and $\hat{a}(\cdot)$ then $\hat{a}(\cdot)$ is stable.

Proof The proof of the theorem may be found in Movchan [21].

6.2.2 Stability of Stationary Disk With Moving Load

The equation of motion for a stationary elastic disk with a spring and mass load system which rotates in concentric circles about the disk is given by (5.1) and boundary conditions (5.2). The solution to (6.1) shall be investigated by the Liapunov Theory.

Let $u(r, \theta, t)$ solve (5.1) and the boundary conditions (5.2). Define the elements of a space M to be

$$a = \left[u(r, \theta, t^*), \ \frac{\partial u}{\partial t}(r, \theta, t^*) \right] \tag{6.1}$$

for some fixed time $t^* \in [0, \infty)$.

Let the space M be composed of all such "a" for all $t^* \in [0, \infty)$ with metric $d: M \times M \to \mathbf{R}$ defined by

$$d(a,b) = \left\{ \iint_D \left[|u-v|^2 + |u_r - v_r|^2 + |u_\theta - v_\theta|^2 + |u_{rr} - v_{rr}|^2 + |u_{\theta\theta} - v_{\theta\theta}|^2 + |u_t - v_t|^2 \right] dA \right\}^{\frac{1}{2}} \tag{6.2}$$

for every $a, b \in M$ such that

$$a = [\, u(r, \theta, t_1), \quad u_t(r, \theta, t_1) \,] \tag{6.3}$$

and $\quad b = [\, v(r, \theta, t_2), \quad v_t(r, \theta, t_2) \,]$

To define the boundary value problem subset of M, let $a(t): [t_0, \infty) \to M \ni$

$$a(t) = [\, u(r, \theta, t_1), \quad u_t(r, \theta, t_1) \,] \tag{6.4}$$

Let $BVP \in M$ be defined as

$$BVP = \{a(t) \mid a(t) = [u(r,\theta,t), \; u_t(r, \theta, t) \,] \text{ with } u \ni \tag{6.5}$$

$$u \text{ satisfies (6.1) and}$$

$$u \text{ satisfies (6.2)} \}$$

$a(t)$ is called a trajectory in the metric space M.

To define the functional f on the metric space M let

$$f(a) = \iint_D \{u_t^2 + V_2(u) + \frac{H(r, \theta)}{A_L}[m_L u_t^2 - \Omega u_\theta^2 + k_L u \,]\} dA \tag{6.6}$$

with

$$V_2 = \frac{Eh^2}{3(1-\nu^2)} \{(\nabla^2 u)^2 + 2(1-\nu)[(\frac{1}{r} u_{r\theta} - \frac{1}{r^2} u_\theta)^2 - u_{rr}(\frac{1}{r^2} u_{\theta\theta} + \frac{1}{r} u_r)]\} \tag{6.7}$$

To show that f is a Liapunov functional it must be shown that f is positive definite, that f admits an infinitesimal upper bound and that f is non-increasing with respect to BVP.

First consider whether f is positive definite. That is, does there exist γ_1 such that $f(a) \geq \gamma_1 d(\hat{a}, 0)$.

Using (6.10) in (6.9), f may be written as

$$f(a) = \iint_D \{ u_t^2 + \frac{H(r,\theta)}{A_L} [m_L u_t^2 + k_L u] - \frac{H(r,\theta)}{A_L} m_L (\Omega^2 u_\theta^2) + \frac{Eh^2}{3(1-\nu^2)} \frac{1}{r^4} u_\theta^2 + \frac{Eh^3}{3(1-\nu^2)} [(\nabla^2 u)^2 - 2(r\nu) u_{rr} (\frac{1}{r^2} u_{\theta\theta} + \frac{1}{r} u_r)] \} dA \tag{6.8}$$

All terms in the integrand of (6.8) are positive for all values of Ω except the terms involving u_θ^2. The coefficient of u_θ^2 will be positive for $\Omega < \Omega^*$ where

$$(\Omega^*)^2 = \frac{Eh^3}{3} \frac{2(1-\nu)}{(1-\nu^2)} / \frac{m_L}{A_L} \tag{6.9}$$

Thus f is positive definite for all values of $\Omega < \Omega^*$.

To show that f admits an infinitesimal upper bound observe that

$$f(a) \leq \iint_D \{ u_t^2 + \frac{1}{A_L} [m_L u_t^2 + k_L u^2] + V_1(u) \} dA \tag{6.10}$$

Let

β = max coefficient of any term in integrand of (6.11). (6.11)

then

$$f(a) \leq \beta \iint_D \{ u_t^2 + u^2 + u_r^2 + u_\theta^2 + u_{rr}^2 + u_{\theta\theta}^2 + u_{r\theta}^2 \} dA$$

$$= \beta\, d(a, 0) \tag{6.12}$$

and f admits an infinitesimal upper bound.

To show that f is non-increasing with respect to BVP:

$$\frac{d}{dt} f(a) = \frac{d}{dt} \iint_D \{ u_t^2 + \frac{H(r, \theta)}{A_L} [m_L (u_t^2 - \Omega^2 u_\theta^2) + k_L u^2] + V_2(u) \} dA \tag{6.13}$$

Integration by parts implies that

$$\frac{d}{dt} f(a) = \iint_D 2 u_t \{ u_{tt} + L_1 u + \frac{H(r, \theta)}{A_L} [m_L (u_{tt} + \Omega^2 u_{\theta\theta}) + k_L u] \} dA$$

$$= \iint_D 2 u_t \{ - \frac{H(r, \theta)}{A_L} m_L u_{\theta t} \} dA$$

$$= \iint_{A_L} 2 u_{\theta t} u_t \, dA$$

$$= 0 \tag{6.14}$$

Thus, the conditions of the stability theorems are satisfied for $\Omega < \Omega_1^*$, and the solution to equation (5.1) will remain bounded for all $t > 0$.

6.2.3 Stability of the Spinning Disk With Stationary Load

The equation of motion for the spinning disk with no load damping is given by

$$u_{tt}+[L_1+L_2](u) = \frac{H(r,\theta)}{A_L}\left[m_L(u_{tt}-2\Omega u_{\theta t}+\Omega^2 u_{\theta\theta})+k_L u\right] \qquad (6.15)$$

If the same metric space is used as previously, then consider the functional f defined by

$$f(a) = \iint_D \left\{u_t^2+V_1(u)+V_2(u)+\frac{H(r,\theta)}{A_L}\left[m_L(u_{tt}-\Omega u_\theta^2)+k_L u^2\right]\right\} dA \qquad (6.16)$$

with V_1 and V_2 given by (2.71) and (2.72).
Arguments similar to those for the stationary disk can be used to show that f is non-increasing and admits an infinitesimal upper bound.

To show for what values of Ω f is positive definite we write

$$\begin{aligned} f(a) = \iint_D \Big\{ & u_t^2+\frac{H(r,\theta)}{A_L}\left[m_L u_t^2+k_L u^2\right] \\ & +\frac{H(r,\theta)}{A_L} m_L\Omega^2 u_\theta^2+\frac{Q(r)}{r^2}u_\theta^2+\frac{Eh^2}{3(1-\nu^2)}2(1-\nu)\frac{1}{r^4}u_\theta^2 \\ & +p(r)u_r^2+\frac{Eh^2}{3(1-\nu^2)}\left[(\nabla^2 u)^2-u_{rr}\left(\frac{1}{r^2}u_{\theta\theta}+\frac{1}{r}u_r\right)\right]\Big\} dA \end{aligned} \qquad (6.17)$$

The only non-positive terms in the integrand of (6.17) involve u_θ^2. Thus f is positive definite for all Ω if $u_\theta = 0$. Also, f is positive

definite for every $\Omega < \Omega_2^*$ where

$$(\Omega_2^*)^2 = \frac{E h^2}{3(1-\nu^2)} \frac{2(1-\nu)}{l} / \left[\frac{m_L}{A_L} - Q_{min}\right] \qquad (6.18)$$

Note that this will be a higher value of Ω^* than for the stationary disk due to the Q term.

Thus for speeds of disk rotation such that $\Omega < \Omega_2^*$ the solution to Equation (6.15) will be stable.

6.3 Matrix Error Bound Theory

Error bounds for approximate eigenvalues of infinite matrices are derived in this section. The error bounds are obtained from an extension of the Gershgorin error bound theorem for finite matrices.

An error bound for the eigenvalues of an infinite matrix A, with components a_{ij}, can be found using Gershgorin's Theorem.

Theorem 6.2 (Gershgorin)

Every eigenvalue λ of an infinite matrix A satisfies at least one of the inequalities

$$|\lambda - a_{ii}| \leq \sum_{\substack{j=1 \\ j \neq i}}^{\infty} |a_{ij}| \qquad i = 1, 2, \ldots \qquad (6.19)$$

with the assumption that the infinite series of (6.19) converge.

The proof may be found in Franklin [30] for the case of finite matrices.

To see how Theorem 6.2 may be used, consider the infinite real

matrix $\mathcal{A}$ given by

$$\mathcal{A} = \left[\begin{array}{c|c} A^N & B^N \\ \hline C^N & A^\infty \end{array}\right] \tag{6.20}$$

with A^N an $N \times N$ matrix.

There exists an orthogonal matrix p^N such that

$$(p^N)^T \; A^N \; p^N = \tilde{A}^N \tag{6.21}$$

with $\tilde{A}^N$ an upper triangular matrix.

Let

$$\mathcal{P} = \left[\begin{array}{c|c} p^N & 0 \\ \hline 0 & I \end{array}\right] \tag{6.22}$$

with

$$I = \begin{bmatrix} 1 & & \\ & \ddots & 0 \\ & \ddots & 1 \\ 0 & & \ddots \end{bmatrix} \tag{6.23}$$

Consider the matrix $\tilde{\mathcal{A}}$ defined by

$$\tilde{\mathcal{A}} = \mathcal{P}^T \; \mathcal{A} \; \mathcal{P} \tag{6.24}$$

$$\tilde{\mathcal{A}} = \left[\begin{array}{c|c} A^N & (p^N)^T \; B^N \\ \hline C^N \, p^N & A^\infty \end{array}\right] \tag{6.25}$$

Let

$$\tilde{\lambda}_k = a_{kk}, \quad k = 1, \ldots, N \tag{6.26}$$

Using (6.26) in $\tilde{\mathcal{A}}$ yields

$$\tilde{\mathcal{A}} = \left[\begin{array}{c|c} \begin{matrix} \tilde{\lambda}_1 & & \neq 0 \\ & \ddots & \\ 0 & & \tilde{\lambda}_N \end{matrix} & (p^N)^T B^N \\ \hline C^N p^N & A^\infty \end{array}\right] \tag{6.27}$$

Call $\{\tilde{\lambda}_k^{(N)}\}_{k=1}^N$ the Nth order approximate eigenvalues of the matrix $\mathcal{A}$.

Assuming the infinite series converge, let

$$d_k = \sum_{\substack{j=1 \\ j\neq k}}^{\infty} |\tilde{a}_{kj}| \quad k = 1, 2, \ldots \tag{6.28}$$

Using (6.27) in (6.28) implies

$$d_k = \begin{cases} \sum_{j=1}^{\infty} |(p^N)^T B^N)_{kj}| + \sum_{j=k+1}^{N} |\tilde{a}_{kj}^N| & \text{for } k < N \\ \sum_{j=1}^{\infty} |(p^{N^T} B_N)_{kj}| & \text{for } k = N \\ \sum_{j=1}^{N} |(C^N p^N)_{kj}| + \sum_{\substack{j=1 \\ j\neq k}}^{\infty} |a_{jk}^\infty| & \text{for } k > N \end{cases} \tag{6.29}$$

The approximate eigenvalues are plotted in the complex plane and disks D_k of radius d_k are constructed about each of the approximate eigenvalues $\tilde{\lambda}_k$. Thus, let

$$D_k = \{ z \in \mathbb{C} \mid |z - \tilde{\lambda}_k| < d_k \} \quad k = 1, 2, \ldots \tag{6.30}$$

Corollary

Let $\mathcal{A}$ be an arbitrary infinite matrix, and let D_k be as in (6.30). If

$$D_k \cap D_n = \phi \quad \forall \; k \neq n, \tag{6.31}$$

then there exists an exact eigenvalue λ of $\mathcal{A}$ within D_n. The proof may be found in Franklin [30] for finite matrices.

Then,

$$| \tilde{\lambda}_n - \lambda | \leq d_n \tag{6.32}$$

and d_k represents an error bound for the approximate eigenvalue $\hat{\mu}_n$.

6.4 Error Bound Theory Applied to Spinning Disk System

To relate the Gershgorin error bound analysis to the N-mode approximation of the spinning disk equation of motion, assume there exist eigenvalues of the infinite mode system related to Equation (4.1) written for the case $m_L = 0$ as

$$(\mathcal{A}^N + \mathcal{B}^N)\, \underset{\sim}{\eta} = \lambda \underset{\sim}{\eta} \tag{6.33}$$

with

$$\mathcal{A}^N = \begin{bmatrix} A^N & & O & \\ & Q^{N+1} & & \\ & & Q^{N+2} & \\ O & & & \ddots \end{bmatrix}$$

and

$$\mathcal{B}^N = \begin{bmatrix} O & B^N & & \\ C^{N+1} & O & B^{N+1} & \\ C^{N+2} & & O & B^{N+2} \\ \vdots & & & \ddots \end{bmatrix} \qquad (6.34)$$

with A^N, Q^k given by (4.2) and (2.100) respectively, and B^k; $k = 1, \ldots$ and C^k; $k = 1, 2, \ldots$ given by

$$B^N = \begin{bmatrix} \mathcal{F}_{1(N+1)} & \mathcal{F}_{2(N+2)} \cdots \\ \vdots & \\ \mathcal{F}_{N\ N+2} & \mathcal{F}_{N\ N+2} \cdots \end{bmatrix}$$

$$B^k = \begin{bmatrix} \mathcal{F}_{k(k+1)} & \mathcal{F}_{k\ k+2} \cdots \end{bmatrix} \text{ for } k > N \qquad (6.35)$$

and

$$C^k = \begin{bmatrix} \mathcal{F}_{k\ 1} & \mathcal{F}_{k\ 2} \cdots & \mathcal{F}_{k\ k-1} \end{bmatrix} \text{ for } k > N$$

with $\mathcal{F}_{ij}$ given by (2.100).

Assume ∃ an N such than $(\mathcal{A}^{N_1})^{-1}$ .Operating on (6.33) with $(\mathcal{A}^{N_1})^{-1}$

$$[\,(\mathcal{A}^{N_1})^{-1}\mathcal{B}^{N} - \lambda\,(\mathcal{A}^{N_1})^{-1}\,]\,\underset{\sim}{\eta} = -\,\underset{\sim}{\eta} \tag{6.36}$$

Assume $\lambda \neq 0$, and let

$$\mu = \frac{1}{\lambda} \tag{6.37}$$

Using (6.37) in (6.36) implies

$$[\,(\mathcal{A}^{N_1})^{-1} - \mu\,(\mathcal{A}^{N_1})^{-1}\mathcal{B}^{N}\,]\,\underset{\sim}{\eta} = \mu\underset{\sim}{\eta} \tag{6.38}$$

Consider the approximate eigenvalue problem associated with (6.38) as

$$(\mathcal{A}^{N_1})^{-1}\,\eta^{N} = \hat{\mu}\,\eta^{N} \tag{6.39}$$

From the form of the matrix $(\mathcal{A}^{N_1})^{-1}$ it is clear that $4N$ eigenvalues of the system (6.39) correspond to the $4N$ eigenvalues of the finite system

$$(A^{N_1})^{-1}\,\underset{\sim}{\xi} = \mu\underset{\sim}{\xi} \tag{6.40}$$

and the rest of the eigenvalues of (6.39) are found from

$$(\Omega^{k})^{-1}\,\underset{\sim}{\xi} = \mu\underset{\sim}{\xi}\,, \quad k > N\,. \tag{6.41}$$

Let the matrix $\mathcal{T}^{N}$ triangularize $(\mathcal{A}^{N_1})^{-1}$. Thus, a similarity transformation of the left hand side of (6.38) yields

$$(\mathcal{P}^N)^T\,[(\mathcal{A}^N)^{-1} - \mu(\mathcal{A}^N)^{-1}\mathcal{B}^N\,]\,\mathcal{P}^N$$

$$= \begin{bmatrix} \hat{\mu}_1 & & \neq 0 & & - \mu (p^N)^T \hat{B}_N \\ & \ddots & & & \\ 0 & & \hat{\mu}_{4N} & & \\ \hline -\mu \hat{C}^{N+1} p^{N+1} & & \hat{\mu}_{4N+1} & & \mu (p^{N+1})^T \hat{B}_{N+1} \\ & & \ddots & & \\ & & & \hat{\mu}_{4N+4} & \\ \hline \vdots & & \vdots & & \vdots \end{bmatrix} \qquad (6.42)$$

with

$$\mathcal{P}^N = \begin{bmatrix} p^N & & & 0 \\ & p^{N+1} & & \\ & & p^{N+2} & \\ 0 & & & \ddots \end{bmatrix} \qquad (6.43)$$

where p^N triangularizes A^N and p^k triangularizes $Q^k \; \forall \; k > N$

and

$$\left.\begin{aligned} \hat{B}_N &= (A^N)^{-1} B_N \\ \text{and} \quad \hat{B}_k &= (Q^N)^{-1} B_k \quad \forall \; k > N \\ \text{and} \quad \hat{C}_k &= (Q^N)^{-1} C_k \quad \forall \; k > N \end{aligned}\right\} \qquad (6.44)$$

Let $(p^N)^T (\hat{B}^N) = (b_{ij})$

Let a_{ij} be the off diagonal elements of $(p^N)^T (A^N)^{-1} p^N$ (6.45)

Let D_k be the kth Gershgorin circle of the matrix (6.42) with radius d_k.

The following theorem gives error bounds for the approximate eigenvalues of the infinite matrix (6.42):

Theorem 6.3

$\exists$ an exact eigenvalue μ of Equation (6.38) such that

$$|\mu - \tilde{\mu}_n| \leq \tilde{d}_n \tag{6.46}$$

where

$$\tilde{d}_k = \frac{|\hat{\mu}_n| \left(\sum_{\substack{j=1 \\ j \neq k}}^{\infty} |b_{kj}| \right) + \left(\sum_{j=1}^{4N} |a_{kj}| \right)}{1 - \sum_{\substack{j=1 \\ j \neq k}}^{\infty} |b_{kj}|} \quad ; \quad \sum_{j=1}^{\infty} |b_{kj}| < 1 \quad , \quad k = 1, 2, \ldots$$

provided

$$\tilde{D}_k \cap \tilde{D}_n = \phi \qquad \forall \; k \neq n$$

where

$$\tilde{D}_k = \left\{ z \in \mathbb{C} \mid |z - \hat{\mu}_k| \leq \tilde{d}_k \right\} \qquad k = 1, 2, \ldots$$

Proof

By definition of the Gershgorin circles,

$$d_k = |\mu| \left(\sum_{j=1}^{\infty} |b_{kj}| \right) + \sum_{\substack{j=1 \\ j=k}}^{4N} |a_{kj}| \ .$$

The triangle inequality implies

$$d_k \le |\mu - \hat{\mu}_n| \left(\sum_{j=1}^{\infty} |b_{kj}| \right) + |\hat{\mu}| \left(\sum_{j=1}^{\infty} |b_{kj}| \right) + \sum_{\substack{j=1 \\ j=k}}^{4N} |a_{kj}|$$

Assume that

$$D_k \cap D_n = \phi \quad \forall \ k \neq n \tag{6.47}$$

Then the corollary to Gershgorin's theorem implies

$$d_n \ge |\mu - \hat{\mu}_n|$$

and

$$|\mu - \hat{\mu}_n| \le d_n \le |\mu - \hat{\mu}_n| \left(\sum_{j=1}^{\infty} |b_{nj}| \right) + |\hat{\mu}_n| \left(\sum_{j=1}^{\infty} |b_{nj}| \right) + \sum_{\substack{j=1 \\ j \neq n}}^{4N} |a_{nj}| \tag{6.48}$$

Let

$$\tilde{d}_k = \frac{|\hat{\mu}_n| \left(\sum_{j=1}^{\infty} |b_{kj}| \right) + \sum_{\substack{j=1 \\ j \neq k}}^{4N} |a_{kj}|}{1 - \sum_{j=1}^{\infty} |b_{kj}|} \qquad k = 1, 2, \ldots$$

Then from (6.48)

$$|\mu - \hat{\mu}_n| \le \tilde{d}_n \ .$$

To check the assumption (6.47) note that

$$d_k \leq \tilde{d}_k \quad k = 1, 2, \ldots$$

$$\Rightarrow \quad D_k \subset \tilde{D}_k \quad k = 1, 2, \ldots$$

By hypothesis $\tilde{D}_k \cap \tilde{D}_n = \phi \ \forall \ k \neq n$. Thus $D_k \cap D_n = \phi \ \forall \ k \neq n$ and the assumption is valid.

Q. E. D.

Theorem 6.3 will now be used to find error bounds for a modal coupling instability of the spinning disk. In order for $\tilde{d}_n$ to be an error bound for $\hat{\mu}_n$ it must be established that no other Gershgorin circle $\tilde{D}_k$ $(k \neq N)$ intersects $\tilde{D}_n$. For the case of the spinning elastic disk, individual cases shall be treated.

For the modal coupling instability between the second and first mode, at speed $\bar{\Omega} = 4.325$ the eigenvalues of $(A^N)^{-1}$ for $N = 4$ are given in Fig. 23. Since the eigenvalues for $(A^N)^{-1}$ satisfy

$$|\hat{\mu}_k| \to 0 \quad \text{as} \quad k \to \infty \tag{6.49}$$

and since $\tilde{d}_k$ for $k > 16$ satisfy

$$\tilde{d}_k \leq (\gamma + \hat{\mu}_{17}) \cdot \left(\sum_{j=1}^{\infty} |b_{nj}| \right) \leq (\gamma + \hat{\mu}_{17}) \, \| \hat{B}^N \| \tag{6.50}$$

then

$$\tilde{d}_k < \tilde{d}_{17} \quad \forall \ k > 4N \tag{6.51}$$

and all Gershgorin circles $\tilde{D}_k$, $k > 17$ lie within D_{17}.

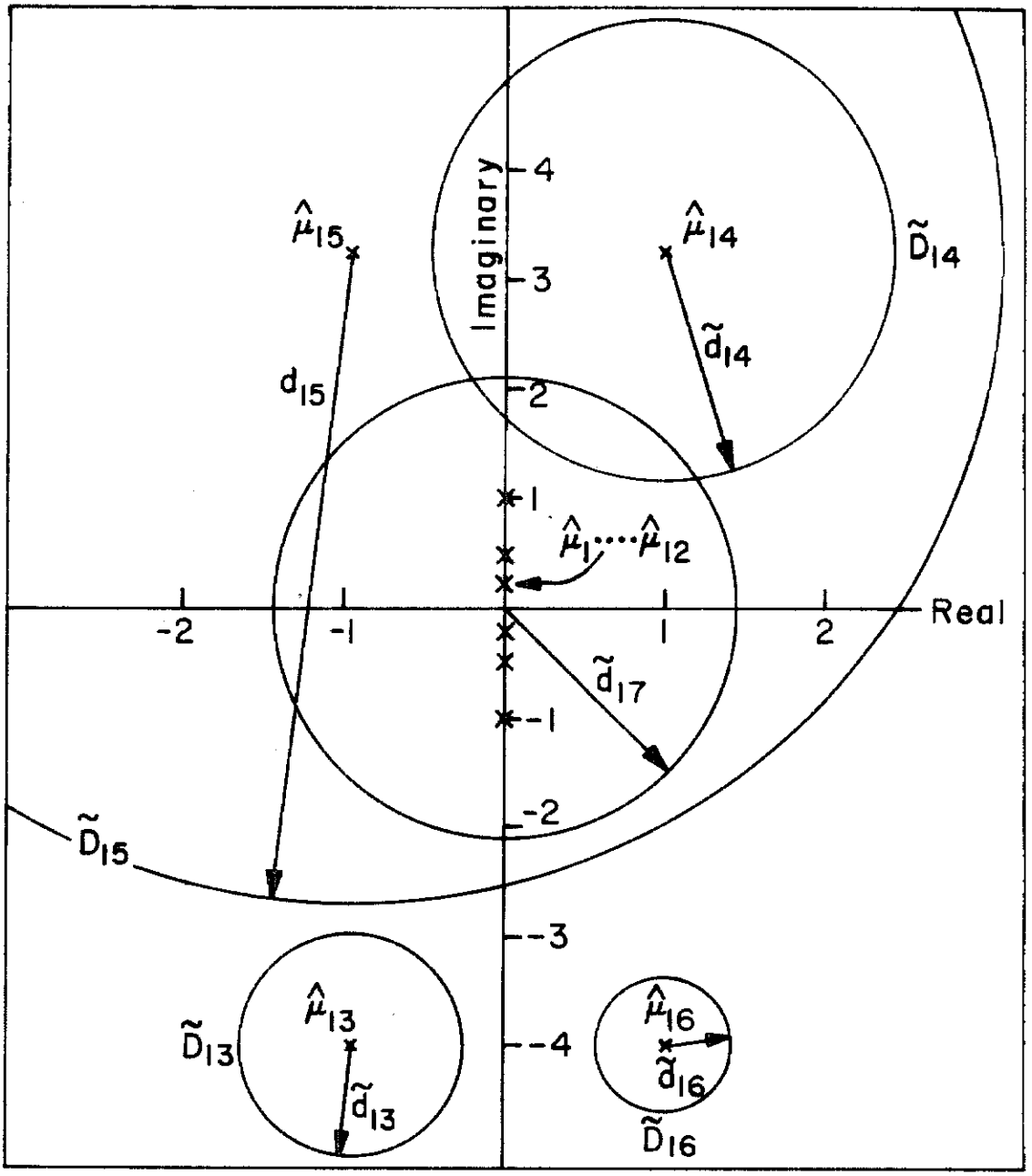

Fig. 23. Error bounds for the eigenvalues of $(a^N)^{-1}$.

Since

$$\tilde{D}_k \cap \tilde{D}_{16} = \phi \quad \forall \; k \neq 16 \tag{6.52}$$

then an exact eigenvalue μ_{16} of the system (6.38) lies within $\tilde{D}_{16}$ and

$$|\mu_{16} - \hat{\mu}_{16}| \leq \tilde{\alpha}_{16} \tag{6.53}$$

Since

$$\text{Real } (\hat{\mu}_{16}) > \tilde{\alpha}_{16} \tag{6.54}$$

it is concluded that

$$\text{Real } (\mu_{16}) > 0 \; . \tag{6.55}$$

Using (6.37) and (6.55) it follows that there exists an eigenvalue λ_{16} of (6.36) which satisfies

$$\text{Real } (\lambda_{16}) > 0 \; . \tag{6.56}$$

Thus the solution to the original infinite system of equations (6.36) is unstable. The error bound for $\hat{\lambda}_{16}$ becomes

$$D_{16}^{\lambda} = \{ z \in \mathbb{C} \mid \frac{1}{z} \in \tilde{D}_{16} \} \tag{6.57}$$

Figure 24 shows this region D_{16}^{λ} corresponding to the eigenvalue $\hat{\lambda}_{16}$ of the modal coupling instability. Figure 25 shows this error bound projected onto the real and imaginary parts of the frequency-speed diagram for this case.

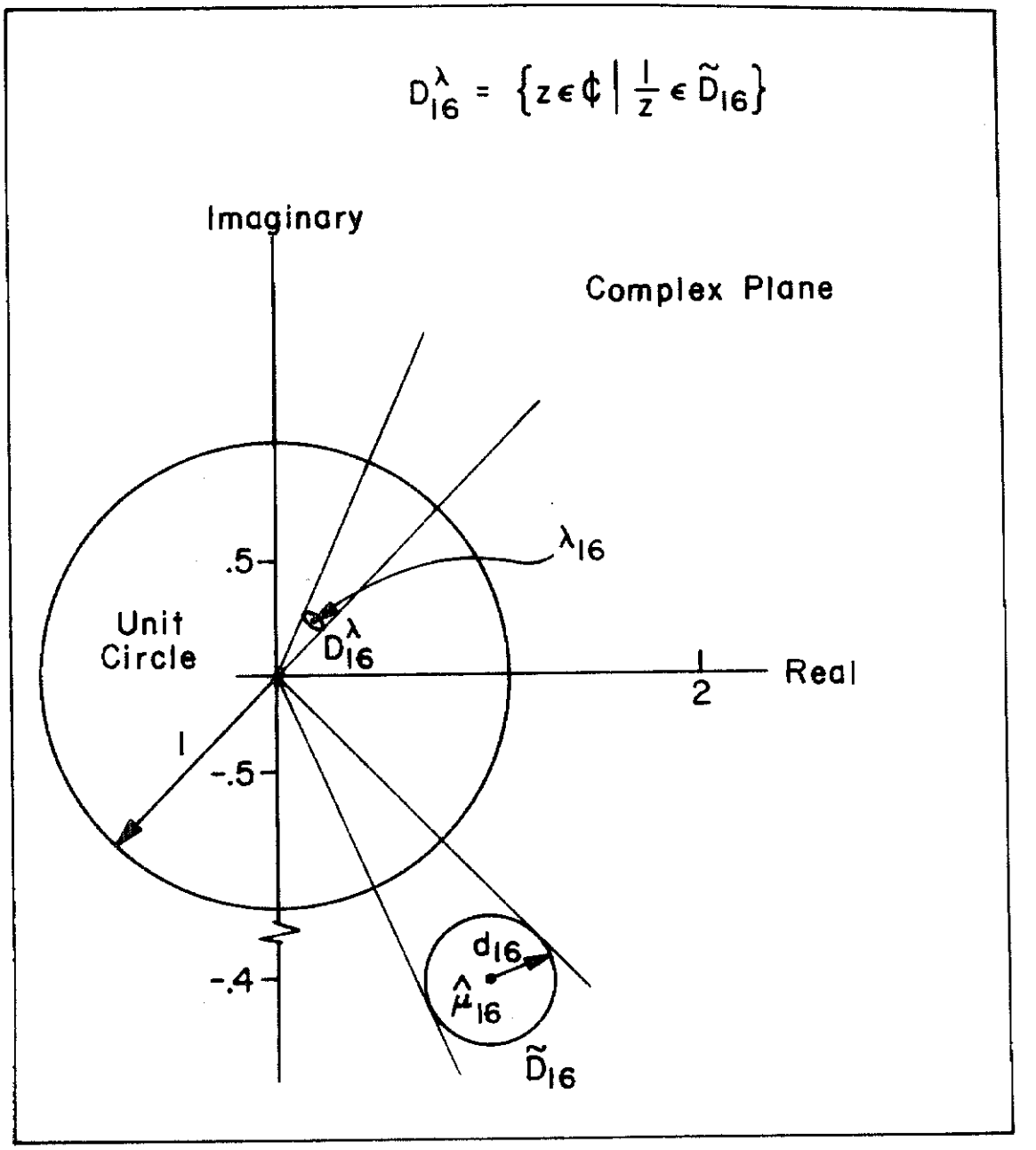

Fig. 24. Error bound for λ_{16} an eigenvalue of $\mathcal{A}^N$.

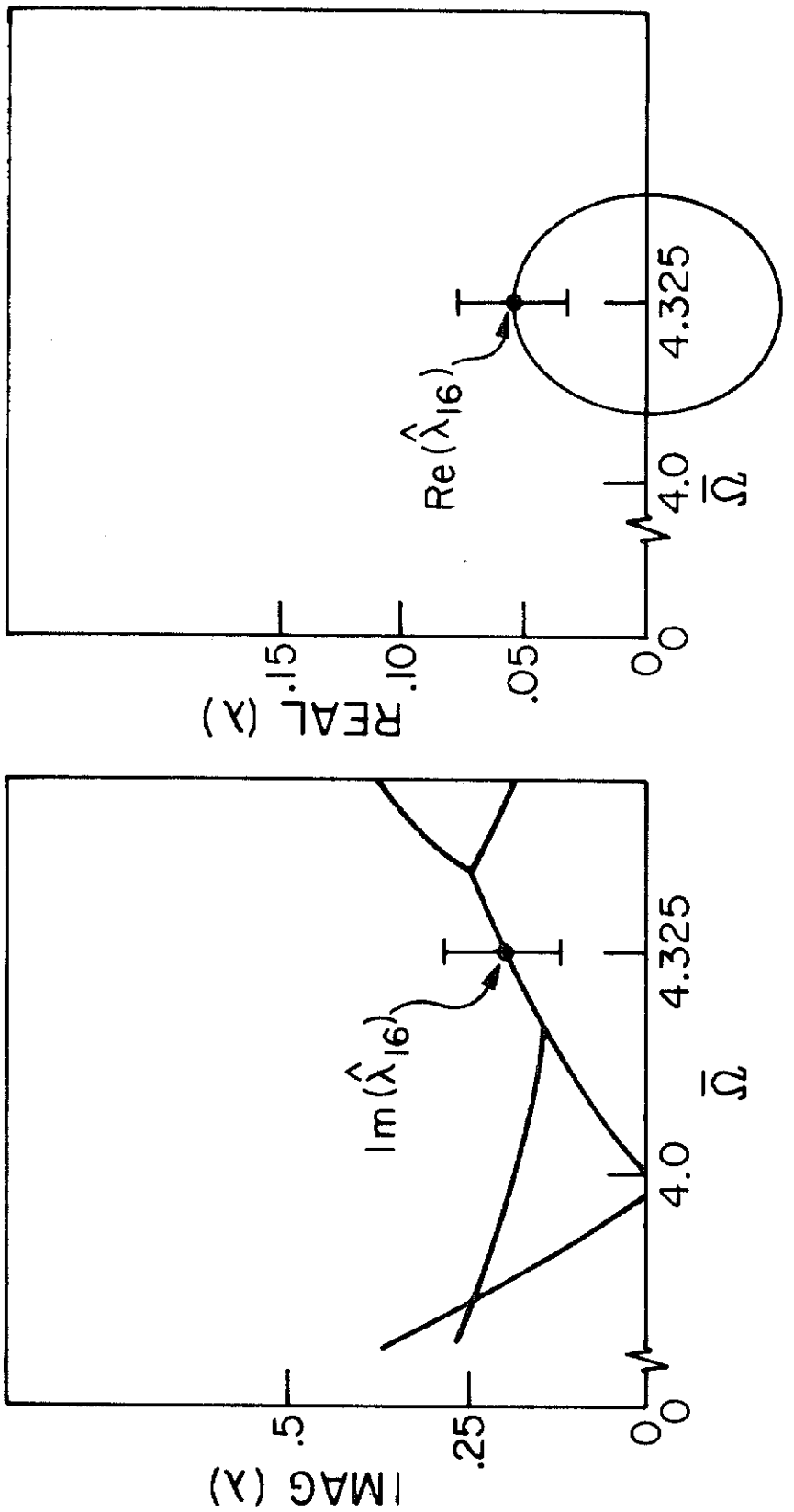

Fig. 25. Frequency-speed diagram for model coupling instability of spinning disk.

6.5 Discussion

In the present investigation, the use of direct stability methods is limited to proving stability at low speed for the spinning disk and stationary disk systems. Since the direct stability analysis gives critical speeds that are much lower than those of the modal analysis, and since the direct stability theorems could not be applied for speeds greater than the critical speeds, other stability methods were also used.

The advantage in using the $(\mathcal{A}^{N_1})^{-1}$ matrix in the error bound analysis is two fold. First, the off-diagonal terms in the triangularized $(\mathcal{A}^{N_1})^{-1}$ matrix are smaller than those of the triangularized $(\mathcal{A}^{N_1})$ matrix. This results in a smaller error bound for the eigenvalues of the $(\mathcal{A}^{N_1})^{-1}$ matrix. Second, by dealing with the eigenvalues of the inverse matrix, the eigenvalues with positive real parts were "spearated" both further from the real axis and further from each other.

The use of Galerkin's method together with a suitable error bound theory is a useful method of predicting stability. The value of the technique is that one needs only to know the form of the original infinite matrix and the eigenvalues of a truncated part of the original matrix to obtain an error bound for the approximate eigenvalues.

VII. CONCLUSIONS

The dynamics of a spinning elastic disk are herein investigated using modal expansion techniques and direct stability methods. An approximate system is derived using approximate eigenfunctions in Galerkin's method. This system is a finite set of constant coefficient ordinary differential equations. The stability of the solution to this system of equations is determined by calculating its eigenvalues.

The Frequency-Speed diagrams showing the real and imaginary parts of the eigenvalues of the approximate system as a function of rotational speed are obtained numerically. All of the eigenvalues of a freely spinning disk are pure imaginary and hence the perturbed motion of the disk is bounded and harmonic. A spinning disk with a massive load can have eigenvalues with non-zero real parts. In this case, the real part gives the rate of growth or decay of amplitude of the transverse vibration of the perturbed disk. Instability regions are defined by the speeds of rotation for which there exist an eigenvalue with positive real part. The approximate modal analysis of the spinning elastic disk with a massive load system indicates that 1) The spring of the load produces an instability in an interval of speed above each of the critical speeds of the spinning disk, 2) The mass and damper of the load system causes terminal instabilities. The magnitude of the mass of the load greatly effects the existence and onset rotation speed of this type of instability. The damping causes the solution to the approximate system of

equations to be unstable for all speeds greater than those of the first stiffness instability. 3) Interaction between the first mode and the reflected branches of any other mode results in a modal coupling instability.

The dynamic behavior of a rotating elastic disk is compared to that of a fixed elastic disk with a rotating load. The effect of the centrifugal stress terms in the rotating disk problem is to eliminate the stiffness instability for the first mode and shift this instability to higher speeds for all other modes. The centrifugal stress also affects the terminal instability arising from the mass of the load, causing it to occur only for values of load mass which are larger than the mass of the disk. Qualitatively the modal coupling instability and the damping instability are unaffected by the centrifugal stress terms.

The direct method of Liapunov is applied to the equation of motion of the spinning disk with massive load and to the stationary disk with rotating massive load. Both systems are shown to be stable at speeds below the first critical speed. The direct stability method produces no results for speeds greater than the first critical speed.

An error bound theory based on Gershgorin's method is used to show the existence of eigenvalues with positive real part for the truncated system implies the same for the full infinite mode system. The theory provides a technique which is useful in the stability analysis of continuous systems. The error bound technique is advan-

tageous when the error bounds calculated by the procedure of Chapter VI are smaller than those calculated using Gershgorin's theorem directly on the system matrix.

REFERENCES

1. Lamb, H., Southwell, R. V., "The Vibrations of a Spinning Disk", Proceedings of the Royal Society (London), Vol. 99, 1921, pp. 272-280.

2. Southwell, R. V., "On the Free Transverse Vibrations of a Uniform Circular Disc Clamped at its Centre; and on the Effects of Rotation", Proceedings of the Royal Society (London), Vol. 101, 1921, pp. 133-153.

3. Barasch, S., Chen, Y., "On the Vibration of a Rotating Disk", Journal of Applied Mechanics, Trans. of ASME, Vol. 39, Series E, No. 4, Dec. 1972, pp. 1143-1144.

4. Moody, A.M.G., Trenton, N. J., "The Axial Vibration of Turbine Disks", Journal of Applied Mechanics, Trans. of ASME, Vol. 67, March 1945, pp. A-48 - A-55.

5. Tobias, S. A., Arnold, R. N., "The Influence of Dynamical Imperfections on the Vibrations of Rotating Disks", Proc. of the Institute of Mechanical Engineers, Vol. 171, 1957, pp. 669-690.

6. Tobias, S. A., "Non-Linear Forced Vibrations of Circular Disks", Engineering, Vol. 186, July 11, 1958, pp. 51-56.

7. Tobias, S. A., "Free Undamped Non-Linear Vibrations of Imperfect Circular Disks", Proc. Instn. Mechanical Engineers, London, Vol. 171, 1957, pp. 691-701.

8. Williams, C. J. H., Tobias, S. A., "Forced Undamped Non-Linear Vibrations of Imperfect Circular Discs", Mechanical Engineering Science, Vol. 5, No. 4, 1963.

9. Nowinski, J. L., "Nonlinear Transverse Vibrations of a Spinning Disk", Journal of Applied Mechanics, Transactions of the ASME, Vol. 31, Ser. E, No. 1, March 1964, pp. 72-78.

10. Williams, C. J. H., "The Stability of Nodal Patterns in Disk Vibrations", International Journal of Mechanical Science, Pergamon Press Ltd., 1966, pp. 421-432.

11. Simmonds, J. G., "Axisymmetric, Transverse Vibrations of a Spinning Membrane Clamped at its Center", American Institute of Aeronautics and Astronautics Journal, Vol. 1, No. 5, May 1963, pp. 1224-1225.

12. Mote, C. D., Jr., "Natural Frequencies in Annuli With Induced Thermal Membrane Stresses", Journal of Engineers for Industry, Nov. 1967, pp. 611-618.

13. Mote, C. D. Jr., "Free Vibrations of Initially Stressed Circular Disks", Journal of Engineers for Industry, Vol. 87, Series E, No. 2, May 1965, pp. 258-264.

14. Advani, S. H., Buckley, P. Z., "Non-Linear Transverse Vibrations and Waves in Spinning Membrane Discs", Journal of Sound and Vibration, Vol. 10, No. 1, Jan. 1969, pp. 59-64.

15. Hegemier, G. A., "On Nonlinear Steady-State Solutions To Moving Load Problems", Quarterly of Applied Math, Vol. 26, No. 2, 1968, pp. 239-248.

16. Iwan, W. D., Stahl, K. J., "The Response of an Elastic Disk With a Moving Mass System", Journal of Applied Mechanics, Trans. of ASME, Vol. 40, Series E, No. 2, June 1973.

17. Stahl, K. J., Iwan, W. D., "On the Response of a Two-Degree-of Freedom Rigid Disk With a Moving Massive Load", Journal of Applied Mechanics, Trans. of ASME, Vol. 40, Series E, No. 1, March 1973, pp. 114-120.

18. Stahl, K. J., "Dynamic Response of Circular Plates Subjected To Massive Loads", Ph. D. Thesis, California Institute of Technology, 1971.

19. Mote, C. D., "Stability of Circular Plates Subjected to Moving Loads", Journal of the Franklin Institute, Vol. 290, No. 4, October 1970, pp. 329-333.

20. Movchan, A. A., "The Direct Method of Liapunov in Stability Problems of Elastic Systems", Journal of Applied Mathematics and Mechanics, Vol. 23, No. 3, 1959, pp. 483-493

21. Movchan, A. A., "Stability of Processes With Respect to Two Metrics", Journal of Applied Mathematics and Mechanics, Vol. 24, No. 6, 1960, pp. 988-1001.

22. Knopps, R. J., Wilkes, E. W., "On Movchan's Theorems for Stability of Continuous Systems", International Journal of Engineering Science, Vol. 4, 1966, pp. 303-329.

23. Dickerson, J. R., Caughey, T. K., "Stability of Continuous Dynamic Systems With Parametric Excitation", Journal of Applied Mechanics, Transactions of the ASME, Vol. 36, Series E, No. 2, June 1969, pp. 212-216.

24. Lee, T. H., Hsu, C. S., "Liapunov Stability Criteria for Continuous Systems Under Parametric Excitation", Journal of Applied Mechanics, Trans. of the ASME, Vol. 39, Series E, No. 1, March 1972, pp. 244-250.

25. D'Souza, A. F., "On the Stability of Continuous Media", Journal of Applied Mechanics, Trans. of ASME, Vol. 39, Series E, No. 2, June 1972, pp. 438-444.

26. Hegemier, G. A., "Stability of Cylindrical Shells Under Moving Loads by the Direct Method of Liapunov", Journal of Applied Mechanics, Trans. of the ASME, Vol, 34, Series E, No. 4, Dec. 1967, pp. 991-998.

27. Mikhlin, S. G., Variational Methods in Mathematical Physics, Pergamon Press, New York, 1964.

28. Bolotin, V. V., Nonconservative Problems of the Theory of Elastic Stability, Pergamon Press, MacMillan Co., New York, 1963.

29. Figueiredo, D. G., "Fixed-Point Theorems for Nonlinear Operators and Galerkin Approximations", Journal of Differential Equations, Vol. 3, 1967, pp. 271-281.

30. Franklin, J. N., Matrix Theory, Prentice Hall, Englewood Cliff, New Jersey, 1968, pp. 161-163.